Nina Bruun

Bio-oils in Contact with Steels and Copper Surfaces

Åbo Akademi University

Bio-oils in Contact with Steels and Copper Surfaces

Nina Bruun

Inorganic Chemistry
Faculty of Science and Engineering
Åbo Akademi University
Åbo, Finland, 2022

Supervisors

Professor Leena Hupa
Åbo Akademi University

and

Docent Fiseha Tesfaye
Åbo Akademi University

and

Docent Juho Lehmusto
Åbo Akademi University

Opponent

D.Sc. (Tech.) Juha Ahola, University lecturer
University of Oulu

Reviewers

Professor Mika Suvanto
University of Eastern Finland

and

Docent Bengt-Johan Skrifvars
Åbo Akademi University

ISBN 978-952-12-4202-1 (printed)
ISBN 978-952-12-4203-8 (digital)
Painosalama, Turku, Finland 2022

Preface

This work was conducted at the Combustion and Materials Chemistry research group of the Johan Gadolin Process Chemistry Centre (PCC) at Åbo Akademi University during the years 2015-2022. The work was financed by the European Regional Development Fund Innovative Cities Programme (INKA) SmartResearch project (4690/31/2014) and the following companies: Crisolteq Oy, Ekolite Oy, Nanol Technologies Oy, VG Shipping Oy, Mirka Oy, Ecomation Oy. Additional funding was provided by the Swedish Cultural Foundation in Finland, Otto A. Malm Foundation, and Rector at Åbo Akademi University. The Åbo Akademi University Foundation and the APC-pool at Åbo Akademi University are acknowledged for financial support of conference participation and open access publications.

I would like to thank my supervisors Professor Leena Hupa, Docent Fiseha Tesfaye, and Docent Juho Lehmusto for their guidance and support during my doctoral studies. I am grateful to Professor Leena Hupa for giving me the opportunity to conduct this work. I especially appreciate the fact that she was always available to help and support me in my work. I would like to express my gratitude for the continuous support I have received from Fiseha, and I am also grateful to Juho for his valuable advice and important feedback.

I am also grateful to my other co-authors: Professor Stefan Willför, D.Sc. Tooran Khazraie Shoulaifar, D.Sc. Abayneh Getaschew Demesa, D.Sc. Meheretu Jaleta Dirbeba, and M.Sc. Jarl Hemming at Åbo Akademi University.

Special thanks go to M.Sc. Jarl Hemming for his expertise in oil chemistry and analysis, which has been of great value in completing this thesis.

I would further like to thank all my colleagues at the Combustion and Materials Chemistry research group for the help they provided and the joy of working together. M.Sc. Berndt Södergård is acknowledged for fruitful discussions and for his contribution to this thesis and Lic.Sc. Tor Laurén for all his guidance and help with practical issues in the laboratory; D.Sc. Emil Vainio, D.Sc. Thomas Kronberg, and M.Sc. Jan-Erik Eriksson for their helpful information. M.Sc. Linus Silvander is acknowledged for his skillful work with SEM-EDS analysis and Mr. Luis Bezerra, Mr. Peter Backman, and Ms. Jaana Paananen for conducting analytical work and providing me with technical support. M.Sc. Kenneth Stenlund is also kindly acknowledged for his technical support during my viscosity and surface tension measurements in the Laboratory of Physical Chemistry at Åbo Akademi University. I would also like to express my gratitude to the very skilled information expert D.Sc. Linda Nisula for her professional support concerning information during my work with this thesis. I would like to thank M.Sc. Eva Höglund, Ms. Mia Mäkinen, Mrs. Annika Fougstedt, Ms. Benita Martiala, and Ms. Maria Ljung for their office support and kind advices.

Docent Jussi Meriluoto in the Biochemistry Laboratory at Åbo Akademi University is also gratefully acknowledged for the fruitful discussions.

I would like to thank my friend D.Sc. Rauni Seppänen at Holmen AB in Stockholm for her positive encouragement and helpful advice during these years. Finally, I must express my gratitude to all my friends, whose support has kept my spirits up during the process of completing this doctoral thesis.

Turku, October 2022
Nina Bruun

Abstract

Bio-oil is a renewable energy source and can be used either in crude or processed forms. The crude bio-oil can be used in marine engines or conventional combustors. Using bio-oils instead of petroleum fossil fuels in marine engines reduces sulfur and phosphorus emissions. Bio-oils originate from animal fats, agricultural crops, and pyrolysis of biomasses. Used cooking oils (UCOs) and fish oils (FOs) are of increasing interest as economic feedstock for bio-oils or biodiesel production. UCOs are non-edible oil residues collected from, e.g., restaurants. During the cooking or frying step, the temperature of the oils can reach 190 °C, which causes the triglycerides in the oil to degrade thermally and chemically. These reactions may form free fatty acids (FFAs), glycerol, monoglycerides, and diglycerides. Some characteristics such as pre-existing organic acids, water content, and any possible sediment in the bio-oil can lead to corrosion of steels and copper in contact with the oil. However, the UCOs must be used within a relatively short period of time after their collection and processing to avoid, e.g., the formation of corrosive degradation components. Certain levels of the acid number, viscosity, density, and water content are essential for approving the bio-oils as fuels. However, the acid number and water do not directly correlate with the bio-oil properties and corrosivity. The roles of different bio-oil components and corrosion inhibitors on the corrosive properties are not thoroughly understood.

In this work, we studied the physicochemical and thermal properties of locally produced UCOs and FOs to determine their applicability as alternative fuels for marine engines. The properties of these locally produced bio-oils were compared to a commercial oil. The corrosive properties were studied by immersing steels or copper rods at room temperature in the UCOs and FOs. Also, the impact of water in oils on the dissolved iron concentration was investigated. Oleic acid and glycerol were studied as corrosion inhibitors in UCOs. Further, changes in the physicochemical and thermal properties were investigated as functions of storage time for up to five years.

The corrosivity of different UCO batches was addressed with three-day immersion tests of steel rods. Furthermore, the roles of contaminants, bio-oil preservatives, and corrosion inhibitors in bio-oil-induced corrosion were examined with oil samples containing added water, short-chain carboxylic acids, and ten different amino acids.

The physicochemical and thermal properties of the bio-oils correlated with their contents of different fats. The acid number of all bio-oils was relatively high and slightly increased with their aging, likely due to the conversion of unsaturated fatty acids. The concentrations of phosphorus and sulfur in the bio-oils were below the limits specified for oils in marine engines. The bio-oils decomposed at higher temperatures than the commercial reference oil but had lower heat content than the commercial oil.

Detailed analysis of various physicochemical properties and the fatty acid composition of the bio-oils suggested that the waste stream-based bio-oils are potential sources of carbon dioxide neutral fuels in marine engines.

However, immersion tests with mild steel rods suggested an increased dissolved iron concentration in the oil at 10 days. Adding oleic acid and glycerol decreased the dissolved iron concentration in the oil. Water content, acid number, and the overall oil composition substantially affected the corrosive behavior of the oils. Among the tested oils, the FO and the reference commercial oil product showed the highest and lowest amounts of dissolved iron, respectively.

The results observed in this work imply that the immersion test of a steel rod can be used as a reliable and cost-effective method to compare the corrosive properties of bio-oils as well as other biofuels.

In general, the oils with the highest water concentrations showed the highest corrosion properties, although their acid numbers were not the highest. The oils with the highest acid numbers contained the highest concentrations of unsaturated free fatty acids, such as oleic acid. The unsaturated free fatty acids were assumed to form a protective layer on the rods, thereby preventing the permeation of oxygen and water to the steel surface. When a very corrosive oil was mixed with a less corrosive oil, the amount of dissolved iron decreased notably. This suggests that mixing different bio-oils decreases the corrosion of steel devices in contact with the oil. Among the ten studied potential corrosion inhibitors, the amino acids L-lycine and L-arginine showed positive effects, also when added at low concentrations. Short-chained carboxylic acids formic or propionic acid also suggested minor corrosion inhibiting effect, most likely due to the thin surface layer that formed on the steel. However, the simultaneous presence of water and carboxylic acid led to corrosion. Furthermore, neither L-lycine nor L-arginine could provide corrosion protection in the presence of both water and a carboxylic acid. This suggests that UCOs containing short-chained carboxylic acids and water increase the corrosion of steel.

The results of this work indicate that the bio-oils may be used as a sustainable, locally sourced alternative fuel as long as they do not contain carboxylic acids and water simultaneously. The impact of water content on the corrosion might be decreased with amino acid-based inhibitors in the absence of carboxylic acid.

Keywords: bio-oil, fish oil, used cooking oil, marine engines, biofuel utilization, corrosion, inhibition, renewable energy sources

Sammanfattning

Bioolja är en förnybar energikälla och kan användas antingen i rå eller förädlad form. Den råa biooljan kan användas i marina motorer eller konventionella brännkammare. Svavel- och fosforutsläppen minskar när biooljor används som bränsle i marina motorer i stället för fossila petroleumbränslen. Biooljor härstammar från animaliska fetter, vegetabiliskt oljeavfall och pyrolysolja från biomassa. Använda matoljor (UCOs) och fiskoljor (FOs) är av ökande intresse som ekonomisk råvara för biooljor eller vid produktion av biodiesel. De använda matoljorna är icke-ätbara rester från t.ex. restauranger. Under tillagnings- och frityrsteget kan temperaturen i oljorna stiga till 190°C, vilket gör att oljornas triglycerider bryts ned termiskt och kemiskt. Dessa reaktioner kan resultera i bildning av fria fettsyror, glycerol, monoglycerider och diglycerider. Vissa kemiska föreningar, såsom redan existerande organiska syror, vatten och eventuella sediment som finns i biooljan, kan orsaka korrosion av stål och koppar vid kontakt med oljan. De använda matoljorna måste dock utnyttjas inom en relativt kort tidsperiod efter insamling och bearbetning för att exempelvis undvika att korrosiva nedbrytningskomponenter bildas. Vissa nivåer av syratal, viskositet, densitet och vattenhalt är avgörande för att biooljorna ska accepteras som bränslen. Syratalet och vattenhalten korrelerar dock inte direkt med biooljans egenskaper och korrosivitet. Det är inte helt klarlagt vilken inverkan de olika biooljekomponenterna och korrosionsinhibitorerna har på de korrosiva egenskaperna.

I detta arbete undersökte vi de fysikalisk-kemiska och termiska egenskaperna hos lokalt producerade, använda matoljor och fiskoljor för att utreda deras användbarhet som alternativa bränslen för marina motorer. Egenskaperna hos dessa lokalt producerade biooljor jämfördes med en kommersiell referensolja. De korrosiva egenskaperna studerades genom ett nedsänkningstest med en stav av stål eller en kopparstav vid rumstemperatur i UCOs eller FOs. Dessutom undersöktes effekten av vatten i oljorna på koncentrationen av löst järn. Oljesyra och glycerol studerades som korrosionsinhibitorer i UCOs. Vidare undersöktes förändringar i de fysikalisk-kemiska och termiska egenskaperna som funktioner av lagringstid i upp till fem år.

Korrosiviteten hos olika UCO-satser undersöktes med tre dagars nedsänkningstest med stavar av stål. Vidare undersöktes rollerna för föroreningar, konserveringsmedel för biooljor och korrosionsinhibitorer i biooljeinducerad korrosion med oljeprover innehållande tillsatt vatten, kortkedjiga karboxylsyror och tio olika aminosyror.

De fysikalisk-kemiska och termiska egenskaperna hos biooljorna korrelerade med deras innehåll av olika fetter. Syratalet för alla biooljor var relativt högt och ökade något under biooljornas åldrande, troligtvis på grund av omvandlingen av omättade fettsyror. Koncentrationerna av fosfor och svavel i biooljorna låg under de angivna gränsvärdena för oljor i marina motorer. Jämfört

med den kommersiella referensoljan nedbröts biooljorna vid högre temperaturer men biooljornas värmeinnehåll var lägre än den kommersiella referensoljans.

En detaljerad analys av olika fysikalisk-kemiska egenskaper samt fettsyrasammansättningen av biooljorna tyder på att avfallsbaserade biooljor kan användas som koldioxidneutrala bränslen i marina motorer. Emellertid visade det sig att nedsänkningstest med stänger av mjukt stål påvisade en högre halt av järn som löste sig i oljorna vid 10 dagar. Vid tillsats av oljesyra och glycerol sjönk halten järn som löste sig i oljan. Vattenhalten, syratalet och den totala oljesammansättningen påverkade väsentligt oljornas korrosiva egenskaper. Bland de testade oljorna visade FO och den kommersiella referensoljeprodukten de högsta respektive lägsta mängderna löst järn.

Resultaten som observerats i detta arbete innebär att nedsänkningstestet med en stav av stål kan användas som en pålitlig och kostnadseffektiv metod för att jämföra de korrosiva egenskaperna hos biooljor såväl som andra biobränslen.

I allmänhet uppvisade oljorna med de högsta vattenkoncentrationerna de högsta korrosionsegenskaperna, även om deras syratal inte var de högsta. Oljorna med de högsta syratalen innehöll de högsta koncentrationerna av omättade fria fettsyror, såsom oljesyra. De omättade fria fettsyrorna antogs bilda ett skyddande skikt på stavarna och därigenom förhindra genomträngning av syre och vatten till stålytan. När en mycket frätande olja blandades med en mindre frätande olja, minskade mängden löst järn markant. Detta tyder på att vid blandning av olika biooljor minskar korrosionen av stålenheter i kontakt med oljan. Bland de tio studerade potentiella korrosionsinhibitorerna visade aminosyrorna L-lycin och L-arginin positiva effekter, även när de tillsattes i låga koncentrationer. Kortkedjiga karboxylsyror myr- eller propionsyra påvisade en lägre korrosionshämmande effekt, troligen på grund av det tunna ytskiktet som bildades på stålet. Den samtidiga närvaron av vatten och karboxylsyra ledde dock till korrosion. Vidare kunde varken L-lycin eller L-arginin ge korrosionsskydd i närvaro av både vatten och en karboxylsyra. Detta tyder på att UCOs som innehåller kortkedjiga karboxylsyror och vatten ökar korrosionen av mjukt stål.

Resultaten av detta arbete indikerar att biooljorna kan användas som ett hållbart, lokalt anskaffat alternativt bränsle så länge de inte innehåller karboxylsyror och vatten samtidigt. Vattenhaltens inverkan på korrosionen kan minskas med aminosyrabaserade inhibitorer i frånvaro av karboxylsyra.

List of original publications

This dissertation is based on the following scientific publications:

I. Bruun, N.; Khazraie Shoulaifar, T.; Hemming, J.; Willför, S.; Hupa, L. Characterization of waste bio-oil as an alternate source of renewable fuel for marine engines. Biofuels 2022, 13, 21–30.

II. Bruun, N.; Demesa, A.G.; Tesfaye, F.; Hemming, J.; Hupa, L. Factors affecting the corrosive behavior of used cooking oils and a non-edible fish oil that are in contact with ferrous metals. Energies 2019, 12, 4812.

III. Bruun, N.; Tesfaye, F.; Hemming, J.; Dirbeba, M. J.; Hupa, L. Effect of storage time on the physicochemical properties of waste fish oils and used cooking vegetable oils. Energies 2021, 14, 101.

IV. Bruun, N.; Lehmusto, J.; Hemming, J.; Tesfaye, F.; Hupa, L. Metal rod surfaces after exposure to used cooking oils. Sustainability 2022, 14, 355.

V. Bruun, N.; Lehmusto, J.; Tesfaye, F.; Hemming, J.; Hupa, L. Amino Acids Reduce Mild Steel Corrosion in Used Cooking Oils. Sustainability 2022, 14, 3858.

Contribution of the author

The following describes the author's contribution to the papers on which this thesis is based. In **Papers I-V,** Bruun wrote the manuscripts. All analyses with ICP-OES, ICP-MS, CHNS-O elemental analyzer, SEM, SEM-EDX, TGA, and FTIR were conducted by laboratory personnel. Bruun was responsible for most of the sample preparations and evaluation of the measured data. In **Papers I-IV,** the GC-FID, GC-MS, GC-MSD, and HPSEC-ELSD analyses and evaluation of the data were carried out by Jarl Hemming.

Paper I
The author planned the experiments with the co-authors. The author carried out the experiments. The results were evaluated by the author together with the co-authors. Jarl Hemming conducted the FTIR analyses and helped evaluate the data.

Paper II
The author planned the experiments with the co-authors. The author carried out the experiments. The results were evaluated together with the co-authors.

Paper III
The author planned the experiments with the co-authors. The author carried out the experiments. The results were evaluated together with the co-authors.

Paper IV
The author planned the experiments with the co-authors. The author carried out the experiments. The results were evaluated together with the co-authors.

Paper V
The author planned the experiments with the co-authors and carried out the experiments. The results were evaluated together with the co-authors.

List of abbreviations and symbols

Abbreviations:

AN	Acid Number
ASTM	American Society for Testing and Materials
BIB	Broad Ion Beam
COref	Reference Commercial Oil Product
EN	European Committee for Standardization
FFA	Free Fatty Acid
FO	Fish Oil
FTIR	Fourier Transform Infrared Spectroscopy
GC-FID	Gas Chromatograph-Flame Ionization Detector
GC-MS	Gas Chromatography-Mass Spectrometry
GC-MSD	Gas Chromatography–Mass Selective Detector
HPSEC-ELSD	High-Performance Size Exclusion Chromatography – Evaporative Light Scatter Detector
HHV	Higher Heating Value
ICP-MS	Inductively Coupled Plasma - Mass Spectrometry
ICP-OES	Inductively Coupled Plasma - Optical Emission Spectrometry
ISO	International Organization for Standardization
KF	Karl Fischer
KOH	Potassium Hydroxide
LB	Liquid Biofuel
n.a.	Not Available
n.d.	Not Detected
SEM-EDS	Scanning Electron Microscopy-Energy Dispersive Spectroscopy
SFS	Suomen Standardisoimisliitto
SOx	Sulfur-oxide
TBA	Tert-Butylamine
TGA	Thermogravimetric Analyser
UCO	Used Cooking Oil
VG	Vegetable Oil

Symbols:

% v/v	Volume percent

Table of contents

1. Introduction

Liquid biofuel is an attractive source of renewable energy, which depends on its similar functionality to petroleum fuel. The liquid biofuel, so-called bio-oil, has a similar heating value as fossil oil. In contrast, its toxicity and usually sulfur content are lower than petroleum fossil oil [1-3]. Bio-oils can be used either in crude or processed forms. The processed bio-oil is currently used as biodiesel in cars and airplanes [4,5], whereas the crude bio-oil can be used in either conventional combustors [6] or marine engines [7]. Most bio-oils originate from animal fats, crops, and pyrolysis of biomasses.

Used cooking oils (UCOs) and fish oils (FOs) are of increasing interest as economic feedstock for bio-oils or biodiesel production [8]. However, they have limited oxidative stability as their source is, i.e., fresh vegetable oils [9].

Bio-oils fulfill the demand of the circular economy. The role of resources in the circular economy can be summarized in four central tenets: reduce, reuse, recycle and recover [10]. UCOs´ contribution to a carbon-neutral energy system is illustrated in Figure 1 [8].

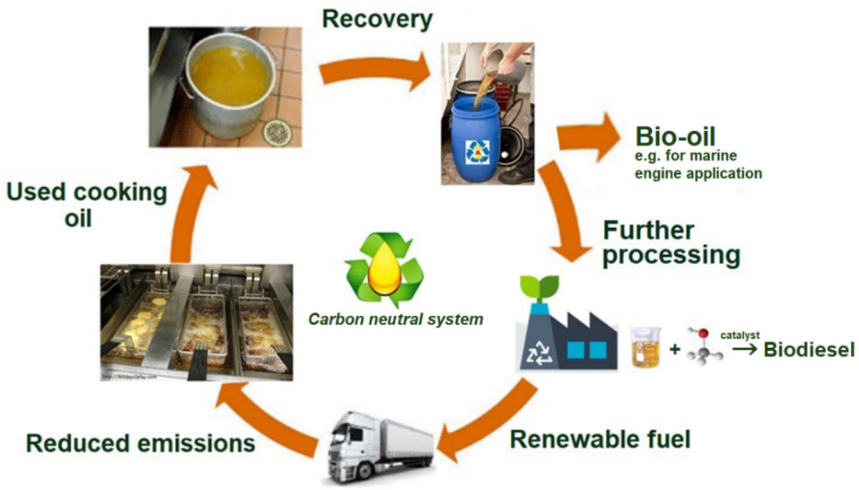

Figure 1. Schematic diagram showing the role of UCOs in enabling a carbon-neutral energy system. Adapted from Paper III.

Among different animal fats, fish oil is produced in large quantity by the fish-processing industry [11]. Fish oil is commonly used in cosmetics, pharmaceuticals, and human dietary complements industries [12,13]. However, in cases where fish oil degrades during storage and handling, the formed low-grade fish oil can be used in marine engines [14].

Cooking oils from vegetable resources are extracted from rapeseed, sunflower, soybean, palm kernel, corn, grapeseed, etc. [15-17]. Recycled vegetable oils or UCOs are non-edible residues from restaurants, households, and the food processing industry. During frying, the temperature of the oils can

reach as high as 190°C [18], which creates favorable conditions for several reactions within the oil and its surroundings. The oils' original properties are significantly affected during the frying step as the triglycerides degrade thermally and chemically [18]. In general, three major types of reactions may take place during frying: oxidation, hydrolysis, and thermal degradation of triglycerides [19]. These reactions may result in the formation of free fatty acids (FFAs), glycerol, monoglycerides, and diglycerides. An increase in saturated and monounsaturated fatty acids can also occur [18,20-24].

The UCO usually needs a cleaning step to avoid blocking or damaging the engine. By removing the contaminants from UCO, the oil can be used either after processing for biodiesel purposes [25] or as is, depending on engine types. Using waste vegetable oils in automotive diesel engines reduced the soot formation and particulate emissions compared to petroleum-based diesel fuel [26].

Bio-oils can be used as fuels, but there might be problems as they can cause corrosion of metal equipment in contact with them. The most common factors to be considered include organic acids (such as acetic, formic, glycolic, and fatty acids), water content, and any possible sediment in the bio-oil. Water participates in forming additional free fatty acids out of any glyceride present in the bio-oil. Water in oils also enhances the growth of microorganisms, resulting in increased corrosion and a high risk of engine malfunction [27-29].

Sulfur and phosphorus emissions are reduced when using bio-oils as fuels in marine engines. In the marine sector, sulfur-oxide (SO_x) emissions from engines cause fine dust generations that can lead to serious health issues and problems such as acid rain, which harms biodiversity [30]. The EU actively promotes and passes legislations for a global maritime emission cut. Recently, the United Nations specialized agency, the IMO–International Maritime Organization, agreed to reduce shipping greenhouse gas emissions by ≥50% until 2050 [31].

According to the revised Sulfur Directive, since the beginning of 2020, the maximum sulfur content of marine fuels was reduced to 0.5%, i.e., down from the 2012 Sulfur Directive limit of 3.5% globally [30]. Bio-oils such as UCOs and FOs with a low sulfur content are thus excellent alternative marine fuels for marine diesel. The ongoing intensive research on bio-oil quality can contribute to the transition towards increased usage of eco-friendly fuels.

Some companies using crude bio-oil have their specifications to measure the quality of the oil. These specifications include limitations on viscosity, density, water content, acid number, sulfur, phosphorus contents, etc. [32]. The specifications come from various challenges the bio-oil cause in the engines [33]. For example, the acid number of crude bio-oils should be below 5.0 mg potassium hydroxide (KOH)/g, and the water content should be less than 0.20% (v/v) [34]. Additionally, the sulfur and phosphorus content should be less than 500 ppm and 100 ppm, respectively.

The source and composition of bio-oils directly influence the quality and behavior of the fuel. Therefore, the physical, chemical, and thermal properties of locally produced fish oils and used cooking oils are studied as fuel candidates in marine engines. All the sources of the oils studied were classified as waste and of

such quality that they could not safely be used, for example, in food production. Thus, their utilization in marine engines instead of crude oil-based fuel offers a means to decrease greenhouse gas emissions.

1.1. Purpose of the work

This work aimed to characterize and better understand the possibilities of using crude bio-oils as fuels in marine engines. The focus is on UCOs and FOs from gutting rests of rainbow trout after extracting fish oil to products other than fuel. The corrosive behavior of bio-oils in contact with steel and copper rod surfaces was experimentally investigated. The high temperature corrosion issue has not been studied in this work.

In particular, the following topics were addressed:

1) The physical, chemical, and thermal properties of locally produced FOs and UCOs as fuel candidates in marine engines (Paper I).

2) The corrosive properties of UCOs and FOs in contact with steel rods. The role of oleic acid and glycerol on corrosion (Paper II).

3) The effect of storage time on the bio-oils' physicochemical and thermal properties (Paper III).

4) The corrosion of steel and copper rods exposed to the UCOs originating from different batches (Paper IV).

5) The role of corrosion inhibitors (different amino acids), water, formic and propionic acids to steel corrosion in contact with different UCO batches (Papers IV and V).

2. Literature review

2.1. Vegetable oils production globally

Some oilseeds can be safely used for human consumption. There are also sources of oils that cannot be used for edible purposes. However, non-edible oils can be used to produce oleo-chemicals for multiple applications in the industry [35].

In the 2021/2022 crop year, the vegetable oil production volume worldwide exceeded 200 million metric tons. Palm oil had the highest production volume among the major categories of vegetable oil, at 75.5 million metric tons. The volume of other oils (given in million metric tons) was 60.3 for soybean oil, 28.3 for rapeseed oil, 22.1 for sunflower seed oil, 8.7 for palm kernel oil, 6.5 for peanut oil, 5 for cottonseed oil, 3.5 for coconut oil, and 3.3 for olive oil [36]. The generation of UCOs is estimated to be around 20-32% of the total vegetable oil consumption [37,38].

2.2. Non-edible vegetable oils as fuel in marine engines

UCOs are waste streams and of great interest as renewable fuels. Thus, they neither compete with the food chain nor utilize farmland for their production. These circumstances make UCOs an attractive feedstock for future transportation fuels for maritime shipping, aviation, and material production [39,40].

Increasing interest in the circular economy and sustainable use of resources has made UCOs and UCO-based biodiesel attractive as renewable fuels for diesel engines, particularly marine engine applications [41].

UCOs are mixtures of triglycerides, diglycerides, monoglycerides, and fatty acids contaminated by derivatives from the food frying process, such as free fatty acids (FFAs), heterocycles, Maillard reaction products, and metal traces originating from pads and food leaching [42-44]. UCOs are also raw materials for other industries, e.g., the production of bio-plasticizers, syngas, and sorbents for volatile organic compounds (VOCs) [45-47].

However, the UCOs must be used relatively quickly after their collection and processing to avoid, e.g., the formation of corrosive degradation components [48,49]. In general, the acid number, viscosity, density, and water content are essential criteria for approving the UCOs as fuels [50]. However, the acid number and water do not directly correlate with the bio-oil properties and corrosivity [51]. The roles of different bio-oil components and corrosion inhibitors in the corrosive properties are not thoroughly understood [51].

Biodiesel is commonly used as a blend with petroleum diesel fuel. Manufacturers of diesel vehicles and engines have approved the use of B5 (a blend containing 5% biodiesel and 95% petroleum diesel). Some approve the use of blends up to B20 (20% biodiesel and 80% petroleum diesel) or higher [62].

The Airbus A380 has in March 2022 completed in Toulouse, France, two trial flights powered on biofuel (which is free of both aromatics and sulfur). Airbus

aircraft can be powered by up to 50% biofuel, blended with traditional kerosene. Airbus plans to bring the world's first zero-emission aircraft to market by 2035 [63].

2.3. Corrosion

2.3.1. Basics of metal corrosion

Metal corrosion is described as an irreversible oxidation-reduction (redox) reaction between the metal and an oxidizing agent present in the environment [52,53]. When iron and steel corrode, they combine with oxygen and water to form hydrated iron oxides, similar in chemical composition to the original ore [54].

In wet corrosion, two principal oxidizing agents are encountered:

Solvated protons and dissolved oxygen. Other oxidizing agents can also cause corrosion in wet environments, such as oxidizing cations (Me^{n+}), oxidizing anions (e.g., OCl^-), and dissolved oxidizing gases (O_2, Cl_2) [52].

While corrosion occurs in different forms, the classification is usually based on one of the following three factors: the corrodent nature, corrosion mechanism, or corroded metal appearance.

Corrosion can be a macroscopically localized or microscopic local attack in which the amount of metal dissolved is minute. In a microscopic local attack, considerable damage can occur before the corrosion becomes visible to the naked eye. In contrast, macroscopic forms of corrosion affect greater areas and are generally observable directly or with low-power magnification devices. Figure 2 classifies macroscopic and microscopic forms of localized corrosion.

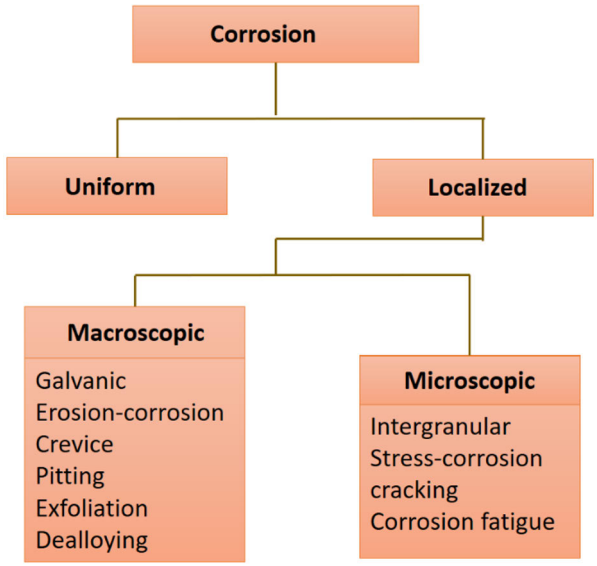

Figure 2. Macroscopic versus microscopic forms of localized corrosion, adapted from [54].

Corrosion can be controlled by five primary methods at room temperature: inhibitors, coatings, material selection, cathodic protection, and design [54]. Common inhibitors are chromates, silicates, and organic amines. The organic amines are adsorbed on anodic and cathodic sites, decreasing the corrosion current. Other inhibitors specifically affect either the anodic or cathodic process. Some inhibitors promote the formation of protective films on the metal surface [54].

When a metal is immersed in a solution, the metal can behave in one of the three following ways. 1) The metal is thermodynamically stable, and corrosion reaction does not occur. This behavior is typical for noble metals, e.g., gold, silver, and platinum. 2) The metal corrodes as it dissolves in the solution and forms soluble, nonprotective corrosion products. This so-called active corrosion is characterized by high weight loss. 3) Passive behavior again means that metal corrodes. However, an insoluble, protective corrosion-product film (passive film) forms on the metal surface. If the passive film is broken or dissolved, the metal reverts to active behavior.

Typical metals that exhibit passivity are iron, chromium, titanium, nickel, aluminum, and their alloys, most notably stainless steels.

Most engineering alloys are passive in their applications. If the environment becomes more corrosive, passive metals might exhibit localized forms of corrosion, e.g., pitting, stress-corrosion, cracking, and crevice corrosion (Figure 2) [54].

The solution's acidity or alkalinity greatly affects its corrosivity for specific metals. For example, nickel is quite resistant to highly alkaline environments, but strongly alkaline environments corrode aluminum.

From the corrosion perspective, the solubility of oxygen in a solution is one of the most significant effects. At any given temperature, the corrosion rate of iron increases with increasing oxygen concentration [54].

Corrosion reactions of iron in oxidizing acidic environment are given by the anode (1) and cathode (2) reactions below:

$$Fe(s) \rightarrow Fe^{2+}(aq) + 2e^{-} \quad (1)$$

$$O_2(g) + 4H^{+}(aq) + 4e^{-} \rightarrow 2H_2O\ (l). \quad (2)$$

In iron corrosion, the ions released into the solution leave electrons at the anodic sites. The corrosion reaction then proceeds as quickly as these electrons are consumed in the cathodic reaction to reduce the dissolved oxygen. Thus, adding oxygen allows more electrons to be consumed, increasing the corrosion rate [53].

2.3.2. Corrosion of metals in biofuels

Although liquid biofuels are usually considered very good replacements for fossil fuel oil in marine engines, their utilization might bring additional challenges [55]. In bio-oils, the presence of water and/or acidic groups (FFAs or short-chain carboxylic acids, which are used as preservatives) might cause corrosion of

storage tanks and fuel injectors [51]. Therefore, the marine engine designers and producers have proposed the acid number (AN) limitations. The acid number expresses the acidity of the oil. For instance, AN above 100 mg KOH/g oil is considered corrosive. On the other hand, AN below 5 mg KOH/g oil means that the oil does not increase the corrosion risk [32].

Also, the presence of some inorganics, especially phosphorus (P) and sulfur (S), could result in hot or cold corrosion in the turbocharger and combustion chambers, respectively [33,56]. However, the corrosion in these conditions was not included in this thesis.

In utilizing UCOs, corrosivity during storage and usage are some of the concerns yet to be investigated for addressing materials compatibility issues with the UCOs. According to Fazal et al. [57], corrosion products consisting of metal oxides, carbonates, and hydroxides can be formed on the surface of metals exposed to biodiesel containing water and dissolved oxygen at room temperature. Figure 3 illustrates the overall phenomena at the interface of a metal and biodiesel as described in the literature [57]. Despite the compositional differences between a typical UCO and biodiesel, the same phenomena depicted in Figure 3 could also occur at metal/UCO interfaces under similar conditions.

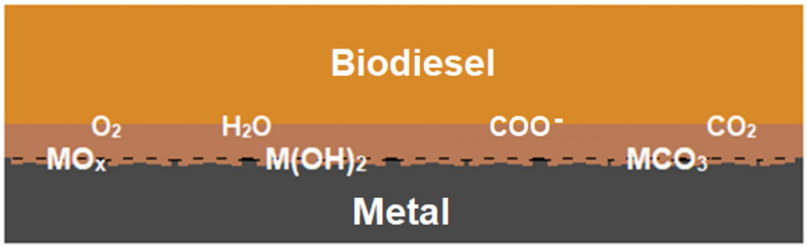

Figure 3. Schematic illustration of the phenomena at the interface of a metal (M) and biodiesel exposed to the atmosphere at room temperature. COO^- represents short-chain radicals formed when breaking down long-chain molecules. Adapted from Paper IV.

The corrosiveness of biodiesel can also depend on the feedstock [58,59]. According to Diaz-Ballote et al. [60], the corrosiveness of biodiesel decreased with decreasing impurities after processing. In addition, the corrosive nature of biodiesel increased with the presence of free water and free fatty acids. Compared to conventional diesel, biodiesel is more prone to water absorption, which leads to an increased risk of corrosion when water condenses on the metallic surfaces in contact with the biodiesel. The composition of the metal in contact with fuel also affects the corrosiveness of the fuel [61].

2.4. Corrosion inhibitors

The corrosivity of bio-oils can be lowered with corrosion inhibitors added in small concentrations to alter the environment into less corrosive [64,65]. Alternatively, the inhibitors interact with the metal to form a protective surface film [65-68]. In this work, the effect of the following compounds to inhibit corrosion on metal surfaces were tested: the surfactant oleic acid [69], glycerol (which is miscible in water, and it is suggested that through microemulsions the water is kept away from the metal surface) [91], amines [69] as well as amino acids are well-known corrosion inhibitors [66].

2.4.1. Oleic acid and glycerol

Surfactants forming a self-assembled monolayer might prevent corrosion by inhibiting the permeation of both water and oxygen to the metal surface. Surfactants such as oleic acid can form monolayers on the surface of metals, thus providing corrosion protection [69]. However, if the concentration is not high enough, the surfactant does not form a protective monolayer, thus allowing corrosion to occur [70].

Glycerol is miscible in water. Glycerol microemulsion forms a barrier between water and iron surfaces, thus reducing corrosion [55]. Besides its binding effect on water molecules, glycerol can form microemulsion in the presence of a surfactant such as oleic acid [55]. Blending glycerol into diesel or gasoline through microemulsification reduced problems associated with stand-alone glycerol fuel use [71,72]. Moreover, glycerol-in-diesel emulsion reduced unwanted combustion emissions [71,72].

2.4.2. Amines and amino acids

Corrosion inhibitors with proven effective performance include those containing multiple bonds, N, O, S, and P organic compounds, and some functional groups [68,73]. Organic compounds with -OH, -COOH, -NH_2, etc., are also excellent corrosion inhibitors, especially in acidic solutions [73]. The environmental legislation on toxicity, biodegradability, and bioaccumulation gives strict regulations and rules for the usage and disposal of corrosion inhibitors in different countries [74].

Inhibitors ethylenediamine, tert-butylamine (TBA), and n-butylamine formed a stable metal oxide protective layer on cast iron and thus retarded the corrosion in biodiesel [75]. However, TBA is classified as an acutely toxic substance and should thus be replaced by environmentally friendly compounds.

Developing green or eco-friendly inorganic and organic corrosion inhibitors with minimal side effects has been considered very important [66,76]. Organic green corrosion inhibitors include surfactants, amino acids, etc. [66]. Proteins in all animal and plant species are composed of twenty different amino acids [77]. Amino acids are biomolecules that are vital to all organisms. They form the building blocks of proteins and many essential substances such as neurotransmitters, hormones, and nucleic acids [78]. Amino acids are relatively

cheap, non-toxic, biodegradable, soluble in aqueous media, and produced at high purity [73,79]. Amino acids possess at least one carboxyl group and one amino group (Figure 4). They can coordinate with metals through nitrogen or oxygen atoms in the carboxyl group [80]. The strength of the inhibitor–metal bond is essential to the corrosion inhibition degree of amino acids [80]. Amino acids can control the corrosion of various metals such as pure iron, carbon steel, copper, zinc, nickel, tin, and aluminum alloys [79-82]. Furthermore, amino acids behave as corrosion inhibitors in acid medium, neutral medium, and de-aerated carbonate solution [80].

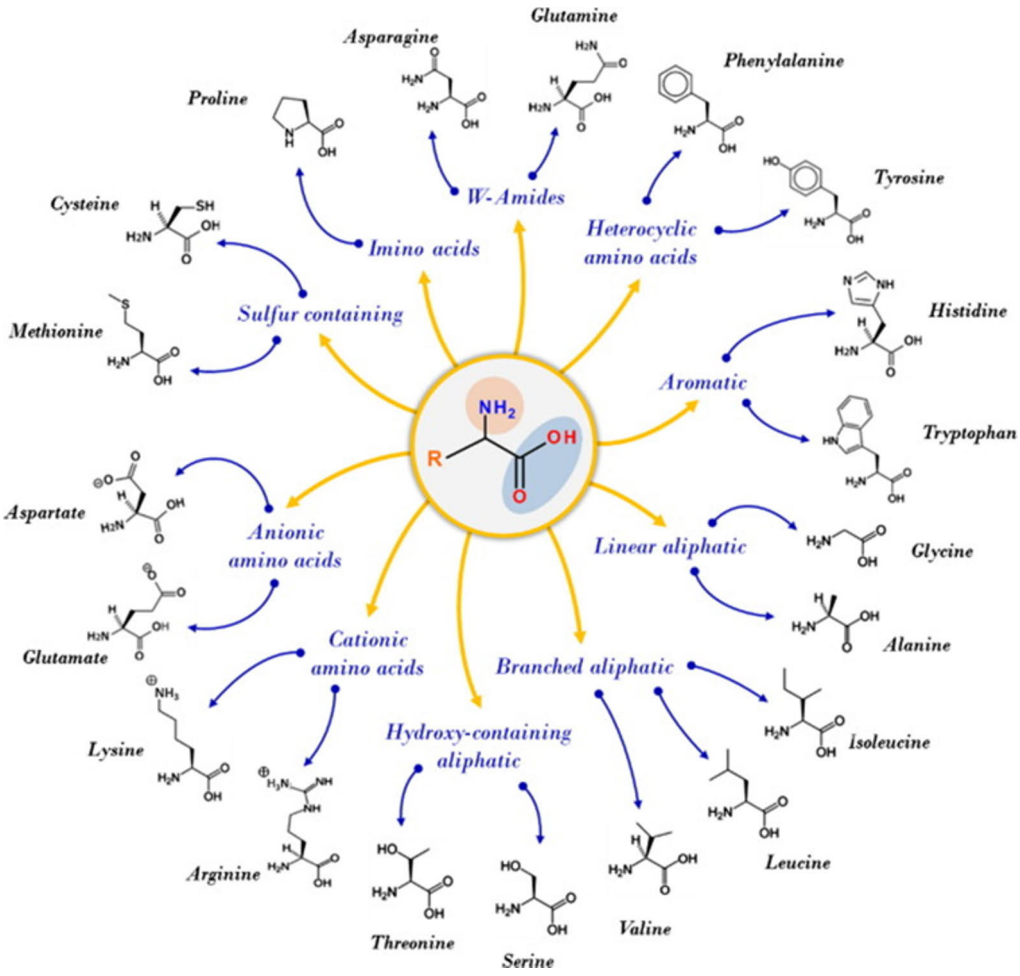

Figure 4. Amino acids and their derivatives as corrosion inhibitors for metals and alloys [66].

3. Materials and methods

This chapter summarizes the materials and methods parts of Papers I-V. All the method parameters are described in detail in the attached original papers. Paper I describes the chemical, physical, and thermal properties of the bio-oils. Paper II studies the corrosion behavior of bio-oils by immersion test of mild steel rods at room temperature. Paper III studies/discusses the effect of storage time on the physicochemical properties of FOs and UCOs. Paper IV describes changes in different metal rod surfaces after exposure to UCOs analyzed using a Scanning Electron Microscopy (SEM). Paper V explores the ability of amino acids to reduce mild steel corrosion in bio-oils.

3.1. Materials

3.1.1. Bio-oils

The composition and properties of fish oils (FOs) and used cooking oils (UCOs) received from VG EcoFuel Oy (Uusikaupunki, Finland) were studied in detail. The company provided the following background information on the bio-oils.

The properties and composition of two waste fish oils (FO1-15 and FO1-18) and six used cooking oils (UCO1-15, UCO2-15, UCO3-15, UCO1-18, UCO2-18, and UCO3-18) were measured and reported in Paper III. The numbers after each sample name FO and UCO refer to the batch and the year of delivery, i.e., for example, FO1-15 means first fish oil sample received in 2015, and UCO1-18 means first used cooking oil sample received in 2018.

Fish oils

The fish oil FO1 (Paper I) had been produced from gutting rests of rainbow trout after extracting fish oil to be used in other products than fuel. FO2 (Paper I) had been extracted from gutting rests stored for some time, and therefore they were naturally aged. FO2 likely contained some formic acid added as a preservative to retard aging. FO3 had been pressed from whole salmon fishes, including bones, and thus contained some phosphorus (Paper I).

Used cooking oils

All the UCOs were produced from vegetable sources. UCO1 (Paper I) was a waste cooking oil from fast food companies and had been filtered and was clear and transparent. UCO2 (Paper I) was waste oil from meat frying. At temperatures below 30°C, the oil separated into a visible white bottom phase (UCO2b) and a clear upper phase (UCO2u). The detailed composition of these two separated phases was analyzed while the physical and chemical properties of the oil were measured for the UCO2 mixture. UCO3 was received from a small-scale used oil recycling (Paper I). The UCOs studied and reported in Papers II, IV-V were received just before the work started.

Reference oils

A commercial oil product (COref) was used as a reference (Papers I-III).

A fresh edible vegetable oil (Keiju from Bunge Finland Oy, Raisio, Finland) and an organic extra virgin olive oil (Pirkka Luomu, Granada, Spain) were used as reference samples in Paper V.

3.1.2. Chemicals

The following chemicals were studied as corrosion inhibitors: tert-butylamine (TBA) and the following amino acids: sulfur-containing L-cysteine and L-methionine, α-amino acid L-glutamic acid, hydroxy-containing aliphatic L-serine, branched aliphatic L-leucine, linear aliphatic L-glycine and L-alanine, heterocyclic L-tyrosine and cationic L-lycine and L-arginine (Papers IV-V).

3.1.3. Steel and copper rods

The following steel and copper rods were used in the immersion tests:

- mild steel (98.64 wt% Fe, 1.00 wt% Mn, 0.21 wt% Si, 0.11 wt% C, 0.03 wt% P, and 0.02 wt% S), i.e., an H44 all-round welding rod with a diameter of 1.6 mm, obtained from Linde (Solna, Sweden) (Papers II, IV-V).
- mild annealed steel (98.79 wt% Fe, 1.0 wt% Mn, 0.15 wt% Si, and 0.06 wt% C) with a diameter of 1.5 mm (Paper IV).
- copper rod (99.9 wt% Cu) with a diameter of 1.0 mm (Paper IV).

Before the experiments, the rods were cut into 85-mm long pieces. The surfaces were first polished with grinding paper Buehler CarbiMetTM, Grit 280 [P320], then with Buehler-Met® II, Silicon Carbide grinding paper, Grit 360 [P600]. The rod ends were polished to a similar visual roughness as the rod surfaces. After polishing, the samples were cleaned ultrasonically using a mixture of toluene and 2-propanol (1:1 v/v) (Papers II, IV-V).

3.2. Experimental Methods

All the experimental parameters are described in detail in the attached original papers (Papers I-V). The standard methods and instruments used to measure the properties of the bio-oils and commercial product are given in Appendix VII.

3.2.1. Immersion test

In Papers II, IV-V, the steel or copper rod immersion tests were carried out at room temperature to investigate the role of bio-oil-induced corrosion. The experiments were performed in test tubes of 15 mL, mounted on a mixer rotated at a constant speed of 56 rpm (Figure 5). The steel or copper rod was placed in 7mL of the oil samples for different periods. After the immersion test, the rods were removed from the oils and cleaned ultrasonically using a mixture (1:1, v:v) of toluene and 2-propanol. Then, the oils were subjected to liquid-liquid extraction using 1 mL of sulfuric acid and 8 mL of deionized water in a test tube,

which was vigorously shaken for 1 min. After the extraction, the mixture was filtered using a quantitative ashless filter paper (Grade No 42, Whatman International Ltd, Maidstone, England), and the filtrate was analyzed spectrophotometrically. Each experiment contained three parallel samples. Further details of the experimental procedures are reported in Papers II, IV-V.

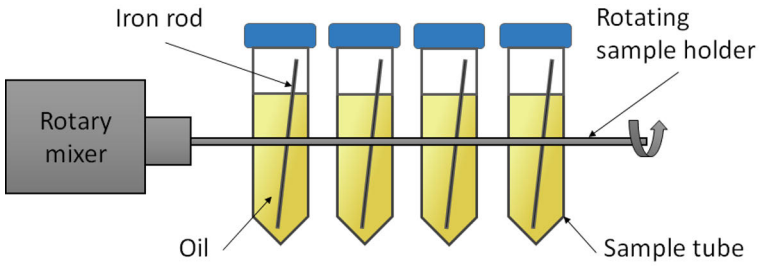

Figure 5. Experimental setup of the immersion test. Adapted from Paper II.

3.2.2. Analysis of iron dissolved in bio-oils

The amount of iron dissolved in oils during the immersions was analyzed in the aqueous phase after the liquid–liquid extraction step using a spectrophotometer (Spectronic Genesys 2PC (Paper II) or (Perkin-Elmer Lambda 25 (Papers IV-V)). Prior to spectrophotometric analysis, the iron in the water solution was reduced to Fe^{2+} with ascorbic acid. The solution was then allowed to react with an excess of ferrozine-reagent to form a magenta-colored complex. A buffer solution containing sodium acetate and acetic acid was used to adjust the pH to 5. The red complex had a maximum absorption peak at 562 nm.

The amount of dissolved iron in oils was also measured using inductively coupled plasma-optical emission spectrometry (ICP-OES, Perkin Elmer Optima 5300 DV) and inductively coupled plasma-mass spectrometry (ICP-MS, PerkinElmer, ELAN 6100 DRC) (Paper II).

3.3. Analytical methods

3.3.1. Characterization of oils

Water content

The water content of the oils was determined with Karl Fischer (KF) titration using an automatic coulometric titrator (Metrohm 851 Titrando instrument) connected to an oven (860 KF Thermoprep). The KF measurements were carried out under a dry nitrogen gas atmosphere with a flow rate of 90 mL/min. The water release of the oil samples was measured at 110°C (Papers I-IV).

Acid number

The acid number (AN), expressing the acidity of the oil, was determined using the ASTM D 664 method. In short, the oil samples were dissolved in toluene,

propan-2-ol, and CO_2-free water (500:495:5, v/v/v) and then titrated with 0.1 M potassium hydroxide (KOH) in propan-2-ol (Merck, Germany) (Papers I-IV).

Oil Composition

Capillary gas chromatography – flame ionization detector (GC–FID) (Perkin Elmer Autosystem XL) was used to quantify the monoglycerides, total (hydrolyzed) fatty acids, free fatty acids, and volatile fatty acids in oils. Individual components were identified using a chromatography–mass spectrometry (GC-MS) with an HP 6890-5973 capillary gas chromatography–mass selective detector (GC-MSD). Di- and triglycerides were analyzed on a wide-bore short column GC-FID (PerkinElmer Clarus 500)(Papers I-IV).

The functional groups of the oil samples were analyzed with a Nicolet iS50 Fourier transform infrared spectroscopy (FTIR) (Nicolet Instrument Corp.) equipped with an iS50 attenuated total reflection (ATR) accessory used together with OMNIC 9 software (Paper I).

Molecular weight distribution

The molecular weight distribution of the oil components was analyzed by high-performance size exclusion chromatography using an evaporative light scattering detector (HPSEC-ELSD, Shimadzu 10A series modular HPLC, Shimadzu Corporation, and ELSD detector, Sedex 85 LT-ELSD, Sedere S.A.)(Paper I-III).

Phosphorus and sulfur contents

Phosphorus and sulfur in the bio-oils were measured using inductively coupled plasma-optical emission spectrometry (ICP-OES, Perkin Elmer Optima 5 300 DV)(Paper I).

Physical properties

The density of all the samples was measured at 21°C using a pycnometer. Dynamic viscosity was measured with a Brookfield digital viscometer Model DV-II at 21°C. Depending on the flowing properties of the oil, the kinematic viscosity was measured using either a Cannon-Fenske (reverse flow) viscometer, capillary 511 20 or 511 13, using the ASTM D 2515 method or an Ostwald viscometer, capillary 509 04, using the ASTM D 445 method, in a thermostatic bath at 40 ± 0.5°C (Papers I-IV).

Thermal properties

The thermal stability of the oil samples was measured using a thermogravimetric analyzer (TGA, TA Instruments Q 600 SDT) (Paper I).

The higher heating values (HHV) of the oils were determined by burning the oil in an adiabatic oxygen-bomb calorimeter (model Parr 1341), according to SFS-EN 14918:2009 (Papers I, III).

3.3.2. Surface characterization techniques

The surface morphologies and the corrosion products were studied with a SEM (LEO Gemini 1530 with a Thermo Scientific Ultra Dry Silicon Drift Detector SDD,

Oberkochen, Baden-Württemberg, Germany) coupled to an elemental X-ray detector (EDS, Energy Dispersive X-Ray Spectroscopy, Thermo Scientific, Madison, WI, USA) (Papers II, IV-V).

Organometallic species at the sample surfaces were identified with Fourier transform infrared spectroscopy (FTIR) using a Perkin-Elmer Spectrum Two™ spectrometer (Perkin-Elmer, Llantrisant, UK) with a spectrum area of 4000–450 cm^{-1} and a resolution of 4 cm^{-1}. The FTIR spectra were interpreted using the spectral analysis function (software KnowItAll Informatics System 2020, John Wiley Sons, Inc., NJ, USA) (Paper V).

4. Results and discussion

4.1. Chemical properties of the bio-oils

The measured physico-chemical properties of the UCOs, FOs, COref, vegetable oil and olive oil are shown in Table 1 and Appendix I-II. The water content of vegetable oil and olive oil were about 600 ppm (Paper V). The lowest water content, 473 ppm, was measured for the fresh fish oil sample, FO1. The water content of the UCOs was between 538–740 ppm, while the measured water content of COref was as low as 37 ppm (Paper I). The water contents of FO1/18 and the UCOs reported in Papers II and IV-V were on a much higher level, 1400–3750 ppm.

The AN of the UCOs, FO1, vegetable oil and olive oil suggested low or negligible corrosion risk (Papers I-V). In contrast, the AN of the naturally aged fish oils FO2, FO3 and FO1/18 was above the limit of 15 mg KOH/g oil set by the engine manufacturer (Paper I-II).

The AN of the FOs and UCOs can be related to their content of free fatty acids. These oils contain high ester groups (-COOR) concentrations, about 150 mg KOH/g oil.

Free fatty acids

The highest unsaturated free fatty acid concentration consisted of the oleic acids (C9-18:1) (Table 2 and Appendix III-IV). Table 1 shows that AN (24.9 mg KOH/g oil) of FO2 is above the limit to be used as fuel. The total FFA of 92.7 mg/g is also high.

Table 1. The physico-chemical properties of FOs, UCOs, COref, vegetable, and olive oils (Paper I-II and IV-V). The Roman numerals in brackets after each sample code indicates the paper numbers where the results are discussed.

Sample	Acid number	Water content	Density 21°C	Kinematic viscosity 40°C	Total FFA	Oleic Acid
	(mg KOH/g oil)	(ppm)	(kg/m^3)	(mm^2/s)	(mg/g)	(mg/g)
FO1(I)	1.7	473	916	31.9	5.9	2.0
FO2(I)	24.9	1070	914	31.6	92.7	38.4
FO3(I)	17.1	1450	914	31.6	71.5	21.7
UCO1(I)	8.9	538	914	40.6	44.8	23.8
UCO2(I)	10.8	706	916	41.3	51.1	27.5/25
UCO3(I)	3.7	740	915	44.3	47	11
COref(I)	0.02	37	873	8.9	-	-
UCO1/18(II)	6.5	1662	916	40.7	29.1	15.2
UCO2/18(II)	8.2	1449	917	40.7	43.3	23.1
UCO3/18(II)	8.1	1403	916	40.3	46.8	24.9
FO1/18(II)	24.8	2473	916	26.6	99.7	42.3
UCO1(IV,V)	6.9	1850	917	39.3	28.4	14.9
UCO2(IV,V)	6.5	1776	917	39.5	28.4	14.8
UCO3(IV,V)	6.9	2180	914	38.7	28.3	16.0
UCO4(IV,V)	7.0	2067	916	39.8	30.0	16.9
UCO5(IV,V)	8.0	2493	917	39.5	32.9	18.7
UCO6(IV,V)	6.7	3748	914	39.4	27.0	15.2
UCO7(IV,V)	6.9	3089	915	39.4	28.0	15.9
UCO8(IV,V)	8.8	2664	915	39.5	37.8	21.7
Vegetable oil(V)	0.1	604	915	35.2	0.5	0.2
Olive oil(V)	0.5	581	910	38.9	0.1	0.4

Table 2. Free fatty acids in oil samples without hydrolysis, measured with GC (mg/g oil) (Paper I).

	FO1	FO2	FO3	UCO1	UCO2u	UCO2b	UCO3
Saturated FA (mg/g oil)							
12:0	3	3	2	3	3	2	3
14:0	16	17	22	2	2	3	2
15:0	1	2	2	n.d.	1	1	n.d.
16:0	74	79	85	87	91	158	72
17:0	1	1	1	1	1	1	1
18:0	22	23	24	23	23	30	24
20:0	3	3	4	6	6	6	6
22:0	2	2	3	3	3	3	4
Unsaturated FA (mg/g oil)							
16:1	24	27	30	2	2	2	4
18:3(1)	7	7	8	n.d.	n.d.	n.d.	n.d.
18:2	152	140	114	166	176	152	182
18:3(2)	52	47	41	50	50	44	51
9-18:1	397	377	338	493	499	437	483
11-18:1	28	30	30	30	29	25	30
cis-5,8,11,14,17-21:5	17	16	29	n.d.	n.d.	n.d.	n.d.
cis-13-21:1	27	32	39	9	8	7	9
5,8,11,14,17-21:5 methyl ester	31	35	40	n.d.	n.d.	n.d.	1
20:5	8	7	12	n.d.	n.d.	n.d.	n.d.
cis-22:1 (1)	16	20	27	n.d.	n.d.	n.d.	n.d.
cis-22:1 (2)	3	4	5	2	1	1	2
Sum saturated FA	121	130	143	124	129	204	112
Sum unsaturated FA	762	744	713	752	765	669	761
Total FA	883	874	856	876	895	873	873
Saturated/Total FA (%)	14	15	17	14	14	23	13
FFA/Total FA (%)	0.7	10.6	8.4	5.1	5.7	5.4	2.5

n.d.= not detected (< 1 mg/g oil)

Table 3 shows the content of all the fats, including triglycerides, diglycerides, and free fatty acids (including monoglycerides) in the fish and used cooking oils measured using HPSEC-ELSD (Appendix V). The highest concentration of

triglycerides, 98.8%, was analyzed in FO1, while FO2 contained the lowest concentration, 81.4%. (Paper I).

Table 3. Main oil component groups in fish and used cooking oils measured with HPSEC-ELSD, given as % of identified compounds (Paper I).

	Free fatty acids*	Diglycerides	Triglycerides	Polymerized triglycerides
FO1	0.7	0.3	98.8	n.d.
FO2	10.3	8.3	81.4	n.d.
FO3	7.3	3.9	88.2	0.5
UCO1	4.2	12.6	77.7	5.6
UCO2u	4.6	13.8	76.0	5.6
UCO2b**	4.4	12.8	78.2	4.6
UCO3	1.7	6.2	87.2	4.8
n.d. = not detected				
*Including monoglycerides				
**Precipitated phase at the bottom				

The UCOs contained about 5% polymerized triglyceride, indicating that the original cooking oils had polymerized during frying. In addition, the share of diglycerides in the UCOs was higher than the share of diglycerides in the FOs, thus also suggesting that the triglycerides had partly degraded during the heating of oils. As explained above, UCO2 had separated into two phases at temperatures below 30°C (Paper I).

The reference oil, COref, was also analyzed using GC–FID. The oil mainly consisted of aliphatic hydrocarbons. The dominating compounds were linear saturated hydrocarbons up to C30, with the largest single compounds in the C14–C26 range.

The FTIR spectra in Figure 6 show the expected strong ester peak around 1743 cm^{-1} (C=O stretching) for FOs and UCOs, while no ester peak was identified for the COref sample. Notably, FO2 and FO3 showed a distinguishable peak around 1712 cm^{-1}, attributable to free fatty acids, in accordance with GC-FID analyses and AN determination. Peaks around 2922 cm^{-1} and 2853 cm^{-1} (C-H stretching) and around 1463 cm^{-1} (C-H bending) appeared in all oil samples, while peaks around 1159 cm^{-1} (C-O stretching) were absent in COref [84–86].

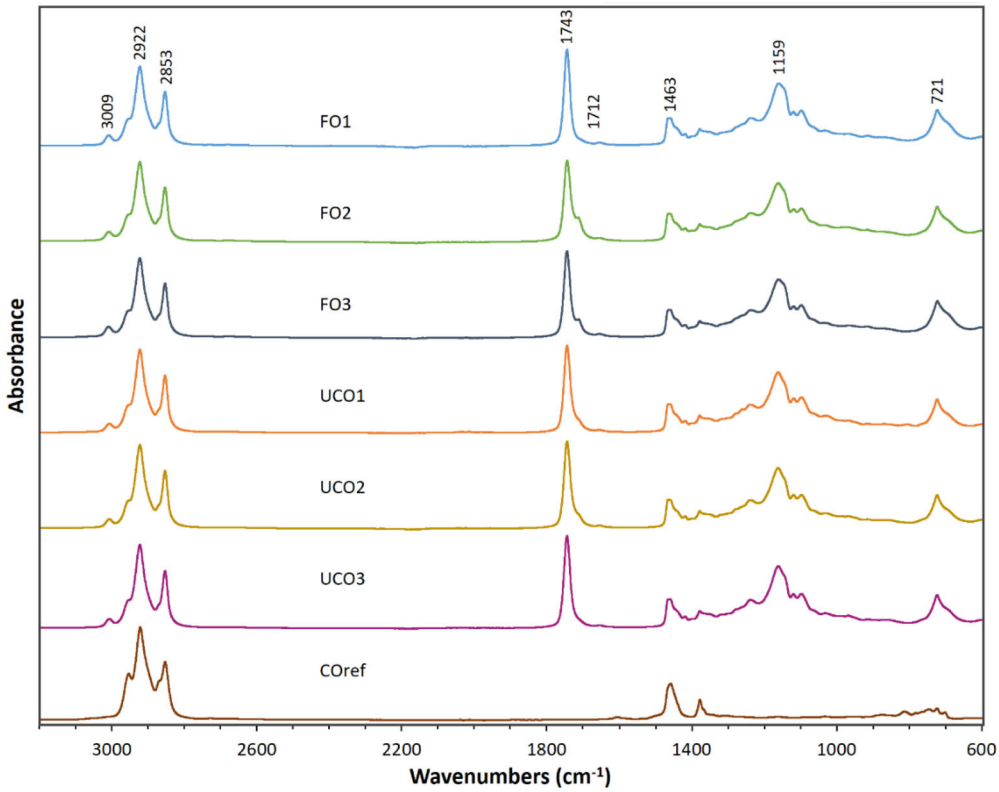

Figure 6. FTIR spectra of FO, UCO, and COref samples (Paper I).

Phosphorus and sulfur

Only FO3 extracted from the whole fish with bones gave a detectable peak of phosphorus corresponding to 28 mg/kg. FO2 and FO3 showed the highest sulfur concentrations, around 50 mg/kg, while the sulfur concentration was below 20 mg/kg for the other samples. The phosphorus concentration of COref was less than 20 mg/kg, and the sulfur concentration was 250 mg/kg. Notably, the sulfur content of COref was higher than in the FOs and UCOs but below the recommended limit (500 mg/kg oil) [34] (Paper I).

4.2. Physical properties

The measured physical properties of importance for fuel applications of the bio-oils are shown in Table 1 and Appendix I-II. The densities of all oils at 21°C were lower than the density of water, 998 kg/m^3. The densities of FOs and UCOs were on the same level, 914–916 kg/m^3, and somewhat higher than the density of the COref, 873 kg/m^3. Finally, all values were clearly lower than the density of heavy fuel oil (940 kg/m^3) [87].

The fuel density affects the dispersion of the fuel injected into the cylinder [88]. Additionally, by increasing the fuel density, more fuel is injected on a mass basis into the engine. It is worth noting that according to the marine diesel engine

manufacturer, the density of the liquid biofuel should be lower than 991 kg/m^3 for 4-stroke engines [67].

The fish oils had lower kinematic viscosity at 40°C than the used cooking oils. The values were highest for the used cooking oils (around 40 mm^2/s), followed by the fish oils (32 mm^2/s), while the viscosity of the COref was lowest (9 mm^2/s). The higher viscosity of the UCOs compared to the other oils was assumed to be due to the nature of the oil and the presence of some impurities like starch, polymerized triglycerides, and meat traces in UCOs (Papers I-IV).

4.3. Thermal properties

The thermal stability of the oils was studied with TGA. The weight change of FO1 and UCO2 as a function of the temperature is shown in Figure 7. In addition, the weight change of COref is given. The TGA curves correlate with the release of the higher molecular weight components present (non-volatile fatty acids and triglycerides) in FO1 and UCO2, and the aliphatic hydrocarbons in COref.

The initial thermal degradation of FO1 and UCO2 started around 200°C. The degradation of UCO2 was slightly faster than that of FO1, and above 360°C, the degradation of both oils was significant. Finally, the oils had degraded approximately at 400°C. The COref started to decompose below 200°C. Already at 300°C, the degradation was completed. The TGA curves suggest that no char formed during the decomposition reactions (Paper I).

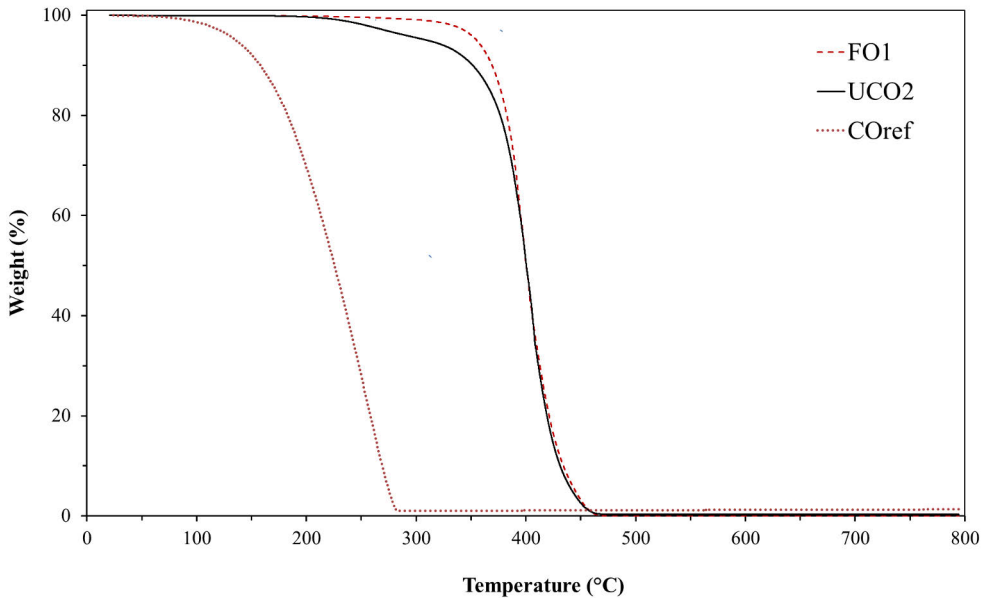

Figure 7. Thermal degradation of the oils - FO1, UCO2, and COref in a nitrogen atmosphere (Paper I).

4.4. Effect of storage

Figure 8 shows the changes in the acid number of the oils when stored in the refrigerator for two or five years. For all but one UCO, the acid number increased. However, the acid number did not increase beyond the limiting value for marine engines for any of the UCOs and FO1-15 (Paper III). As already mentioned in chapter 4.1 the naturally aged FO1-18 was above the limit of 15 mg KOH/g oil set by the engine manufacturer (Paper I-II).

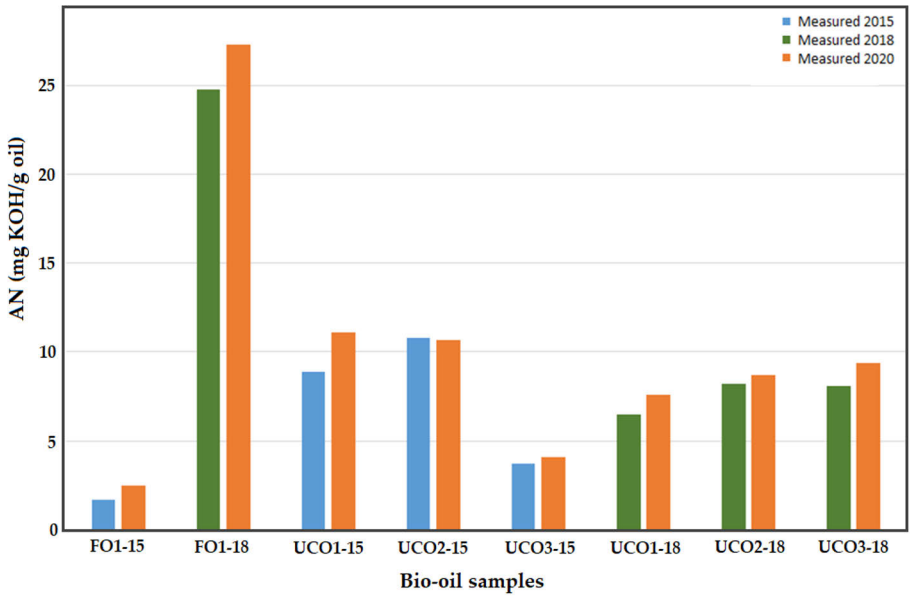

Figure 8. The acid numbers for bio-oils in 2015, 2018, and 2020 (Paper III).

The presence of water in bio-oil decreases the heating value. In addition, water in oil might induce corrosion of the equipment and containers during the storage and use of the oil [83]. When using bio-oils with relatively high water contents in marine engines, the possibility of water accumulation in tanks must be considered and remedied by careful dewatering.

In general, the amount of ester groups shows the potential to provide fatty acid methyl esters (FAME) in the transesterification process when biodiesel is produced. Therefore, the fish and used cooking oils containing high concentrations of compounds with ester groups have good potential to be converted into biodiesel using a transesterification process (Paper I). The content of oleic acids in different cooking oils in this work varied considerably depending on the oil origin, thus making comparisons with different oils relevant only if their detailed composition is available (Papers I). For example, comparing the fatty acid contents in FO2 before and after storing suggest that triglycerides in FO2 had degraded during storing to di- and monoglycerides due to natural aging or acid hydrolysis (Paper I).

The density of the fuel affects the dispersion of the fuel injected into the cylinder [88]. Additionally, by increasing the fuel density, more fuel is injected on a mass basis to the engine. The engines are designed based on their optimum yields; for instance, the lower the density, the better the atomization and mixture formation achieved; however, the higher the density, the better penetration in the combustion chamber [88]. As the densities of the studied bio-oils are in between the values for the heavy fuel oil and the commercial reference oil, no engine modifications due to density values would be needed if the FOs and UCOs were used in marine engines. It is worth noting that according to a manufacturer of marine diesel engines, the density of the liquid biofuel should be lower than 991 kg/m^3 for four-stroke engines [34]. The viscosity of the engine fuel plays a dominant role during spraying the fuel into the chamber or mixing it with other fuels [89]. Additionally, high viscosity in bio-oil causes high operating temperature leading to fuel boiling in injection pumps. Therefore, a very high viscosity (> 100 mm2/s) is not desirable for bio-oils [32]. The higher viscosities of the bio-oils compared to COref must be compensated, for example, by changes in the fuel delivery system to the engine when replacing the fuel [33]. The TGA curves correlated with the release of the higher molecular weight components present (non-volatile fatty acids and triglycerides) in FO1 and UCO2 as well as the aliphatic hydrocarbons in COref. The TGA curves suggested that no char formed during the decomposition reactions (Paper I).

4.5. Steel and copper rod surfaces exposed to bio-oils

4.5.1. Iron dissolved in oils

The effect of the immersion time on the concentration of iron dissolved from mild steel rods into the oils was studied for up to ten days. As shown in Figure 9, the amount of iron in UCOs increased with immersion time (Appendix VI). At ten days, the highest iron content was analyzed in UCO1/18 and UCO2/18. On the other hand, iron concentration in UCO3/18 and COref showed no significant change after one day of immersion. The highest dissolved iron concentration (170 ppm) was measured in FO1/18 at five days. However, the iron content was lower at higher time points. The relatively high dissolved iron concentration in the fish oil at all time points could be attributed to the chemical properties of the oil, i.e., the high water content and AN (see Table 1). Water content and acid number are known to increase the corrosivity of the oils (Paper II).

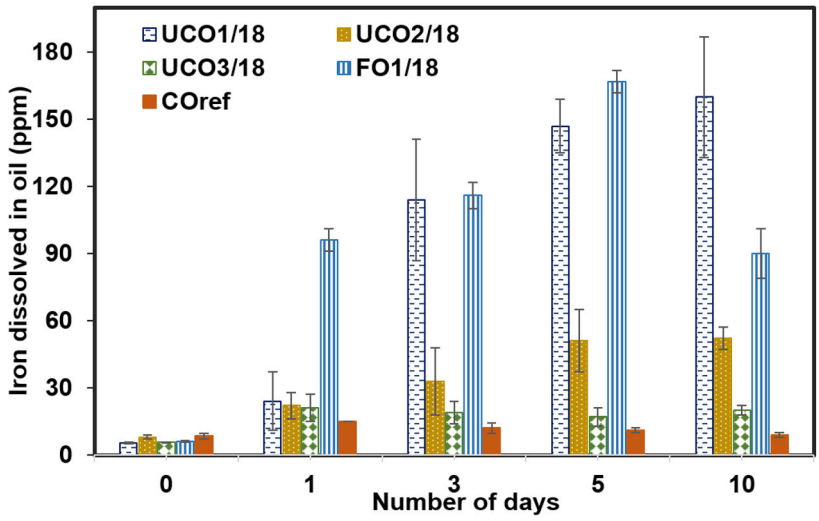

Figure 9. The effect of immersion time on the concentration of iron dissolved from the mild steel rods into the oils (Paper II).

Iron concentration dissolved from the unpolished reference mild steel rod surfaces into UCO2 increased during the test from 58 ppm (1 d), 84 ppm (3 d), 308 ppm (5 d) to 370 ppm (10 d) (see Figure 10 and Appendix VI). The values are averages of three parallel samples. For polished mild steel rod, the iron concentration in UCO2 first increased to 406 ppm (5 d) but then decreased to 351 ppm at 10 days. A similar increasing trend during the five first days followed by a lower concentration at 10 days was measured for mild annealed polished steel rods in UCO2. In general, lower ion concentrations were measured for the mild annealed steel rods than for the polished mild steel rods. For the polished samples, the iron concentration increased up to five days, after which the concentration started slowly decreasing. The decrease suggested the formation of iron-containing precipitates. This was, however, not verified. Unlike the polished samples, iron continued dissolving from the untreated mild steel rod, probably because the dissolved iron concentration did not reach saturation during the experiment. No precipitates could be verified on the rod surfaces nor in oils (Paper IV). Cu ion concentration dissolved from polished copper rod into UCO2 was 14 ppm after 1 d but increased to 25.9 ± 0.7 ppm (3–10 d) (Paper IV). The copper rods withstood corrosion in UCO2 much better than the mild steel rods. Hu et al. [92] reported that the effects of biodiesel induced corrosion of copper and carbon steel, while stainless steel showed good resistance in two-month immersion tests at 43 °C. Fazal et al. [61] found that copper was a strong catalyst for oxidizing palm biodiesel.

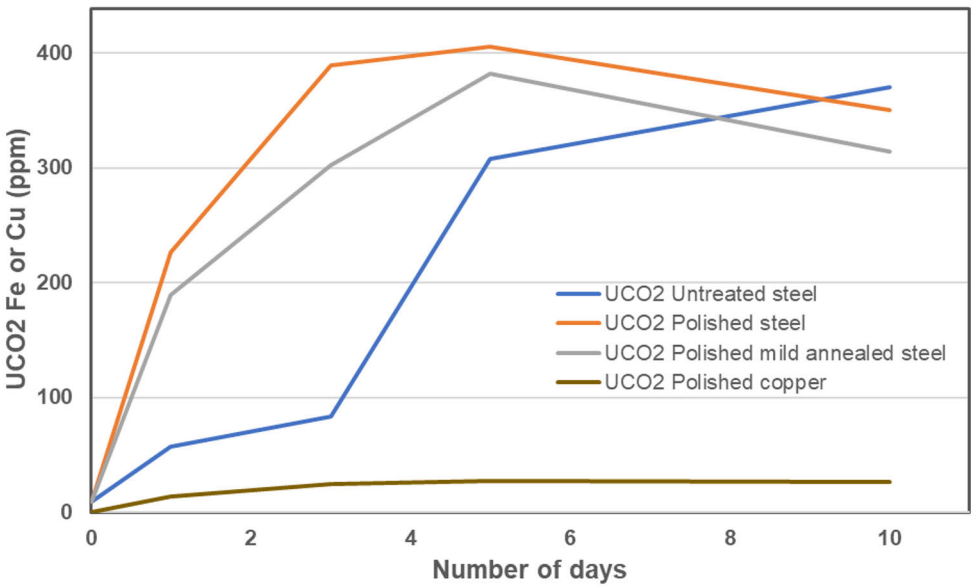

Figure 10. Changes in iron and copper concentrations dissolved from untreated and polished mild steel rods, polished mild annealed steel rods, and polished copper rods into UCO2 as a function of exposure time. The total error for the measured values is 3% (Paper IV).

The more corrosive UCO2 was mixed with the low corrosive UCO4 in ratios of 9:1, 8:2, 7:3, and 1:1. Figure 11 shows the iron concentrations dissolved in oils after immersion of polished mild steel rods for 3 d. For UCO2, the average dissolved iron concentration was 277 ppm. As mixtures with decreasing UCO2 content were tested, the iron concentration in the oil also decreased. Thus, the corrosive properties gradually decreased by adding the low corrosive UCO4 to the very corrosive UCO2. This suggests that the corrosive properties of UCOs might be decreased by mixing oils from different sources (Paper IV). However, it would be relevant to understand which component in the oil provides corrosion protection.

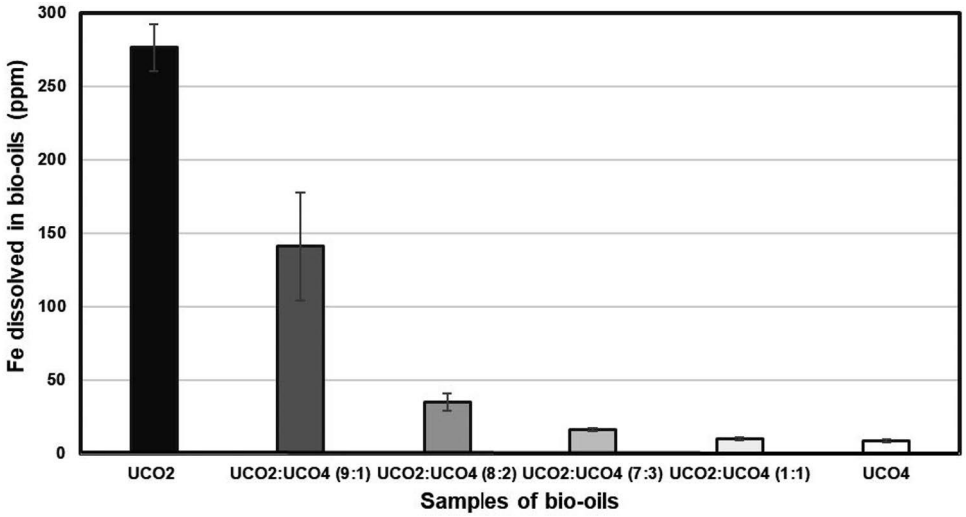

Figure 11. Iron concentration dissolved from polished mild steel rods into various mixtures of UCO2 and UCO4 (Paper IV).

The effect of oleic acid and glycerol additions in UCO1/18 and UCO3/18 on the dissolved iron concentration from mild steel rods was measured after three days of immersion (Figure 12). The concentrations of oleic acid (21 mg/g oil) and glycerol (2.31 mg/g oil) were calculated to give 50 mg/g of free fatty acids in oils. In addition, the combined effect of oleic acid and glycerol (3:1 molar ratio) on the dissolved iron concentration in the UCOs was investigated. According to Figure 12, oleic acid reduced the dissolved iron concentration in the UCOs by 57%. The acid number of the UCOs increased by almost 50% due to the oleic acid addition. However, much less iron was dissolved in oils. Active surface groups in oleic acid were assumed to have formed a protective film layer at the surface of the mild steel rod, thus suppressing the corrosion (Paper II).

The addition of glycerol showed a more profound effect than oleic acid, resulting in a 92% and 63% reduction in dissolved iron in UCO1/18 and UCO3/18, respectively (Figure 12). The combined effect of oleic acid and glycerol resulted in iron levels similar to those obtained with glycerol only. Besides its binding effect on water molecules, glycerol can form microemulsion in the presence of a surfactant such as oleic acid [55]. Both oleic acid and glycerol considerably reduced the amount of iron dissolved in the oil phase. However, a more predominant effect was observed with glycerol than oleic acid when protecting the mild steel rod from corrosion (Paper II).

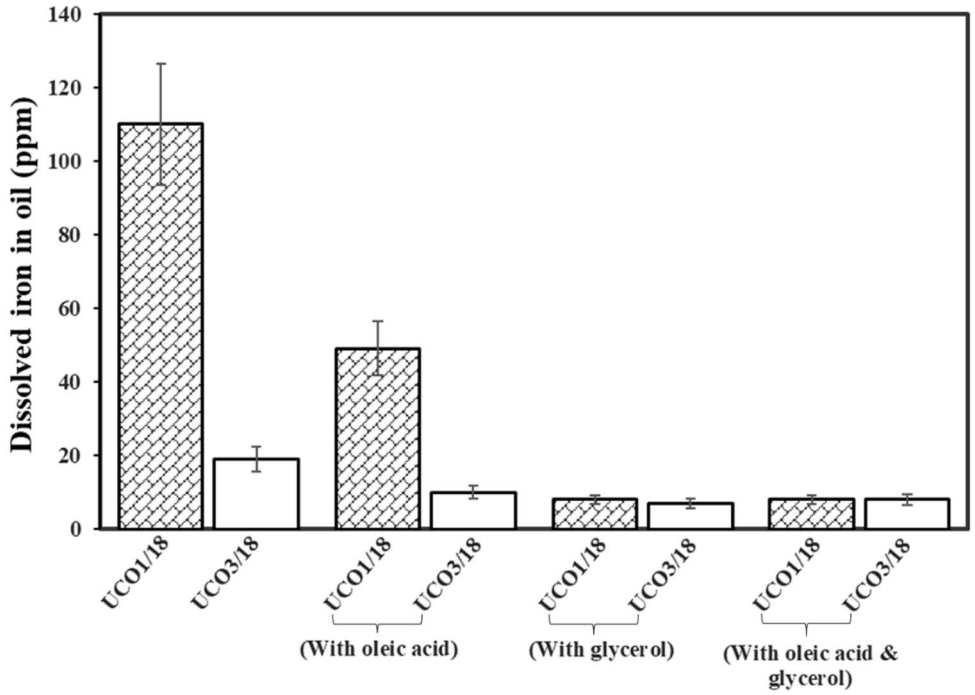

Figure 12. The effect of oleic acid and glycerol additions on the dissolved iron concentration in UCO1/18 and UCO3/18 after three days (Paper II).

The effect of several potential corrosion inhibitor additions in UCO2 was tested using polished mild steel rods. During the three-day test 310 ppm iron dissolved in UCO2 without any inhibitor. Adding 0.025 wt% TBA into UCO2, decreased the iron concentration to 9 ppm (Paper IV and Appendix VI). Inhibitors ethylenediamine, TBA, or n-butylamine form a stable metal oxide protective layer and thus inhibit the corrosion in biodiesel [75]. It should be noted that TBA is classified as an acutely toxic substance, thus limiting its utilization.

Figure 13 shows iron concentration after immersion of the mild steel rods in UCO2 with various amino acid concentrations. Although significant differences were measured between the corrosion-inhibiting effects, all amino acids decreased the amount of iron dissolved during the three-day immersion. These results are in accordance with the published results of utilizing amino acids and their derivatives to prevent corrosion of metals and alloys in aqueous media [66,81]. The best corrosion inhibition was achieved with the cationic acids L-lycine and L-arginine. Low concentrations of these two amino acids almost totally inhibited the corrosion.

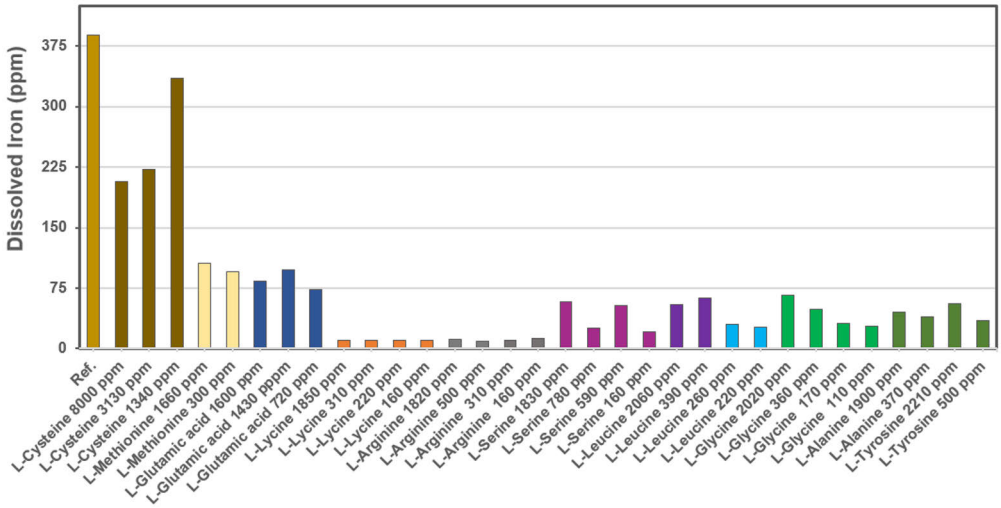

Figure 13. Iron dissolved (ppm) from the mild steel rods during 3d immersion in UCO2 without and with different additions of amino acids (Paper IV).

UCO batches with more than 3000 ppm water (UCO6 and UCO7 in Table 1) dissolved more iron than UCO2 with 1800 ppm water. Whether L-lycine and L-arginine were effective also in the presence of higher water content was tested by adding water to UCO2 and its mixtures with the two amino acids. Table 4 gives the water and amino acid contents in UCO2 and the measured average Fe concentration of three parallel samples with each UCO2 mixture. The corrosivity of UCO2 increased with the water content. As indicated by the small amounts of dissolved iron in Table 4, both L-lycine and L-arginine effectively inhibited corrosion by the oil with higher water contents.

Table 4. Impact of water, L-lycine, and L-arginine content (ppm) in UCO2 on iron released from the mild steel rod during the three-day immersion test (Paper V).

Chemicals in UCO2 (ppm)			Dissolved Fe
H_2O	L-lycine	L-arginine	(ppm)
1800			490
5500			530
4200	430		10
3400		380	10

The corrosion inhibiting effects of L-lycine on mild steel corrosion was also tested in the presence of water and a carboxylic acid (formic or propionic acid) in UCO6 and UCO7 (Paper V).

After three days, the iron concentration in UCO6 without additives was 450 ppm. However, in the presence of formic acid and added water, the iron content

was lower, around 230 ppm. After immersion in UCO6 containing formic acid and added water, the iron content was lower, around 230 ppm. Adding 300 ppm L-lycine to the UCO6 mixture with formic acid and water slightly decreased the iron content to 180 ppm. Similar trends were also seen in UCO7, i.e., the iron content in the oil decreased from 570 ppm (no additives) to 190 ppm (formic acid and water) and further to 140 ppm (formic acid, water and L-lycine).

Immersion of mild steel for up to 10 days showed that the chemical properties of the bio-oil, i.e., water content and AN, increased the corrosivity (Paper I). Less iron dissolved from polished mild annealed steel rods than polished mild steel rods into UCO2. The iron concentration increased during the five first days but then decreased slowly. The decrease suggested precipitation of iron-containing species. However, no precipitates could be verified on the rod surfaces or in oils (Paper IV).

As expected, copper rods corroded much less than mild steel rods during immersion in UCO2 (Paper IV).

Mixing UCO4, a low corrosive oil, with a very corrosive UCO2 oil decreased the corrosive properties of the mixture. Thus, blending different batches might minimize the corrosive properties of UCOs. It should be pointed out that whether a particular component in the UCO provides corrosion protection could not be verified in this work (Paper IV).

In general, corrosion of the mild steel rod was suppressed by oleic acid and glycerol. The surface-active groups in oleic acid were assumed form a protective layer at the surface of mild steel rod (Paper II).

4.5.2 Steel appearance after oil exposure

SEM secondary electron images of the polished rods (Fig. 14b and c) showed steep scratches on the surfaces. After oil immersion, the surface morphologies had changed, thus suggesting corrosion, as also indicated by the increased iron concentrations in the oil (Fig. 14 d-f) (Paper IV). This agrees with the measured ion concentration in the oil after the exposure (Paper IV). The SEM secondary electron images in Figure 15 show that corrosion on the steel rod surface after three days of exposure to UCO2 can be seen, but when UCO4 was tested, a very smooth surface with low corrosion was noticed. Figure 16 shows SEM secondary electron images of polished mild steel rod surfaces after immersion in UCO2 with the different amino acids. The immersion affected the surface morphology of the rods for all other UCO2 additives but L-lycine and L-arginine. Thus, the images suggest only minor corrosion, further supported by low iron concentrations in UCO2, around 10 ppm Fe with L-lycine and 12 ppm Fe with L-arginine (Paper V). The SEM images in Figures 16 and 17 do not explain the corrosion inhibition mechanism induced by the amino acids. According to Rafiquee et al. [90], the inhibitive effect occurs when the inhibitors adsorb on the mild steel surface, thereby decreasing corrosion.

The SEM images of the steel surface after immersion in UCOs with additions of formic acid (10,000 ppm), water (10,000 ppm), and L-lycine (300 ppm) show a surface layer of large (>10 μm) particles (Figure 18). The surface layer

structure is similar to that reported by Rafiquee et al. [90] for mild steel after being in contact with a 20% formic acid solution.

SEM-EDS analysis suggested that the layer consisted mainly of carbon and oxygen, with some iron and manganese. The layer was removed from the rod surface and analyzed by FTIR. The results suggest that the layer consisted of formic acid and iron salt (Paper V).

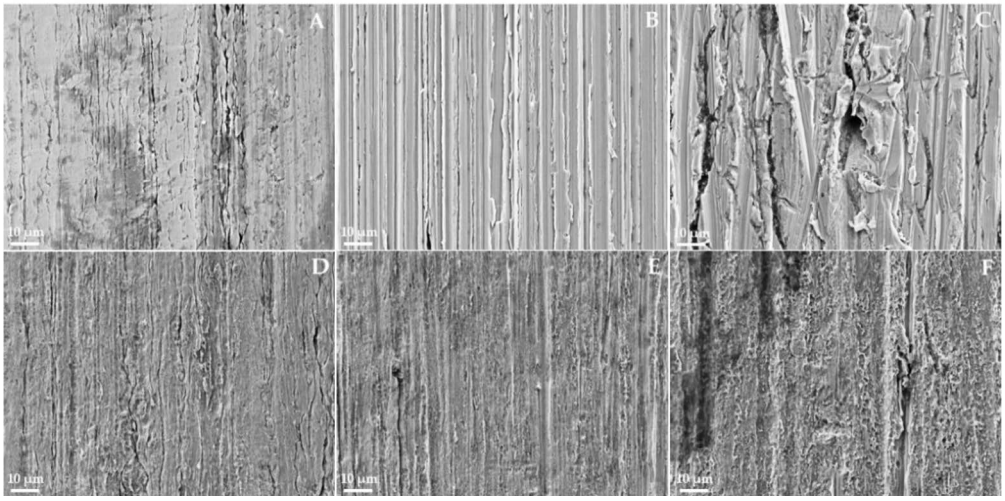

Figure 14. SEM images before oil exposure of (A) untreated mild steel, (B) polished mild steel, and (C) polished mild annealed steel. SEM images after 10 days of exposure to UCO2 (D) untreated mild steel, (E) polished mild steel, and (F) polished mild annealed steel (Paper IV).

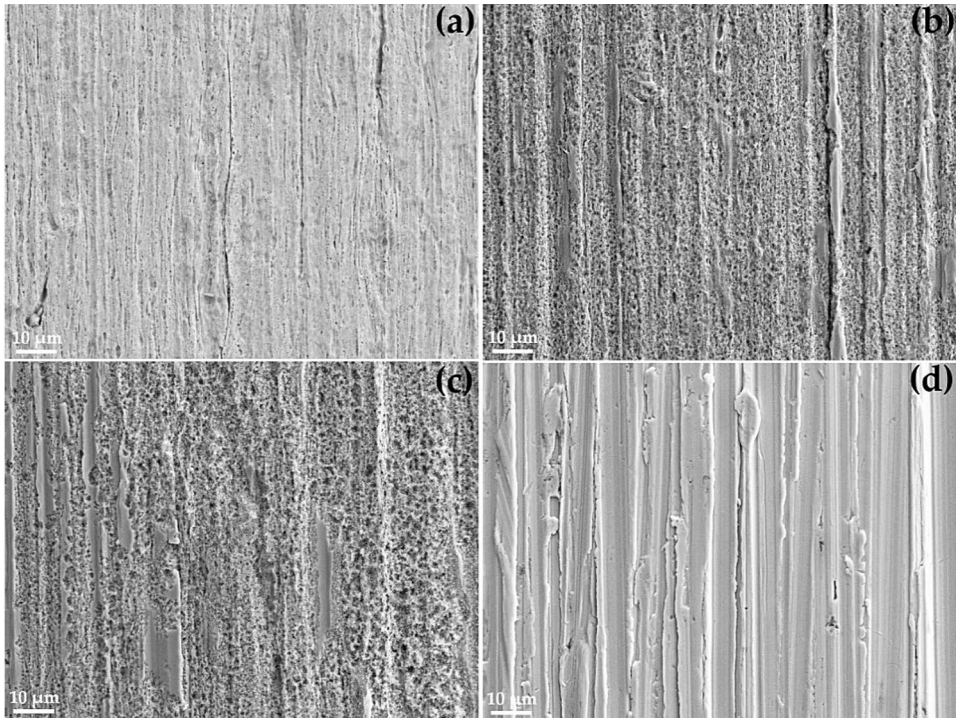

Figure 15. SEM secondary electron images of polished mild steel rod surfaces after 3 days of exposure to: (a) UCO2, (b) UCO2:UCO4 (9:1), (c) UCO2:UCO4 (8:2), and (d) UCO4 (Paper IV).

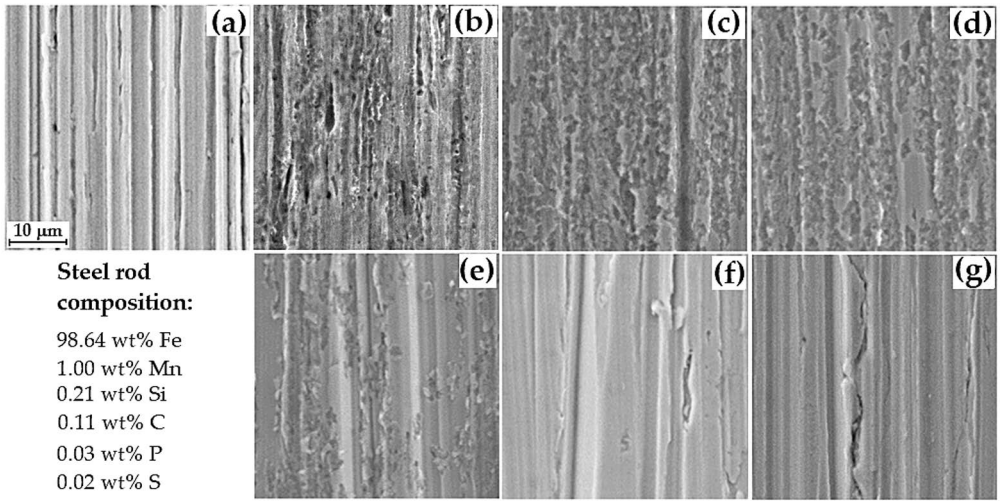

Figure 16. SEM images of polished mild steel surface exposed to UCO2 and amino acid additives: (a) before exposure, (b) after exposure without any additive, (c) with 300 ppm L-methionine, (d) 720 ppm L-glutamic acid, (e) 220 ppm L-leucine, (f) 160 ppm L-lycine, (g) 160 ppm L-arginine. All images have the same magnification (Paper V).

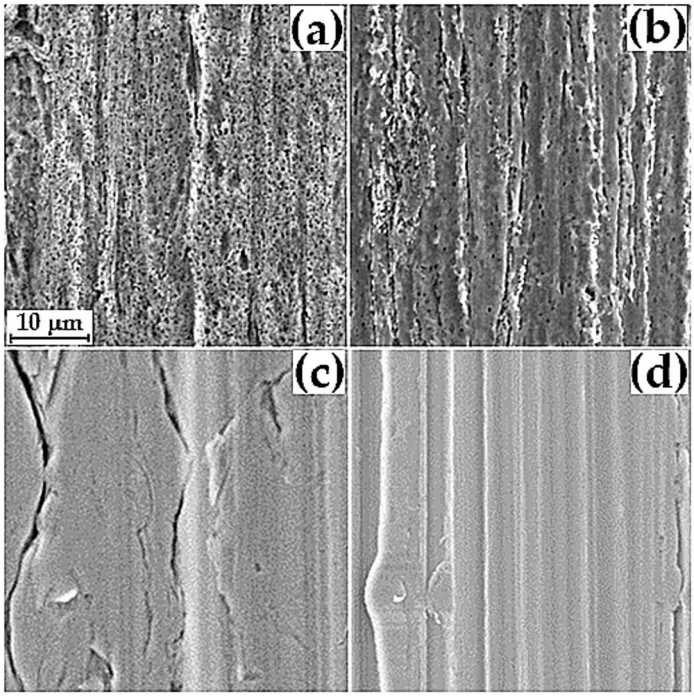

Figure 17. SEM secondary electron images of mild steel rod surfaces after immersion in UCO2 with (a) no additives, 1800 ppm water, (b) 5500 ppm water, (c) L-lycine 430 ppm+ 4200 ppm water, and (d) L-arginine 380 ppm+ 3400 ppm water. The magnification is the same for all images (Paper V).

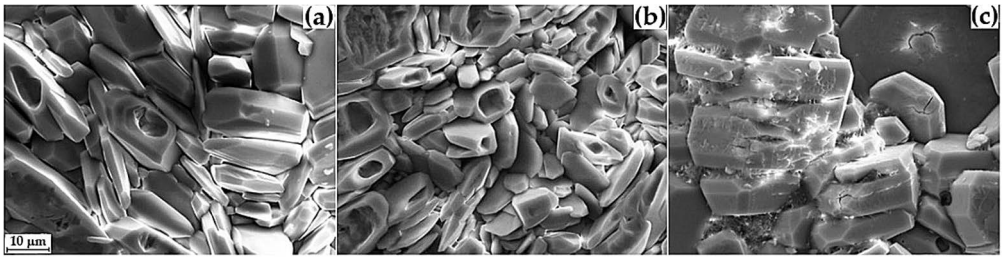

Figure 18. SEM images of rod surfaces after immersion in oils with formic acid (10,000 ppm), water (10,000 ppm), and L-lycine (300 ppm): (a) UCO6, (b) UCO7, and (c) UCO8. The magnification is the same for all images (Paper V).

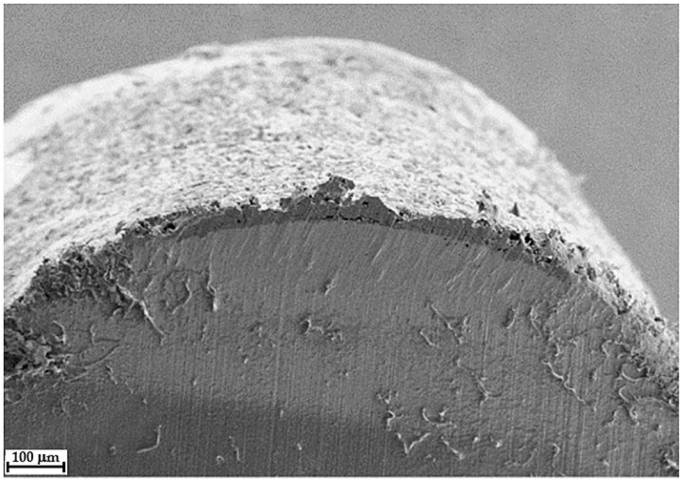

Figure 19. SEM image of rod surface layer after 3 days in UCO6 + formic acid, water, and L-lycine (Paper V).

5. Conclusions

The properties and chemical composition of bio-oils derived from waste sources were explored with respect to their utilization as fuels in marine engines. The properties of the locally produced bio-oils were compared to commercial oil and typical values for heavy fuel oils. Detailed analysis of various physicochemical properties of the bio-oils suggested their potential as carbon dioxide neutral fuels in marine engines. In general, the physicochemical and thermal properties of the bio-oils correlated with their contents of different fats. The acid number was relatively high and slightly increased with the aging of the bio-oils, likely due to the conversion of unsaturated fatty acids. The concentrations of phosphorus and sulfur in the bio-oils were below the limits specified for oils in marine engines. The bio-oils decomposed at higher temperatures than the commercial reference oil. Also, the bio-oils had lower heat content than the commercial oil. These thermal properties might affect the utilization of the bio-oils in conditions where more effect is needed.

The impact of bio-oils on steel or copper rod corrosion was studied at room temperature. The iron content dissolved into the oils markedly varied depending on the oil sample. The steel or copper rod immersion tests were reliable and cost-effective for comparing the corrosive properties of bio-oils. Water content, acid number, and the overall oil composition substantially affected the corrosive behavior of the oils. The acid number did not have as strong a correlation as the water content on the corrosion. Interestingly, the oils with the highest acid numbers contained the highest concentrations of unsaturated free fatty acids, such as oleic acid. The unsaturated free fatty acids were assumed to form a protective layer on the rods, thereby preventing the permeation of oxygen and water to the metal surface. Mixing a corrosive oil with a non-corrosive oil led to a marked decrease in the dissolved iron concentration. Thus, mixing bio-oils containing high concentrations of unsaturated free fatty acids with corrosive oils might prevent corrosion of fuel tanks and engines.

Adding oleic acid and glycerol to used cooking oils decreased the iron dissolution. Glycerol showed a more profound effect than oleic acid, resulting in up to a 92% reduction in the amount of dissolved iron in used cooking oils. Amino acids L-lycine and L-arginine showed noticeable corrosion inhibition effects, even at low concentrations in used cooking oil. More importantly, corrosion inhibition was maintained even after adding water to the oil. Short-chained carboxylic acids formic and propionic acid slightly decreased the corrosivity of the oils. The improved corrosion resistance was assumed to be due to a thin carboxylic acid layer formed on the steel surface. However, the simultaneous presence of water and carboxylic acids led to corrosion of the steel rods. Furthermore, neither L-lycine nor L-arginine provided any notable/special corrosion protection in the presence of both water and carboxylic acid. This suggests that used cooking oils contaminated with water and containing short-chained carboxylic acids increase the corrosion of mild steel. This should be considered when selecting the materials for oil storage vessels.

The information gained in this study not only helps the bio-oil producers to refine their oil to meet engine requirements but also aids the engine designers in adjusting the engines for future renewable fuels. Overall results indicate that the bio-oils may be a sustainable, locally sourced alternative fuel.

6. References

1. Adeoti, I.A.; Hawboldt, K. A review of lipid extraction from fish processing byproduct for use as a biofuel. Biomass Bioenergy 2014, 63, 330–40.
2. Westbrook C.K. Biofuels Combustion. Annu. Rev. Phys. Chem. 2013, 64, 201–219.
3. Kalligeros, S.; Zannikos, F.; Stournas, S.; Lois, E.; Anastopoulos, G.; Teas, Ch.; Sakellaropoulos, F. An investigation of using biodiesel/marine diesel blends on the performance of a stationary diesel engine. Biomass Bioenergy 2003, 24, 141–149.
4. Ma, F.; Hanna, M.A. Biodiesel production. A review. Bioresour. Technol. 1999, 70, 1–15.
5. Daggett, D.; Hadaller, O.; Hendricks, R.; Walther, R. Alternative Fuels and Their Potential Impact on Aviation. Technical Memorandum; NASA/TM-2006-214365. NASA: Cleveland, OH, USA, 2006.
6. Preto, F.; Zhang, F.; Wang, J. A study on using fish oil as an alternate fuel for conventional combustors. Fuel 2008, 87, 2258–2268.
7. Ushakov, S.; Valland, H.; Aesoy, V. Combustion and emissions characteristics of fish oil fuel in a heavy duty diesel engine. Energy Convers. Manage. 2013, 65, 228–238.
8. Bruun, N.; Tesfaye, F.; Hemming, J.; Dirbeba, M.J.; Hupa, L. Effect of storage time on the physicochemical properties of waste fish oils and used cooking vegetable oils. Energies 2021, 14, 101.
9. Mannekote, J.K.; Kailas, S.V. The effect of oxidation on the tribological performance of few vegetable oils. J. Mater. Res. Technol. 2012, 1, 91–95.
10. The Explorer. How the Circular Economy is Changing Business. Available online: https://www.theexplorer.no/stories/renewable-resources/an-introduction-to-the-circular-economy/?gclid=CjwKCAjwxZqSBhAHEiwASr9n9AEz9swG6tiXEDvFuMZppbh2MvreAmOImWb-eIC84NEhDIZq1aGc7hoCSxEQAvD_BwE (accessed on 12 March 2022).
11. Steigers, J.A. Demonstrating the use of fish oil as fuel in a large stationary diesel engine. In Advances in Seafood Byproducts: 2002 Conference Proceedings, Proceedings of the 2nd International Seafood Byproduct Conference, Anchorage, AK, USA, 10–13 November 2002; Bechtel, P.J. Ed.; Alaska Sea Grant College Program: Fairbanks, AK, USA, 2003; pp. 187–199.
12. Ward, O.P.; Singh, A. Omega-3/6 fatty acids: Alternative sources of production. Process Biochem. 2005, 40, 3627–3652.
13. Jafari, S.M.; Assadpoor, E.; Bhandari, B.; He, Y. Nano-particle encapsulation of fish oil by spray drying. Food Res. Int. 2008, 41, 172–183.
14. Boran, G.; Karacam, H.; Boran, M. Changes in the quality of fish oils due to storage temperature and time. Food Chemistry 2006, 98, 693–698.
15. Lligadas, G.; Ronda, J.C.; Galia, M.; Cadiz, V. Renewable polymeric materials from vegetable oils: a perspective. Mater. Today. 2013, 6, 337–343.
16. Biermann, U.; Bornscheuer, U.; Meier, M.A.R.; Metzger, J.O.; Schäfer, H.J. Oils and fats as renewable raw materials in chemistry. Angew. Chem. Int. Ed. 2011, 50, 3854–3871.

17. Giannelos, P.N.; Zannikos, F.; Stournas, S.; Lois, E.; Anastopoulos, G. Tobacco seed as an alternative diesel fuel: physical and chemical properties. Ind. Crops Prod. 2002, 16, 1–9.
18. Santos, J.C.O.; Santos, I.M.G.; Souza, A.G. Effect of heating and cooling on rheological parameters of edible vegetable oils. J. Food Eng. 2005, 67, 401–405.
19. Di Pietro, M.E.; Mannu, A.; Mele, A. NMR determination of free acids in vegetable oils. Processes 2020, 8, 410.
20. Kulkarni, M.G.; Dalai, A.K. Waste cooking oil—An economical source for biodiesel: A review. Ind. Eng. Chem. Res. 2006, 45, 2901–2913.
21. Talbot, G. The stability and shelf life of fats and oils. In The Stability and Shelf Life of Food, 2nd ed.; Subramaniam, P., Ed.; Elsevier: Amsterdam, The Netherlands, 2016; pp. 461–503.
22. Marmesat, S.; Rodrigues, E.; Velasco, J.; Dobarganes, C. Quality of used frying fats and oils: Comparison of rapid tests based on chemical and physical oil properties. Int. J. Food Sci. Technol. 2007, 42, 601–608.
23. Totani, N.; Yawata, M.; Mori, T.; Hammond, E.G. Oxygen content and oxidation in frying oil. J. Oleo Sci. 2013, 62, 989–995.
24. Gnanasekaran, D. Green fluids from vegetable oil: Power plant. In Vegetable Oil based Bio-lubricants and Transformer Fluids: Applications in Power Plants; Gnanasekaran, D., Chavidi, V.P., Eds.; Springer Nature: Singapore, 2018; pp. 3–26.
25. Zhang, Y.; Dube, M.A.; McLean, D.D.; Kates, M. Biodiesel production from waste cooking oil: 1. Process design and technological assessment. Bioresour.Technol. 2003, 89, 1–16.
26. Corsini, A.; Marchegiani, A.; Rispoli, F.; Sciulli, F.; Venturini, P. Vegetable oils as fuels in diesel engine. Engine performance and emissions. Energy Procedia 2015, 81, 942–949.
27. Munoz, R.A.A.; Fernandes, D.M.; Santos, D.Q.; Barbosa, T.G.G.; Sousa, R.M.F. Biodiesel: Production, characterization, metallic corrosion and analytical methods for contaminants. In Biodiesel: Feedstocks, Production and Applications; Fang, Z., Ed.; IntechOpen: London, UK, 2012; pp. 129–176.
28. Johnston, P.A.; Brown, R.C. Evaluation of bio-oil corrosion characteristics. In Sustainable engineering forum: Core programming topic at the 2012 AIChE annual meeting, Proceedings of the 2012 AIChE Annual Meeting, Pittsburg, PA, USA, 28 October–2 November 2012; AIChE: New York, NY, USA, 2013; p. 952.
29. Hau, J.L.; Yepez, O.J.; Torres, L.H.; Vera, J.R. Measuring naphthenic acid corrosion potential with the Fe powder test. Rev. Metal. 2003, 39, 116–123.
30. Moirangthem, K. Alternative Fuel for Marine and Inland Waterways: An Exploratory Study; European Commission JRC: Luxembourg, 2016; pp. 1–44.
31. European Commission (EC). Reducing Emissions from the Shipping Sector. Available online: https://ec.europa.eu/clima/policies/transport/shipping_en (accessed on 7 December 2020).
32. Ollus, R.; Juoperi, K. Alternative fuels experiences for medium-speed diesel engines. In 25th CIMAC World Congress 2007, Proceedings of the 25th CIMAC World Congress on Combustion Engines, Vienna, Austria, 21–24 May 2007; CIMAC: Frankfurt, Austria, 2007; pp. 538–552.

33. Opdal, O.A.; Hojem, J.F. Biofuels in Ships: A Project Report and Feasibility Study into the Use of Biofuels in the Norwegian Domestic Fleet; Zero Emission Resource Organisation: Oslo, Norway, 2007.
34. Juoperi, K.; Ollus, R. Alternative fuels for medium-speed diesel engines. Wärtsilä Technical Journal 2008, 1, 24–28.
35. El-Hamidi, M.; Zaher, F.A. Production of vegetable oils in the world and in Egypt: an overview. Bulletin of the National Research Centre 2018, 42, 19.
36. USDA Foreign Agricultural Service, Oilseeds: World Markets and Trade. Available online:https://downloads.usda.library.cornell.edu/usda-esmis/files/tx31qh68h/0c484n813/6d5712933/oilseeds.pdf (accessed on 14 April 2022).
37. Ribau, M.; Nogueira, R.; Nunes, L.M. Quantitative assessment of the valorisation of used cooking oils in 23 countries. Waste Manag. 2018, 78, 611–620.
38. Orjuela, A. Industrial Oleochemicals from Used Cooking Oils (UCOs): Sustainability Benefits and Challenges. In Advances in Carbon Management Technologies: Biomass Utilization, Manufacturing, and Electricity Management; Sikdar, S.K., Princiotta, F., Eds.; CRC: Boca Raton, FL, USA, 2021; Volume 2, pp. 74–96.
39. Moretti, C.; Junginger, M.; Shen, L. Environmental life cycle assessment of polypropylene made from used cooking oil. Resour. Conserv. Recycl. 2020, 157, 104750.
40. van Grinsven, A.; van den Toorn, E.; van der Veen, R.; Kampman, B.; Oil, C. Used Cooking Oil (UCO) as Biofuel Feedstock in the EU; CE Delft: Delft, The Netherlands, 2020.
41. Stathatou, P.M.; Bergeron, S.; Fee, C.; Jeffrey, P.; Triantfyllou, M.; Gershenfeld, N. Towards decarbonization of shipping: Direct emissions & life cycle impacts from a biofuel trial aboard an ocean-going dry bulk vessel. Available online: https://pubs.rsc.org/en/content/articlehtml/2022/se/d1se01495a (accessed on 15 January 2022).
42. Panadare, D.C.; Rathod, V.K. Applications of waste cooking oil other than biodiesel: A review. Iran. J. Chem. Eng. 2015, 12, 55–76.
43. Chung, T.Y.; Eiserich, J.P.; Shibamoto, T. Volatile compounds identified in headspace samples of peanut oil heated under temperatures ranging from 50 to 200 °C. J. Agric. Food Chem. 1993, 41, 1467–1470.
44. Wu, C.M.; Chen, S.Y. Volatile compounds in oils after deep frying or stir frying and subsequent storage. J. Am. Oil Chem. Soc. 1992, 69, 858–865.
45. Singhabhandhu, A.; Tezuka, T. The waste-to-energy framework for integrated multi-waste utilization: Waste cooking oil, waste lubricating oil, and waste plastics. Energy 2010, 35, 2544–2551.
46. Mannu, A.; Ferro, M.; DiPietro, M.E.; Mele, A. Innovative applications of waste cooking oil as raw material. Sci. Prog. 2019, 102, 153–160.
47. Lhuissier, M.; Couvert, A.; Amrane, A.; Kane, A.; Audic, J.-L. Characterization and selection of waste oils for the absorption and biodegradation of VOC of different hydrophobicities. Chem. Eng. Res. Des. 2018, 138, 482–489.
48. Fu, J.; Turn, S.Q.; Takushi, B.M.; Kawamata, C.L. Storage and oxidation stabilities of biodiesel from waste cooking oil. Fuel 2016, 167, 89–97.

49. Pölczmann, G.; Tóth, O.; Beck, Á.; Hancsók, J. Investigation of storage stability of diesel fuels containing biodiesel produced from waste cooking oil. J. Clean. Prod. 2016, 111, 85–92.
50. Tsoutsos, T.; Tournaki, S.; Gkouskos, Z.; Paraíba, O.; Giglio, F.; García, P.Q.; Braga, J.; Adrianos, H.; Filice, M. Quality characteristics of biodiesel produced from used cooking oil in Southern Europe. ChemEngineering 2019, 3, 19.
51. Bruun, N.; Lehmusto, J.; Hemming, J.; Tesfaye, F.; Hupa, L. Metal rod surfaces after exposure to used cooking oils. Sustainability 2022, 14, 355.
52. Landolt, D. The corrosion of metals. In Corrosion and surface chemistry of metals; Landolt, D., Ed.; EPFL: Lausanne, Switzerland, 2003; pp. 1–13.
53. Schweitzer, P.A. Corrosion mechanisms. In Fundamentals of Corrosion; Mechanisms, Causes, and Preventative Methods; Schweitzer, P.A., Ed.; CRC Press: Boca Raton, FL, USA, 2010; pp. 5–26.
54. Davis, J.R. The effects and economic impact of corrosion. In Corrosion: Understanding the Basics; Davis, J.R., Ed.; ASM International: Materials Park, OH, USA, 2000; pp. 1–20.
55. Leng, L.; Yuan, X.; Zeng, G.; Chen, X.; Wang, H.; Li, H.; Fu, L.; Xiao, Z.; Jiang, L.; Lai, C. Rhamnolipid based glycerol-in-diesel microemulsion fuel: Formation and characterization. Fuel 2015, 147, 76–81.
56. Shifler, D. Meeting materials needs in extreme naval corrosive and oxidative environments. Mater. High Temp. 2015, 32, 148–159.
57. Fazal, M.A.; Haseeb, A.S.M.A.; Masjuki, H.H. Corrosion mechanism of copper in palm biodiesel. Corros. Sci. 2013, 67, 50–59.
58. Kaul, S.; Saxena, R.C.; Kumar, A.; Negi, M.S.; Bhatnagar, A.K.; Goyal, H.B.; Gupta, A.K. Corrosive behaviour of biodiesel from seed oils of Indian origin on diesel engine parts. Fuel Process. Technol. 2007, 88, 303–307.
59. Maru, M.M.; Lucchese, M.M.; Legnani, C.; Quirino, W.G.; Balbo, A.; Aranha, I.B.; Costa, L.T.; Vilani, C.; de Sena, L.A.; Damasceno, J.C.; dos Santos Cruz, T.; Lidízio, L.R.; Silva, R.F.; Jorio, A.; Achete, C.A. Biodiesel compatibility with carbon steel and HDPE parts. Fuel Process. Technol. 2009, 90, 1175–1182.
60. Diaz-Ballote, L.; Lopez-Sansores, J.F.; Maldonado-Lopez, L.; Garfias-Mesias, L.F. Corrosion behaviour of aluminium exposed to a biodiesel. Electrochem. Commun. 2009, 11, 41–44.
61. Fazal, M.A.; Haseeb, A.S.M.A.; Masjuki, H.H. Comparative corrosive characteristics of petroleum diesel and palm biodiesel for automotive materials. Fuel Process. Technol. 2010, 91, 1308–1315.
62. U.S. Department of Energy, Office of Energy Efficiency and Renewable Energy. Straight Vegetable Oil as a Diesel Fuel? Available online: https://afdc.energy.gov/files/u/publication/straight_vegetable_oil_as_diesel_fuel.pdf (accessed on 12 April 2022).
63. CNN. An A380 Superjumbo Just Completed a Flight Powered by Cooking Oil. Available online: https://www.citizen.digital/lifestyle/an-a380-superjumbo-just-completed-a-flight-powered-by-cooking-oil-n295778 (accessed on 4 April 2022).
64. Sanyal, B. Organic compounds as corrosion inhibitors in different environments—A review. Prog. Org. Coat. 1981, 9, 165–236.

65. Raja, A.S.; Rajendran, S.; Sathiyabama, J.; Angel, P. Corrosion control by aminoacetic acid (glycine)—An overview. Int. J. Innov. Res. Sci. Eng. Technol. 2014, 3, 11455–11467.
66. El Ibrahimi, B.; Jmiai, A.; Bazzi, L.; El Issami, S. Amino acids and their derivatives as corrosion inhibitors for metals and alloys. Arab. J. Chem. 2020, 13, 740–771.
67. Kovács, A.; Tóth, J.; Isaák, G.; KereszténYi, I. Aspects of storage and corrosion characteristics of biodiesel. Fuel Process. Technol. 2015, 134, 59–64.
68. Fazal, M.A.; Sazzad, B.S.; Haseeb, A.S.M.A.; Masjuki, H.H. Inhibition study of additives towards the corrosion of ferrous metal in palm biodiesel. Energy Convers. Manag. 2016, 122, 290–297.
69. Komatsu, D.; Souza, E.C.; de Souza, E.C.; Canale, L.C.F.; Totten, G.E. Effect of antioxidants and corrosion inhibitor additives on the quenching performance of soybean oil. Stroj. Vestn. J. Mech. Eng. 2010, 56, 121–130.
70. Bruun, N.; Demesa, A.G.; Tesfaye, F.; Hemming, J.; Hupa, L. Factors affecting the corrosive behavior of used cooking oils and a non-edible fish oil that are in contact with ferrous metals. Energies 2019, 12, 4812.
71. Eaton, S.J.; Harakas, G.N.; Kimball, R.W.; Smith, J.A.; Pilot, K.A.; Kuflik, M.T. Formulation and combustion of glycerol–diesel fuel emulsions. Energy Fuels 2014, 28, 3940–3947.
72. Mize, E.; Lucio, A.J.; Fhaner, C.J.; Pratama, F.S.; Robbins, L.A.; Karpovich, D.S. Emulsions of crude glycerin from biodiesel processing with fuel oil for industrial heating. J. Agric. Food Chem. 2013, 61, 1319–1327.
73. Hamadi, L.; Mansouri, S.; Oulmi, K.; Kareche, A. The use of amino acids as corrosion inhibitors for metals: A review. Egypt. J. Pet. 2018, 27, 1157–1165.
74. Sastri, V.S. Green Corrosion Inhibitors: Theory and Practice; Wiley: Hoboken, NJ, USA, 2011; pp. 257–258.
76. Singh, B.; Korstad, J.; Sharma, Y.C. A critical review on corrosion of compression ignition (CI) engine parts by biodiesel and biodiesel blends and its inhibition. Renew. Sustain. Energy Rev. 2012, 16, 3401–3408.
76. Moretti, G.; Guidi, F.; Grion, G. Tryptamine as a green iron corrosion inhibitor in 0.5 M deaerated sulphuric acid. Corros. Sci. 2004, 46, 387–403.
77. Raja, P.B.; Sethurama, M.G. Natural products as corrosion inhibitor for metals in corrosion media—A review. Mater. Lett. 2008, 62, 113–116.
78. Kilberg, M.S.; Häussinger, D. Amino acid transport in liver. In Mammalian Amino Acid Transport: Mechanisms and Control; Kilberg, M.S., Häussinger, D., Eds.; Springer: Boston, MA, USA, 1992; pp. 133–148.
79. Wu, G. Amino Acids: Biochemistry and Nutrition, 2nd ed.; CRC Press: Boca Raton, FL, USA, 2022; pp. 1–32.
80. Mendonça, G.L.F.; Costa, S.N.; Freire, V.N.; Casciano, P.N.S.; Correia, A.N.; de Lima-Neto, P. Understanding the corrosion inhibition of carbon steel and copper in sulphuric acid medium by amino acids using electrochemical techniques allied to molecular modelling methods. Corros. Sci. 2017, 115, 41–55.
81. Gowri, S.; Sathiyabama, J.; Rajendran, S. Corrosion inhibition by amino acids—An over review. Eur. Chem. Bull. 2012, 11, 470–476.

82. Gece, G.; Bilgiç, S. A theoretical study on the inhibition efficiencies of some amino acids as corrosion inhibitors of nickel. Corros. Sci. 2010, 52, 3335–3443.
83. Adeoti I.A,; Hawboldt K. Comparison of biofuel quality of waste derived oils as a function of oil extraction methods. Fuel 2015, 158, 183–190.
84. Yang, H.; Irudayaraj, J.; Paradkar, M.M. Discriminant analysis of edible oils and fats by FTIR, FT-NIR and FT-Raman spectroscopy. Food Chem. 2005, 93, 25–32.
85. Guillen, M.D.; Cabo, N. Infrared spectroscopy in the study of edible oils and fats. J. Sci. Food Agric. 1997, 75, 1–11.
86. Klaypradit, W.; Kerdpiboon, S.; Singh, R.K. Application of artificial neutral networks to predict the oxidation of menhaden fish oil obtained from fourier transform infrared spectroscopy method. Food Bioprocess Technol. 2011, 4, 475–480.
87. Mohan, D.; Pittman, C.U. Jr.; Steele, P.H. Pyrolysis of wood/biomass for bio-oil: A critical review. Energy Fuels. 2006, 20, 848–889.
88. Canakci, M.; Sanli, H. Biodiesel Production from various feedstocks and their effects on the fuel properties. J Ind Microbiol Biotechnol. 2008, 35, 431–441.
89. Choi, C.Y.; Reitz, R.D. A numerical analysis of the emissions characteristics of biodiesel blended fuels. J Eng Gas Turbines Power. 1999, 121, 31–37.
90. Rafiquee, M.Z.A.; Khan, S.; Saxena, N.; Quraishi, M.A. Influence of some thiadiazole derivatives on corrosion inhibition of mild steel in formic acid and acetic acid media. Port. Electrochim. Acta 2007, 25, 419–434.
91. Leng, L.; Yuan, X.; Zeng, G.; Chen, X.; Wang, H.; Li, H.; Fu, L.; Xiao, Z.; Jiang, L.; Lai, C. Rhamnolipid based glycerol-in-diesel microemulsion fuel: Formation and characterization. Fuel 2015, 147, 76–81. doi:10.1016/j.fuel.2015.01.052.
92. Hu, E.; Xu, Y.; Hu, X.; Pan, L.; Jiang, S. Corrosion behaviors of metals in biodiesel from rapeseed oil and methanol. Renew. Energy 2012, 37, 371–378.

Appendix I

Physicochemical properties of the bio-oils, commercial product, and heavy fuel oil (HFO). Limit values for marine engines: liquid biofuel (LB) and vegetable oil (VO).

Sample	Density 21 °C (kg/m^3)	Kinematic viscosity 40 °C (mm^2/s)	Water content (ppm)	Measured Acid number (mg KOH/g oil)
FO1(I)	916	31.9	473	1.7
FO2(I)	914	31.6	1070	24.9
FO3(I)	914	31.6	1450	17.1
UCO1(I)	914	40.6	538	8.9
UCO2(I)	916	41.3	706	10.8
UCO3(I)	915	44.3	740	3.7
COref(I)	873	8.9	37	0.02
COref**(I)	879	9.1	<100	<0.10
HFO(I)	940	50****	n.a.	
LB(I)	<991*****	min 1.8-2.8 max 100	2000	<5.0
VO(I)	920-960*****	30-40	<500	<4***
FO1/18/0d(II)	916	26.6	2473	24.8
UCO1/18/0d(II)	916	40.7	1662	6.5
UCO2/18/0d(II)	917	40.7	1449	8.2
UCO3/18/0d(II)	916	40.3	1403	8.1
COref(II)	873	8.9	37	0.02
COref**(II)	879	9.1	<100	<0.10

n.a. = not available
* Precipitated phase at the bottom.
** From manufacturer's specifications.
*** Total acid number (TAN)
**** Measured at 50 °C.
***** Measured at 15 °C.

After each sample name the numbers in brackets, i.e., FO1(I) indicates that more information about the measurements is available in Paper I and similarly UCO1(IV,V) means that in Papers IV and V more information is available.

Appendix II

Physicochemical properties of the bio-oils and vegetable oil and virgin olive oil.

Sample	**Density 21 °C (kg/m^3)**	**Kinematic viscosity 40 °C (mm^2/s)**	**Water content (ppm)**	**Measured Acid number (mg KOH/g oil)**
FO1-15 (2015)(III)	916	31.9	473	1.7
FO1-15 (2020)(III)	917	36.4	900	2.5
UCO1-15 (2015)(III)	914	40.6	538	8.9
UCO1-15 (2020)(III)	915	43.6	1094	11.1
UCO2-15 (2015)(III)	916	41.3	706	10.8
UCO2-15 (2020)(III)	916	43.6	1015	10.7
FO1-18 (2020)(III)	919	35.7	2720	27.3
UCO1-18 (2018)(III)	916	40.7	1662	6.5
UCO1-18 (2020)(III)	916	41.0	1773	7.6
UCO2-18 (2018)(III)	917	40.7	1449	8.2
UCO2-18 (2020)(III)	914	40.0	1734	8.7
UCO3-18 (2018)(III)	916	40.3	1403	8.1
UCO3-18 (2018)(III)	918	41.7	1686	9.4
UCO1(IV,V)	917	39.3	1850	6.9
UCO2(IV,V)	917	39.5	1776	6.5
UCO3(IV,V)	914	38.7	2180	6.9
UCO4(IV,V)	916	39.8	2067	7.0
UCO5(IV,V)	917	39.5	2493	8.0
UCO6(IV,V)	914	39.4	3748	6.7
UCO7(IV,V)	915	39.4	3089	6.9
UCO8(IV,V)	915	39.5	2664	8.8
mean value UCO1-UCO8(IV,V)	916±1.3	39.4±0.3	2483.0±672	7.2±0.8
Vegetable oil(V)	915	35.2	604	0.1
Virgin Olive oil(V)	910	38.9	581	0.5

Appendix III

Chemical properties of bio-oils and liquid biofuel (LB).

Sample	Ester group (mg KOH/ g oil)	Unsaturated fatty acids (g jodine/ 100g oil)	Total FFA (mg/g oil)	Oleic acid (mg/g oil)
FO1(I)	156	131	5.9	2.03
FO2(I)	156	129	92.7	38.4
FO3(I)	154	133	71.5	21.7
UCO1(I)	150	103	44.8	23.8
UCO2(I)	149	102		
UCO2u(I)			51.1	27.5
UCO2b(I)			47	25
UCO3(I)	157	104	21.7	11
LB(I)	n.a.	<120	n.a.	n.a.

n.a.= not available.
LB = liquid biofuel.
UCO2u = UCO2 upper phase
UCO2b = UCO2 bottom phase

Appendix IV

Chemical properties of the bio-oils, vegetable oil and virgin olive oil.

Sample	**Total FFA (mg/g oil)**	**Oleic acid (mg/g oil)**
FO1/18/0d(II)	99.7	42.3
FO1/18/10d(II)	93.9	41.0
UCO1/18/0d(II)	29.1	15.2
UCO1/18/10d(II)	33.7	18.0
UCO2/18/0d(II)	43.3	23.1
UCO2/18/10d(II)	45.2	24.0
UCO3/18/0d(II)	46.8	24.9
UCO3/18/10d(II)	47.0	25.1
UCO1-15 (2015)(III)	44.8	23.8
UCO1-15 (2020)(III)	41.7	23.1
UCO2-15 (2015)(III)	51.1	27.5
UCO2-15 (2020)(III)	45.1	25.1
UCO3-15 (2015)(III)	21.7	11.0
UCO3-15 (2020)(III)	17.8	9.8
UCO1-18 (2018)(III)	29.1	15.2
UCO1-18 (2020)(III)	30.8	16.6
UCO2-18 (2018)(III)	43.3	23.1
UCO2-18 (2020)(III)	43.4	19.8
UCO3-18 (2018)(III)	46.8	24.9
UCO3-18 (2020)(III)	39.6	20.6
UCO1(IV,V)	28.4	14.9
UCO2(IV,V)	28.4	14.8
UCO3(IV,V)	28.3	16.0
UCO4(IV,V)	30.0	16.9
UCO5(IV,V)	32.9	18.7
UCO6(IV,V)	27.0	15.2
UCO7(IV,V)	28.0	15.9
UCO8(IV,V)	37.8	21.7
mean value		
UCO1-UCO8(IV,V)	30.1±3.6	16.8±2.4
Vegetable oil(V)	0.5	0.2
Virgin Olive oil(V)	1.0	0.4

Appendix V

Main component groups of fish and used cooking oils measured by high-performance size exclusion chromatography using an evaporative light scattering detector (% of identified compounds).

Sample	Free fatty acids incl.monoglycerides	Diglycerides	Triglycerides	Polymerized triglycerides
FO1(I)	0.7	0.3	98.8	n.d.
FO2(I)	10.3	8.3	81.4	n.d.
FO3(I)	7.3	3.9	88.2	0.5
UCO1(I)	4.2	12.6	77.7	5.6
UCO2u(I)	4.6	13.8	76.0	5.6
UCO2b*(I)	4.4	12.8	78.2	4.6
UCO3(I)	1.7	6.2	87.2	4.8
FO1/18/0d(II)		9.7		n.d.
FO1/18/10d(II)		10.3		n.d.
UCO1/18/0d(II)		7.1		1.2
UCO1/18/10d(II)		7.6		1.5
UCO2/18/0d(II)		7.7		1.3
UCO2/18/10d(II)		7.8		1.4
UCO3/18/0d(II)		7.7		1.3
UCO3/18/10d(II)		7.8		1.3

n.d. = not detected.

* Precipitated phase at the bottom.

Appendix VI

The effect of immersion time on the amount of iron or copper dissolved in the bio-oil, vegetable and virgin olive oil samples. Iron concentration was measured spectrophotometrically. Copper dissolved in the bio-oil was measured using ICP-OES.

Sample	**Immersion Test (3d)**	**Immersion Test (10d)**	**Immersion Test (3d) TBA 0.025 wt% added**	**Immersion Test (3d)**
	Fe (ppm)	**Fe (ppm)**	**Fe (ppm)**	**Cu (ppm)**
FO1/18(II)	129±31			
FO1/18(II)		97±15		
UCO1/18(II)	128±30			
UCO1/18(II)		178±30		
UCO2/18(II)	38±17			
UCO2/18(II)		62±3		
UCO3/18(II)	22±6			
UCO3/18(II)		22±2		
COref(II)	14±3			
COref(II)		10±1		
UCO1(IV,V)	12			
UCO2(IV,V)	390		9	25.3±0.3
UCO3(IV,V)	102			
UCO4(IV,V)	14			
UCO5(IV,V)	74			
UCO6(IV,V)	449			
UCO7(IV,V)	571			
UCO8(IV,V)	59			
mean value UCO1-UCO8(IV,V)	209±223			
Vegetable oil(V)	8			
Virgin Olive oil(V)	8			

Appendix VII

Standard methods and instruments used to measure properties of the bio-oils and commercial product.

Compound	Method	Instrument	Paper
Acid number	ASTM D 664	Metrohm 888 Titrando titrator and a Solvotrode glass electrode	I-IV
Theoretical Acid number		GC-FID	III, IV
Ester groups	ASTM D 5558		I
Unsaturated fatty acids	ISO 3961		I
Monoglycerides		GC-FID	I-IV
Total fatty acids		GC-FID	I-IV
Free fatty acids		GC-FID	I-IV
Volatile fatty acids		GC-FID	I
Di- and triglycerides		GC-FID	I-IV
Polymerized triglycerides		GC-FID	I-IV
Molecular weight		HPSEC-ELSD	I
Functional groups		FTIR	I
Ageing test		Metrohm 888 Titrando titrator and a Solvotrode glass electrode	I
Phosphorus and Sulfur		ICP-OES	I
Density		Pycnometer	I-IV
Kinematic viscosity	ASTM D 2515, ASTM D 445	Viscometer: Cannon-Fenske 511 20 or 511 13 or Ostwald 509 04	I-IV
Water content		Karl Fischer coulometric titrator (Metrohm 851 Titrando)	I-IV
Surface Tension		du Noüy KSV Sigma 70 tensiometer	III
Volatility of oils		Thermogravimetric analyzer	I
Higher Heating value	SFS-EN 14918:2009	Adiabatic oxygen-bomb calorimeter	I, III
Immersion test		Metal rod dissolved in oil (1d, 3d, 5d, 10d)	II, IV, V
Iron dissolved in oil		Spectrophotometer, ICP-OES, ICP-MS	II, IV, V

Appendix: Original publications (I-V)

Nina Bruun, Tooran Khazraie Shoulaifar, Jarl Hemming, Stefan Willför and Leena Hupa

Characterization of waste bio-oil as an alternate source of renewable fuel for marine engines

Biofuels 2022, 13, 21–30.

I

https://www.tandfonline.com/doi/abs/10.1080/17597269.2019.1628481?journalCode=tbfu20

Nina Bruun, Abayneh Getachew Demesa, Fiseha Tesfaye, Jarl Hemming and Leena Hupa

II

Factors Affecting the Corrosive Behavior of Used Cooking Oils and a Non-Edible Fish Oil That Are in Contact with Ferrous Metals

Energies 2019, 12, 4812, 1–12.

Supplementary Materials: Table S1 and Table S2

http://www.mdpi.com/1996-1073/12/24/4812/s1

energies

MDPI

Article

Factors Affecting the Corrosive Behavior of Used Cooking Oils and a Non-Edible Fish Oil That Are in Contact with Ferrous Metals

Nina Bruun *, Abayneh Getachew Demesa, Fiseha Tesfaye, Jarl Hemming and Leena Hupa

Johan Gadolin Process Chemistry Centre, Åbo Akademi University, Piispankatu 8, FI-20500 Turku, Finland; abayneh.demesa@abo.fi (A.G.D.); fiseha.tesfaye@abo.fi (F.T.); jarl.hemming@abo.fi (J.H.); leena.hupa@abo.fi (L.H.)

* Correspondence: nina.bruun@abo.fi; Tel.: +358-50343-6637

Received: 1 November 2019; Accepted: 16 December 2019; Published: 17 December 2019

Abstract: The corrosion behavior of three used cooking oils and one non-edible fish oil was experimentally investigated by the immersion test of iron rods at room temperature. The corrosivity of the tested oils was indirectly determined from the amount of the dissolved iron in the tested oils after the immersion test. Different factors that affect the corrosive behavior of the tested oils were assessed. Among the tested oils, the fish oil showed the highest amount of dissolved iron owing to its chemical properties such as high water content and acid number. In general, water content and acid number have direct effects on the amount of dissolved iron. The addition of oleic acid to the used cooking oil resulted in a 60% less amount of dissolved iron. It was suggested that the addition of oleic acid prompted the formation of a monolayer, which inhibited the permeation of oxygen and water to the surface of the iron rod. Moreover, the addition of glycerol gave the lowest amount of dissolved iron in the oil sample owing to its ability to bind water molecules and form microemulsions in the presence of a surfactant (for example, oleic acid).

Keywords: corrosion; used cooking oil; fish oil; bio-oil; renewable energy

1. Introduction

The need for an alternative fuel source is becoming increasingly apparent mainly due to environmental concerns and depletion of fossil fuel reserves. In this context, liquid biofuel, such as bio-oil, has become more attractive as an alternative fuel owing to its environmental benefits as CO_2 neutral fuel and the fact that it is obtained from renewable sources [1]. Bio-oils can be used in either processed form, as in car and airplane engines [2,3], or in their crude form for conventional combustors [4] and marine engines [5].

Despite several advantages of bio-oils, their corrosiveness during storage and use are two of the concerns related to compatibility issues, thus limiting the potential of direct substitution of bio-oils for petroleum fuels. Several characteristics of bio-oils can cause corrosion of metals, but the most common ones include pre-existing organic acids (such as acetic, formic, glycolic, and fatty acids), water content, and any possible sediment present in the bio-oil. Besides its ability to produce additional free fatty acids out of any glyceride present in the bio-oil, water enhances the growth of microorganisms, which in turn results in increased corrosion and a high risk of engine malfunction [6–8].

Oxidation of biodiesel is also an important factor that needs to be taken into consideration as it reconverts esters into different mono-carboxylic acids such as formic acid, acetic acid, propionic acid, and caproic acid, which increase corrosion of metals [9]. According to Barabás and Todorut [10], the composition of a bio-oil or biodiesel determines how well it can withstand oxidation, polyunsaturated

fatty acids being more susceptible to oxidation in the presence of a suitable catalyst [10]. Therefore, the rate at which any degradation (aging or oxidation) occurs must be kept to a minimum since the degradation affects the quality of bio-oil or biodiesel while prompting corrosion as a result of introduced peroxides and fatty acids [11]. In addition to oxidation, hydrolytic degradation can take place when the bio-oil/biodiesel reacts with water [10].

It has also been reported that the corrosiveness of biodiesel depends on its feedstock [12,13]. According to Diaz-Ballote et al. [14], the corrosiveness of biodiesel was found to decrease when decreasing the impurities remaining after processing. In addition, the corrosive nature of biodiesel was increased by the presence of free water and free fatty acids. Compared to conventional diesel, biodiesel is more prone to water absorption, which in turn leads to an increased risk of corrosion when water is condensed on the metallic surfaces that are in contact with the biodiesel. The composition of the metal in contact with fuel has also its own characteristics that would affect the corrosiveness of the fuel [15].

In general, biodiesels tend to show a much higher affinity for corrosion than the conventional petroleum-based fuels, predominantly because of their much higher tendency to absorb water [11]. Despite the corrosive behavior of bio-oils and the mechanisms for the observed corrosion that might be very complex to understand, the corrosion itself can be measured using different techniques. In our previous work [16], the physicochemical, as well as thermal properties of fish oils and used cooking oils, were investigated to determine their applicability as alternative fuels for marine engines. The objective of this work, which is a continuation from our previous publication [16], was to experimentally examine the corrosive properties of crude bio-oils (used cooking oils and non-edible fish oil) that are in contact with ferrous metals.

2. Materials and Methods

2.1. Materials

The composition and properties of fish oil (FO1/18), which was obtained from gutting remains of rainbow trout after edible oil was extracted, and three used cooking oils (UCO1/18, UCO2/18, and UCO3/18) delivered by VG EcoFuel Oy in Finland were studied in detail. In the abbreviations of the oils, numbers are given to identify different types of oils, and the number 18 indicates the year 2018 (in which the oils were prepared).

All the used cooking oils (filtered) had vegetable sources and they were obtained from fast food companies. The used cooking oils (UCO), as well as the fish oil, were stored in a refrigerator before experimental use. For both oils, a commercially available product (COref) was used as a reference.

The iron rod used in the immersion tests was an H44 all-round welding rod with a diameter 1.6 mm obtained from AGA (Finland). It was manufactured according to SFS 2369 G-132, and is composed of (in wt.%) 98.64 Fe, 1.00 Mn, 0.21 Si, 0.11 C, 0.03 P, and 0.02 S. It is a brightly drawn welding wire intended for unalloyed construction steel and some pressure vessel steel with the highest minimum breaking strength of 430 N/mm^2. The rods were cut in 85 mm long pieces, and the ends of the iron rod were polished to a similar roughness (visually) as the surfaces of the rod. The rods were cleaned ultrasonically for 2 min using a mixture of toluene and 2-propanol (1:1 *v*/*v*), and cleaned for 1 min with acetone ultrasonically. The rods were dried with compressed air before each immersion test.

All chemicals and solvents used in the experiments were of analytical reagent grade. Ferrozine iron reagent (>95%) and monosodium monohydrate (95%) were purchased from Hach Lange GmbH, Dὺsseldorf, Germany. L-Ascorbic acid (99%) was obtained from Sigma-Aldrich, Saint Louis, MO, USA. Acetic acid (98%) was supplied by Merck, Darmstadt, Germany. Sodium acetate (99%), sulfuric acid (95%), potassium hydrogen phthalate (>99.5%), and glycerol (99.5%) were purchased from VWR International, Helsinki, Finland. Toluene (HPLC grade) was obtained from Fisher Scientific, Kandel, Germany. Hydranal Coulomat for Karl Fischer titration was supplied by Fluka, Bucharest, Romania. Oleic acid (97%) was purchased from Acros Scientific, Geel, Belgium.

2.2. Methods

2.2.1. Experimental Setup and Procedure

A room temperature immersion test was applied to investigate the corrosion behavior of used cooking oils and non-edible fish oil on an iron rod (length 85 mm and diameter 1.6 mm). The experiments were conducted in test tubes (15 mL) mounted on a rotary mixer, rotating at a constant speed of 56 rpm. The iron rod was placed in a 7 mL oil sample and the test was conducted over a period of 1, 3, 5, and 10 days. During the experiments, the samples were wrapped around with duct tape in order to avoid exposure to light. After the immersion test, the iron rod was separated from the oil and cleaned ultrasonically using a mixture of toluene and 2-propanol (1:1 *v*/*v*). The oils from each experiment were subjected to liquid–liquid extraction using 1 mL of sulfuric acid (95%) and 8 mL of deionized water in a test tube, which was then vigorously shaken for 1 min. After the extraction, the mixture was filtered using Whatman™ quantitative filter paper grade No 42 (ashless, Whatman International Ltd, Maidstone, England) and the aqueous solution was taken for subsequent spectrophotometric analysis. Each experiment was repeated in triplicates. The experimental setup developed in this work for the immersion test is shown in Figure 1.

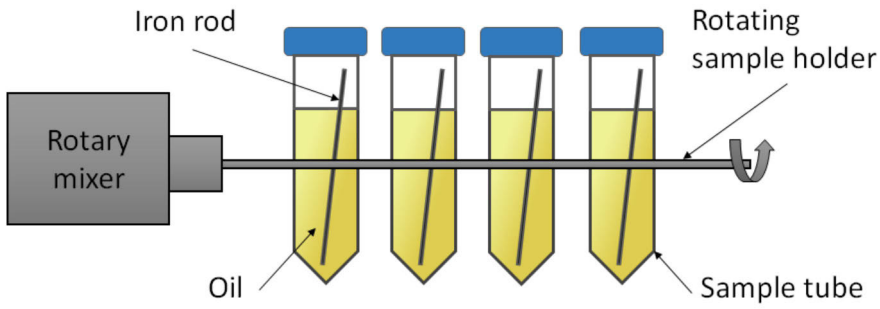

Figure 1. Experimental setup of the immersion test.

2.2.2. Analytical Methods

- Iron Content Measurement

The amount of iron dissolved in the oils during the experiment was determined using a spectrophotometer (Spectronic Genesys 2PC) by analyzing the amount of total dissolved iron in the aqueous phase after the liquid–liquid extraction step. Prior to spectrophotometric analysis, the iron in the water solution was reduced to Fe^{2+} with the aid of ascorbic acid. The solution was then allowed to react with an excess of ferrozine-reagent to form a magenta-colored complex. A buffer solution containing sodium acetate and acetic acid was used to adjust the pH to 5. The red complex had a maximum absorption peak at 562 nm. The molar absorptivity used for the analysis was $27,900\left(\frac{\text{mol}}{\text{l}}\right)^{-1}\text{cm}^{-1}$, which was selected according to the report by Stookey [17]. It is known that the red complex follows the Beer–Lambert law [18] up to the absorbance value 1. The final solutions were made to achieve an absorbance value between 0.5 and 1.

In addition to the spectrophotometric analysis, the amount of the dissolved iron in the oil was measured using inductively coupled plasma-optical emission spectrometry (ICP-OES, Perkin Elmer Optima 5300 DV) and inductively coupled plasma-mass spectrometry (ICP-MS, PerkinElmer, ELAN 6100 DRC). Prior to the analysis, 65% HNO_3 and 30% H_2O_2 were added to the samples and digested in a microwave oven (Anton Paar, Multiwave 3000). In the ICP-MS analysis, a commercial multi-element standard was used for the calibration and ammonia was used as a reaction gas. A minimum of five replications per each sample were performed in each case.

- Acid Number Measurement

The acid number (AN) of the crude bio-oil was measured by the ASTM D 664 method using Metrohm 888 Titrando titrator with the Solvotrode glass electrode. Samples of the crude bio-oils were dissolved in 125 mL solution of toluene, propan-2-ol, and deionized water (500:495:5 *v/v/v*), and then titrated with 0.1 M KOH in propan-2-ol. The amount of KOH in propan-2-ol was determined by titration of potassium hydrogen phthalate. The blank test was done three times.

- Water Content Analysis

Karl Fischer (KF) titration with an automatic coulometric titrator (Metrohm 851 Titrando instrument) was used to measure the water content of the samples. The KF titrator was connected to an oven (860 KF Thermoprep), which was adjusted to 110 °C. About 0.1 g of the sample sealed in a glass bottle was placed in the sample holder. In the KF measurements, a dry N_2 (gas) with a flow rate of 90 mL/min was used. During the measurement of the water content of the reference commercial product, about 0.5 g of the sample was injected into the reactor, since the flashpoint of the sample is relatively low (about 60 °C). Three runs were performed for each sample and no dry N_2 (gas) was used.

- SEM-EDS Analysis

The surface of the iron rod was analyzed with a scanning electron microscopy (SEM) LEO Gemini 1530 with a Thermo Scientific UltraDry Silicon Drift Detector (SDD) coupled to an elemental X-ray detector (EDS, Energy Dispersive X-Ray Spectroscopy, Thermo Scientific, Madison, WI, USA).

- Oil Composition Measurements

A capillary gas chromatography–flame ionization detector (GC-FID) (Perkin Elmer Autosystem XL) was used to quantify the number of monoglycerides and free fatty acids in the oil samples. All samples were silylated before the GC analysis. The column used was an Agilent J&W HP-1, 25 m (L) × 0.200 mm (ID) with film thickness 0.11 μm. Hydrogen was used as a carrier gas with a flow rate of 0.8 mL/min. The temperature of the oven was increased at a rate of 6 °C/min from 120 °C (1 min hold) to 320 °C (15 min hold), and with an injector program at a rate of 8 °C/min from 160 °C to 260 °C (10 min hold). The detector temperature was 320 °C. The identification of individual components was performed by GC-MS analysis with an HP 6890-5973 GC-MSD instrument, using a similar GC column, but using helium as the carrier gas.

A wide-bore short column GC-FID (PerkinElmer Clarus 500, Shelton, CT, USA) was used to analyze the diglycerides. The column parameters were: Agilent HP-1/SIMDIST, ~6 m (length) × 0.530 mm (inner diameter), film thickness 0.15 μm. The hydrogen carrier gas was fed at 7 mL/min. The wide-bore GC-oven temperature program was increased from 100 °C (after a 0.5 min hold) at a rate of 12 °C/min to 340 °C (5 min hold), and with an injector program from 80 °C (0.1 min hold) at a rate of 50 °C/min to 110 °C, and at a rate of 15 °C/min to 330 °C (7 min hold), while the temperature of the detector was maintained at 340 °C.

A high-performance size exclusion chromatography with an evaporative light scattering detector (HPSEC-ELSD, Shimadzu 10A series modular HPLC, Shimadzu Corporation (Shimadzu, Japan), and ELSD detector, Sedex 85 LT-ELSD, S.E.D.E.R.E. S.A.) was used to detect polymerized triglycerides.

3. Results and Discussion

3.1. Physicochemical Properties

The physical and chemical properties of the bio-oils were experimentally studied to evaluate the suitability of the oils for fuel applications.

It is well known that the density of fuel affects the dispersion of the fuel injected into the cylinder, whereas the viscosity of the fuel plays a significant role when the fuel is sprayed into the chamber or

while mixing it with other fuels [19,20]. High water content and acidity in bio-oils can substantially increase the risk of corrosion during the storage and the use of the oils [21–23]. Moreover, the presence of water in a bio-oil decreases the heating value of the oil [16]. The measured physicochemical properties of the bio-oils are summarized in Table 1.

Table 1. Physicochemical properties of the bio-oils and a commercially available product.

Sample	Density 21 °C (kg/m^3)	Kinematic Viscosity 40 °C (mm^2/s)	Water Content (ppm)	Acid Number (mg KOH/g Oil)
UCO1/18	916	40.7	1662	6.5
UCO2/18	917	40.7	1449	8.2
UCO3/18	916	40.3	1403	8.1
FO1/18	916	26.6	2473	24.8
COref	873	8.9	37	0.02
COref *	879	9.1	<100	<0.10

* From manufacturer's specification.

According to the results in Table 1, the density of the fish oil and used cooking oils were on the same level, but slightly denser than the commercial product used as a reference. All the values were apparently lower than the density of water or the density of heavy fuel oil, 940 kg/m^3 [24]. The fuel density affects the design of an engine since the higher the density, the better the penetration is in the combustion chamber. A lower density facilitates mixture formation and atomization to be attained [19]. It has been reported that the density of the liquid biofuel for the marine engine should be lower than 991 kg/m^3 [25]. Our results indicate that the densities of the studied oils are lower than 991 kg/m^3 and are between the values for the heavy fuel oil and the reference commercial product, thus avoiding the need for engine modification due to density values.

On the other hand, the used cooking oils showed the highest kinematic viscosity (40.7 mm^2/s) compared to the fish oil (26.6 mm^2/s) or reference product (9 mm^2/s). The high kinematic viscosity of the used cooking oils can be attributed to the presence of some impurities like starch, polymerized triglycerides, and meat traces in the used cooking oils. In general, a very high viscosity (>100 mm^2/s) is not desirable as it causes high operating temperature and the fuel in the injection pumps starts to boil [20]. However, the higher viscosity of the used cooking oils relative to conventional fuels can be lowered by changing the temperature of the oil.

Among the tested oils, FO1/18 had the highest water content (2473 ppm) while the water content of UCO1/18, UCO2/18, and UCO3/18 was between 1403 and 1662 ppm. The commercial product has the lowest water content (37 ppm) among the tested oils. It is important to consider the possibility of water accumulation in tanks when using the bio-oils with relatively high water content. Consequently, careful dewatering operation might be needed to alleviate such problems.

With regard to the acidity of the bio-oils, FO1/18 had the highest acid number (24.8 mg KOH/g oil) while UCO1/18, UCO2/18, and UCO3/18 had an acid number (AN) between 6.5 and 8.2 mg KOH/g oil. The reference product had the lowest AN (0.02 mg KOH/g oil) compared to the rest of the oils. The acid number of a bio-oil is an important property that directly affects the expected lifetime of engine components by increasing the risk of corrosion. For example, according to marine engine designers and producers, an acid number above 100 mg KOH/g oil is regarded as highly corrosive [23]. According to the oil delivered to these laboratory tests, UCO1/18, UCO2/18, and UCO3/18 have been successfully tested for marine engines without the requirement for any modification of engine components. In contrast, the AN of the fish oil (FO1/18) was above the limit of 15 mg KOH/g oil set by the engine manufacturer, hence testing was not permitted [16]. The content of free fatty acids in the tested oils can have a profound effect on increasing the acid number of the oils.

3.2. Oil Composition

The amount of total free fatty acids and diglycerides in the oil samples were analyzed using gas chromatography (GC). High-performance size exclusion chromatography with an evaporative light scattering detector (HPSEC-ELSD) was used to measure the amount of polymerized triglycerides in the oil samples. In addition, the changes in the composition of the oil samples after 10 days of immersion test were investigated. The results are summarized in Table 2.

Table 2. Comparison of changes in the composition of the original used cooking oils and fish oil samples after 10 days of contact with an iron rod. n.d. is not detected. FFA is free fatty acid.

Sample	Total FFA (mg/g Oil)	Diglycerides (mg/g Oil)	Polymerized Triglycerides (%)
UCO1/18/0 d	29.1	7.08	1.17
UCO1/18/10 d	33.7	7.55	1.50
UCO2/18/0 d	43.3	7.65	1.28
UCO2/18/10 d	45.2	7.83	1.40
UCO3/18/0 d	46.8	7.65	1.34
UCO3/18/10 d	47.0	7.75	1.34
FO1/18/0 d	99.7	9.70	n.d.
FO1/18/10 d	93.9	10.30	n.d.

The GC results, presented in Table 2, indicate that during the 10 days of immersion test, the amount of total free fatty acids and diglycerides for the UCO1/18 sample increased approximately by 16% and 7%, respectively. In addition, the HPSEC-ELSD results showed that the amount of polymerized triglycerides in the UCO1/18 sample significantly increased (28%) during the 10-day test period. For the UCO2/18 sample, the total FFA increase was as low as 4%, for the diglycerides 2.3% and for the polymerized triglycerides 9.4%. For UCO3/18, the amounts of diglycerides and polymerized triglycerides did not markedly change at all during the 10-day test period, whereas the change in the amount of total FFA was insignificant (<1%). Analysis with GC showed that fish oil has the highest total free fatty acid content compared to the used cooking (vegetable) oils. However, unlike UCO1/18, UCO2/18, and UCO3/18, the total amount of FFA in FO1/18 decreased as much as 6% during the 10-day period. This could be explained by the fact that the FFA in the fish oil had quickly undergone autoxidation with an iron rod catalyzing the reaction. On the other hand, the amount of diglyceride in the fish oil increased by almost 6% during the test period of 10 days. Compositional analysis of the COref was also performed using GC-FID and GC-MS. The result indicated that the sample mainly composed of aliphatic hydrocarbons predominantly composed of linear saturated hydrocarbons up to C30 with the largest compounds in the C14 to the C26 range [16]. Detailed oil composition results can be found in Tables S1 and S2.

3.3. Effect of Immersion Time

The effect of the immersion time on the total amount of dissolved iron was tested over a period of 0–10 days. As shown in Figure 2, the amount of iron in the cooking oils seems to increase with increasing immersion time. Among the cooking oils, the maximum effect was exhibited by UCO1/18 and UCO2/18, with the highest content of dissolved iron analyzed at 10 days. On the other hand, for UCO3/18 and COref, the amount of dissolved iron did not show any significant change over the course of 1–10 days. The fish oil sample had the highest amount of dissolved iron (170 ppm, 5 days) compared to all the tested oils; however, the iron content started to decrease when increasing the reaction period beyond five days. The relatively high amounts of dissolved iron the fish oil at all time points could be attributed to the chemical properties of the oil; i.e., the high water content and AN (see Table 1). Water content and acid number typically affect the corrosive behavior of oils.

A comparison of iron concentrations in the oil samples after 10 days of immersion was made using spectrophotometry, inductively coupled plasma-optical emission spectrometry (ICP-OES), and

inductively coupled plasma-mass spectrometry (ICP-MS). As shown in Figure 3, the iron concentrations measured with the spectrophotometric method corresponded well with those measured with ICP-OES and ICP-MS. Since the results for one and the same oil using the three methods were of the same level, the spectrophotometric method was selected for the subsequent experiments as it is a relatively cheap method and, according to the two other methods, provided reliable results.

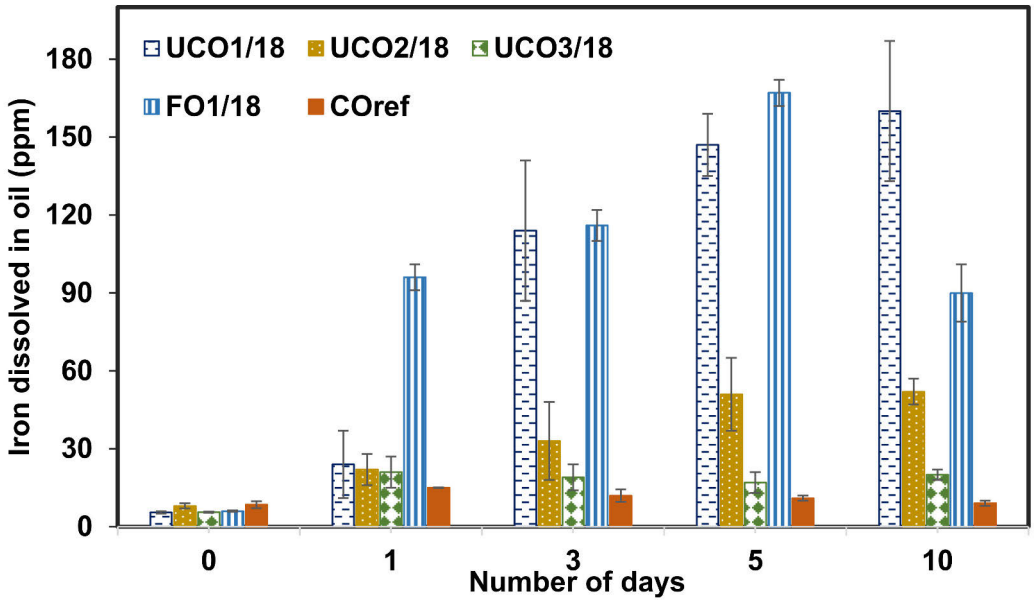

Figure 2. The effect of immersion time on the amount of iron dissolved in the oil samples. Iron concentration was measured spectrophotometrically.

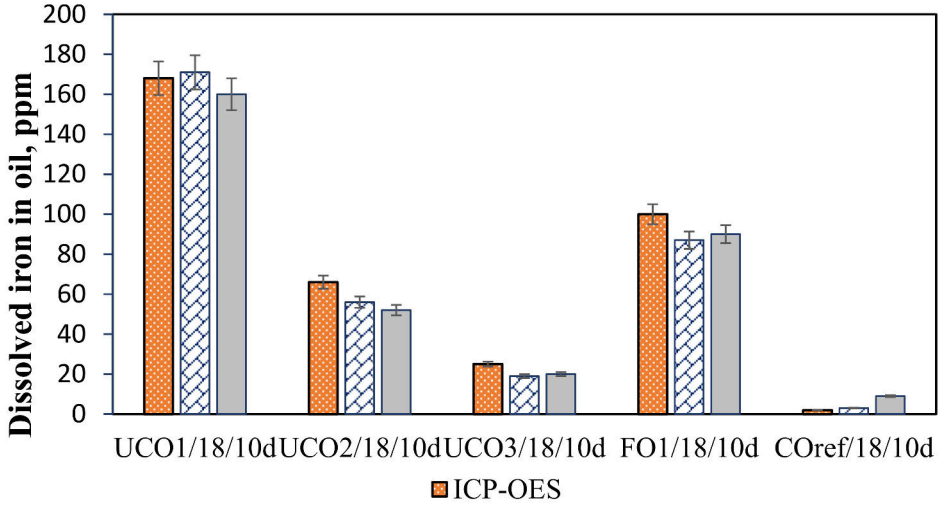

Figure 3. Comparison of dissolved iron from the rods in the experimental and reference oils after 10 days of immersion using different analysis methods.

3.4. Effect of Water Content

The effect of water content of the bio-oils on the concentration of dissolved iron was investigated using the UCO3/18 sample. An amount of 240–5130 ppm water was added to an oil sample of 50 g

and the concentration of dissolved iron was measured spectrophotometrically after three days of immersion. Water content measurements were conducted using the Karl Fischer (KF) titration method. The concentration of iron as a function of the water content in the oil is shown in Figure 4. Iron in the oil increased with the water content up to around 2600 ppm, after which the iron concentration was constant, thus indicating saturation as shown in Figure 4. In general, the water content of the bio-oils has shown to have a direct effect on the amount of iron dissolved, thus enhancing the corrosive property of the bio-oils.

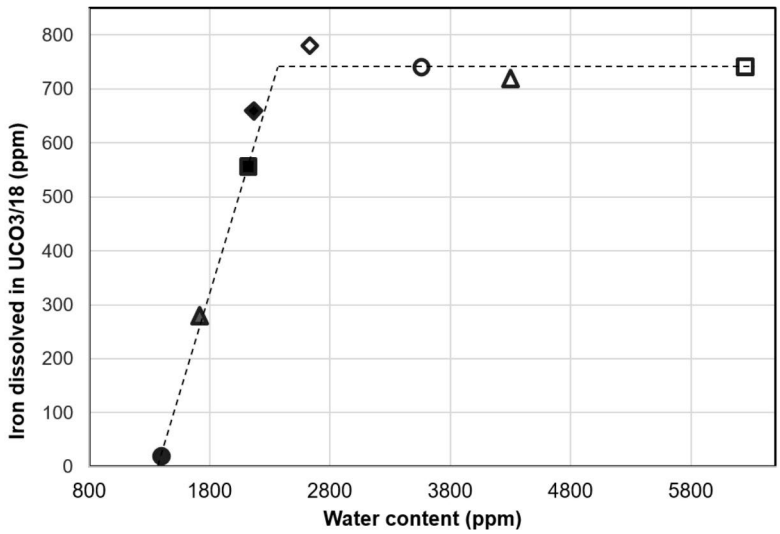

Figure 4. The amount of dissolved iron versus different water contents of used cooking oils (UCO) 3/18 sample after three days of immersion test. The initial water content of the UCO3/18 sample was 1400 ppm.

3.5. Effect of Oleic Acid and Glycerol

The effect of oleic acid and glycerol on the amount of dissolved iron after three days of immersion of iron was investigated using the UCO1/18 and UCO3/18 oils (see Figure 5). For this study, oleic acid (21 mg/g oil) and glycerol (2.31 mg/g oil) were added to give the total units 50 mg/g oil of free fatty acids for UCO1/18 and 68 mg/g oil for UCO3/18. In addition, the combined effect of oleic acid and glycerol (3:1 molar ratio) on the amount of dissolved iron in the UCOs was investigated. According to Figure 5, the addition of oleic acid resulted in a 57% reduction of dissolved iron in both UCOs. Despite a significant reduction in the concentration of iron, the acid number of the used cooking oils was found to increase by almost 50% due to the addition of oleic acid. In contrast to the trends seen for the acid number and water content of the original oils (Table 1), an increase in the acid number did not enhance the dissolution of iron in the oils with added oleic acid. It was assumed that the active surface group in oleic acid had formed a protective film layer at the surface of the iron rod (see Figure 6). The self-assembled monolayer might furthermore prevent corrosion by inhibiting the permeation of both water and oxygen, thus protecting the metal surface from the exposure to the corrosive environment. This is also in agreement with results from the literature according to which surfactants such as oleic acid can be used for protection against corrosion, owing to their ability to form monolayers on the surface of metals [26]. However, it is worth noting that at very low concentrations of oleic acid/surfactants, adsorption of the corrosion inhibitor might be insufficient to form a monolayer, thus allowing corrosion to occur.

The addition of glycerol showed a more profound effect than oleic acid, resulting in 92% and 63% reduction in the amount of dissolved iron in UCO1/18 and UCO3/18, respectively, as shown in Figure 5. This can be due to the fact that glycerol is miscible in water and through microemulsions

keeping the water away from the iron rod [27]. The combined effect of oleic acid and glycerol resulted in comparable values of dissolved iron to those obtained when glycerol was used without oleic acid. Besides its binding effect toward water molecules, glycerol can form microemulsion in the presence of a surfactant such as oleic acid [27]. The formation of a microemulsion produces a thermodynamically stable dispersion system that might have less risk of phase separation in the long term use of bio-oils. It has also been reported that blending glycerol into diesel or gasoline through microemulsification reduced problems associated with stand-alone glycerol fuel use [28,29]. Moreover, glycerol-in-diesel emulsion performed well without fail while showing positive effects on the reduction of unwanted combustion emissions [28,29]. In general, both oleic acid and glycerol considerably reduced the amount of iron dissolved in the oil phase; however, a more predominant effect was observed with glycerol than with oleic acid when protecting the iron rod from corrosion.

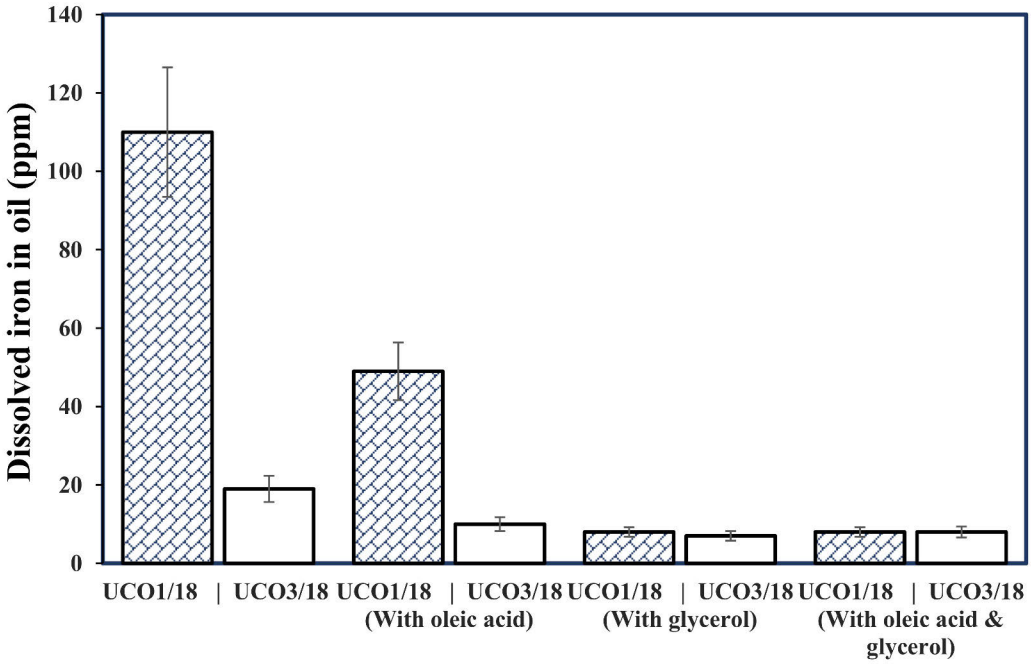

Figure 5. The effect of addition of oleic acid and glycerol on the amount of dissolved iron in the UCO1/18 and UCO3/18 oils during three days of immersion test.

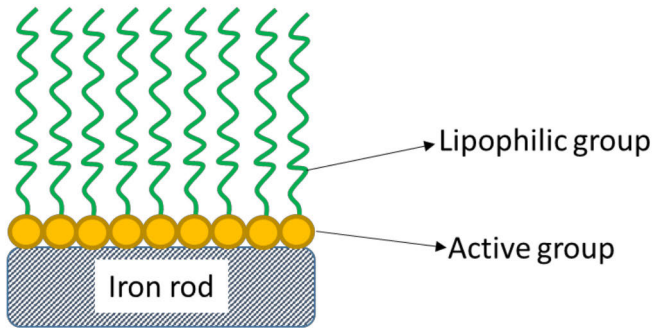

Figure 6. Formation of a monolayer on a ferrous surface. Adapted from [26].

3.6. SEM-EDS Analysis

The SEM images in Figure 7 shows the surface morphology of the original rod and the corroded iron rod after 10 days of exposure to UCO1/18. Figure 7b does not show any large pits and thus suggests a rather uniform corrosion of the rod surface. The iron rod used is a common low carbon steel with a composition of 98.64 wt.% Fe. Future experimental investigations may reveal the effects of different compositions of the test rod on the corrosivity of the bio-oils.

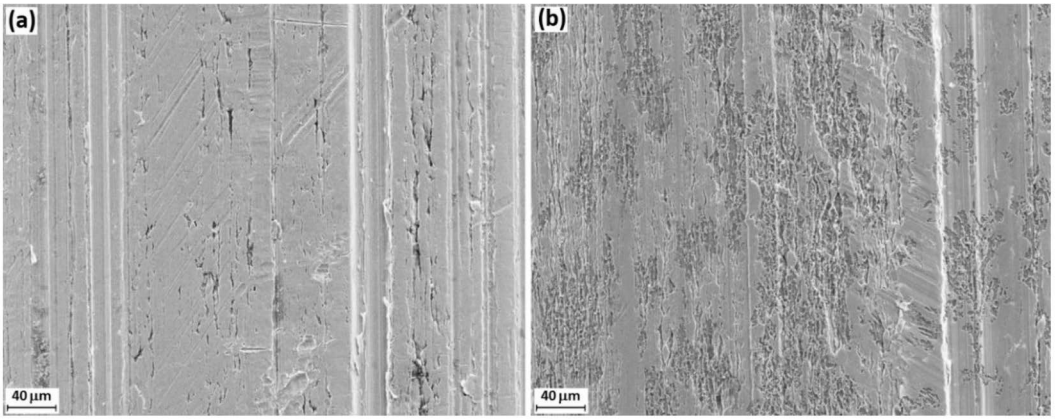

Figure 7. SEM images of (**a**) original surface and (**b**) corroded surface of the iron rod after 10 days of exposure to UCO1/18.

4. Conclusions

The corrosion behavior of used vegetable cooking oils and a non-edible fish oil was investigated by an immersion test with an iron rod at room temperature. A prolonged immersion time, in general, resulted in an increased amount of dissolved iron. The effect of increased water content of the bio-oils on the concentration of dissolved iron was investigated using one of the bio-oils with added water between 240 and 5130 ppm. The results from three days of immersion testing indicated that the amount of dissolved iron in the oil increased with the water content up to 2600 ppm, after which more iron did not dissolve further.

The addition of oleic acid and glycerol had a clear effect in preventing the iron dissolving into the oil. However, the addition of glycerol showed a more profound effect than oleic acid, resulting in up to a 92% reduction in the amount of dissolved iron in the different samples of the used cooking oils. This can be attributed to the characteristics of glycerol to bind water molecules and keep them away from the iron rod surface, thus preventing corrosion. The results also suggest that the blending of glycerol through microemulsification could be a promising approach for reducing problems associated with the corrosive properties of the crude bio-oils.

Water content, acid number, and the overall oil composition were observed to have substantially affected the corrosive behavior of the oils. Among the tested oils, the fish oil and the reference commercial product showed the highest and lowest amounts of dissolved iron, respectively. In general, the dissolved iron concentrations measured spectrophotometrically were in good agreement with those measured by the ICP-OES and ICP-MS techniques. The results observed in this work imply that the immersion test of a low carbon iron rod can be used as a reliable and cost-effective method to compare the corrosive properties of crude bio-oils as well as other biofuels.

Supplementary Materials: The following are available online at http://www.mdpi.com/1996-1073/12/24/4812/s1: Table S1: Composition of used cooking oil samples (0 d and 10 d samples) measured with gas chromatography (mg/g oil). n.d. is not detected (<0.02 mg/g oil); Table S2: Composition of fish oil samples (FO1/18/0 d, FO1/18/10 d), measured with gas chromatography (mg/g oil). n.d. is not detected (<0.02 mg/g oil).

Author Contributions: Conceptualization, N.B. and L.H.; methodology, N.B. and J.H.; formal analysis, N.B., A.G.D. and J.H.; investigation, N.B., A.G.D., J.H. and F.T.; writing—original draft, N.B. and A.G.D.; writing—review & editing, F.T. and L.H.; supervision, F.T. and L.H.; project administration, L.H.; funding acquisition, N.B., L.H. and F.T.

Funding: This research was funded by the Swedish Cultural Foundation in Finland, Business Finland, the European Regional Development Fund INKA SmartResearch project (decision no. 4690/31/2014), the scholarship programme by the Johan Gadolin Process Chemistry Centre at Åbo Akademi University, and the Academy of Finland project "Thermodynamic investigation of complex inorganic material systems for improved renewable energy and metals production processes" (decision no. 311537). The APC was funded by Åbo Akademi University. VG EcoFuel Oy and Neste Oyj are gratefully acknowledged for providing the oil samples.

Conflicts of Interest: The authors declare no conflicts of interest.

References

1. Haseeb, A.S.M.A.; Masjuki, H.H.; Ann, L.J.; Fazal, M.A. Corrosion characteristics of copper and leaded bronze in palm biodiesel. *Fuel Process. Technol.* **2010**, *91*, 329–334. [CrossRef]
2. Ma, F.; Hanna, M.A. Biodiesel production: A review. *Bioresour. Technol.* **1999**, *70*, 1–15. [CrossRef]
3. Daggett, D.; Hadaller, O.; Hendricks, R.; Walther, R. *Alternative Fuels and Their Potential Impact on Aviation*; (Technical Memorandum; NASA/TM-2006-214365); NASA: Cleveland, OH, USA, 2006.
4. Preto, F.; Zhang, F.; Wang, J. A study on using fish oil as an alternate fuel for conventional combustors. *Fuel* **2008**, *87*, 2258–2268. [CrossRef]
5. Ushakov, S.; Valland, H.; Aesoy, V. Combustion and emissions characteristics of fish oil fuel in a heavy duty diesel engine. *Energy Convers. Manag.* **2013**, *65*, 228–238. [CrossRef]
6. Munoz, R.A.A.; Fernandes, D.M.; Santos, D.Q.; Barbosa, T.G.G.; Sousa, R.M.F. Biodiesel: Production, Characterization, Metallic Corrosion and Analytical Methods for Contaminants. *Biodiesel Feed. Prod. Appl.* **2012**, 48. [CrossRef]
7. Johnston, P.A.; Brown, R.C. Evaluation of Bio-oil Corrosion Characteristics. In Proceedings of the 2012 AIChE Annual Meeting, Pittsburg, PA, USA, 28 October–2 November 2012.
8. Hau, J.L.; Yepez, O.J.; Torres, L.H.; Vera, J.R. Measuring naphthenic acid corrosion potential with the Fe powder test. *Rev. Metal.* **2003**, *39*, 116–123. [CrossRef]
9. Tsuchiya, T.; Shiotani, H.; Goto, S.; Sugiyama, G.; Maeda, A. Japanese standards for diesel fuel containing 5% fame blended diesel fuels and its impact on corrosion. *SAE Tech. Pap.* **2006**, *1*, 3303. [CrossRef]
10. Barabás, I.; Todorut, I.-A. Biodiesel Quality, Standards and Properties. In *Biodiesel Quality, Emissions and By-Products*; InTech: Rijeka, Croatia, 2011; pp. 5–12.
11. Kovács, A.; Tóth, J.; Isaák, G.; Kereszténvi, I. Aspects of storage and Determination of bio-oil induced corrosion characteristics of biodiesel. *Fuel Process. Technol.* **2015**, *134*, 59–64. [CrossRef]
12. Kaul, S.; Saxena, R.C.; Kumar, A.; Negi, M.S.; Bhatnagar, A.K.; Goyal, H.B.; Gupta, A.K. Corrosive behaviour of biodiesel from seed oils of Indian origin on diesel engine parts. *Fuel Process. Technol.* **2007**, *88*, 303–307. [CrossRef]
13. Maru, M.M.; Lucchese, M.M.; Legnani, C.; Quirino, W.G.; Balbo, A.; Aranha, I.B.; Costa, L.T.; Vilani, C.; DeSena, L.A.; Damasceno, J.C.; et al. Biodiesel compatibility with carbon steel and HDPE parts. *Fuel Process. Technol.* **2009**, *90*, 1175–1182. [CrossRef]
14. Diaz-Ballote, L.; Lopez-Sansores, J.F.; Maldonado-Lopez, L.; Garfias-Mesias, L.F. Corrosion behaviour of aluminium exposed to a biodiesel. *Electrochem. Commun.* **2009**, *11*, 41–44. [CrossRef]
15. Fazal, M.A.; Haseeb, A.S.M.A.; Masjuki, H.H. Comparative corrosive characteristics of petroleum diesel and palm biodiesel for automotive materials. *Fuel Process. Technol.* **2010**, *91*, 1308–1315. [CrossRef]
16. Bruun, N.; Khazraie Shoulaifar, T.; Hemming, J.; Willför, S.; Hupa, L. Characterization of waste bio-oil as an alternate source of renewable fuel for marine engines. *J. Biofuels* **2019**, 1–10. [CrossRef]
17. Stookey, L.L. Ferrozine—A new spectrophotometric reagent for iron. *Anal. Chem.* **1970**, *42*, 779–781. [CrossRef]
18. Swinehart, D.F. The Beer-Lambert Law. *J. Chem. Educ.* **1962**, *39*, 333–335. [CrossRef]
19. Canakci, M.; Sanli, H. Biodiesel Production from various feedstocks and their effects on the fuel properties. *J. Ind. Microbiol. Biotechnol.* **2008**, *35*, 431–441. [CrossRef] [PubMed]

20. Choi, C.Y.; Reitz, R.D. A numerical analysis of the emissions characteristics of biodiesel blended fuels. *J. Eng. Gas Turb. Power* **1999**, *121*, 31–37. [CrossRef]
21. Wexler, H. Polymerization of drying oils. *Chem. Rev.* **1964**, *64*, 591–611. [CrossRef]
22. European Biomass Industry Association. Transformation of used cooking oil into biodiesel: From waste to resource. In *UCO to Biodiesel 2030*; EUBIA: Brussels, Belgium, 2015.
23. Ollus, R.; Juoperi, K. Alternative Fuels Experiences for Medium-Speed Diesel Engines. In Proceedings of the 25th CIMAC Congress on Combustion Engine Technology, Vienna, Austria, 21–27 May 2007; International Council on Combustion Engines: Frankfurt, Germany, 2007.
24. Mohan, D.; Pittman, C.U., Jr.; Steele, P.H. Pyrolysis of wood/biomass for bio-oil: A critical review. *Energy Fuels* **2006**, *20*, 848–889. [CrossRef]
25. Juoperi, K.; Ollus, R. Alternative fuels for medium-speed diesel engines. *Wärtsilä Tech. J.* **2008**, *1*, 24–28.
26. Komatsu, D.; Souza, E.C.; de Souza, E.C.; Canale, L.C.F.; Totten, G.E. Effect of Antioxidants and Corrosion Inhibitor Additives on the Quenching Performance of Soybean Oil. *Stroj. Vestn. J. Mech. Eng.* **2010**, *56*, 121–130.
27. Leng, L.; Yuan, X.; Zeng, G.; Chen, X.; Wang, H.; Li, H.; Fu, L.; Xiao, Z.; Jiang, L.; Lai, C. Rhamnolipid based glycerol-in-diesel microemulsion fuel: Formation and characterization. *Fuel* **2015**, *147*, 76–81. [CrossRef]
28. Eaton, S.J.; Harakas, G.N.; Kimball, R.W.; Smith, J.A.; Pilot, K.A.; Kuflik, M.T. Formulation and combustion of glycerol–diesel fuel emulsions. *Energy Fuels* **2014**, *28*, 3940–3947. [CrossRef]
29. Mize, E.; Lucio, A.J.; Fhaner, C.J.; Pratama, F.S.; Robbins, L.A.; Karpovich, D.S. Emulsions of crude glycerin from biodiesel processing with fuel oil for industrial heating. *J. Agric. Food Chem.* **2013**, *61*, 1319–1327. [CrossRef] [PubMed]

energies

MDPI

Supplementary Materials

Table S1. Composition of used cooking oil samples (0d and 10d samples) measured with gas chromatography (mg/g oil). n.d. is not detected (<0.02 mg/g oil).

	UCO1/18/0 d	U UCO1/18/10 d	UCO2/18/0 d	UCO2/18/10 d	UCO3/18/0 d	UCO3/18/10 d
Saturated FFA						
C12:0	n.d.	0.04	n.d.	0.02	n.d.	0.07
C14:0	0.04	0.08	0.07	0.09	0.11	0.08
C16:0	2.18	2.42	3.01	3.19	3.41	3.59
C17:0	0.06	0.04	0.10	0.16	0.14	0.06
C18:0	1.04	1.11	1.48	1.53	1.57	1.59
C20:0	0.25	0.32	0.41	0.38	0.32	0.41
C22:0	0.25	0.26	0.28	0.24	0.28	0.27
Unsaturated FFA						
C16:1	0.08	0.15	0.15	0.12	0.12	0.21
C18:2	6.63	7.30	9.65	9.74	10.18	10.24
C18:3	1.77	1.93	2.60	2.56	2.70	2.55
9-18:1	15.15	18.03	23.05	24.02	24.88	25.05
11-18:1	1.13	1.44	1.82	2.23	2.18	2.02
cis-13-21:1	0.33	0.37	0.45	0.59	0.53	0.48
C22:1	0.18	0.21	0.27	0.28	0.38	0.36
Monoglycerids						
MG (1)	0.18	0.09	0.18	0.20	0.23	0.19
MG (2)	0.48	0.50	0.69	0.67	0.95	0.93
MG (3)	1.11	1.14	1.59	1.58	2.18	2.15
Sterols						
cholesterol	0.12	0.12	0.10	0.10	0.09	0.10
campesterol	0.33	0.36	0.28	0.28	0.29	0.28
sitosterol	0.63	0.62	0.57	0.55	0.54	0.57
sitostanol	0.07	0.14	0.11	0.07	n.d.	0.09
Sum saturated FFA	3.8	4.3	5.4	5.6	5.8	6.1
Saturated FFA/Sum FFA	13.1%	12.7%	12.4%	12.5%	12.5%	12.9%
Sum unsaturated FFA	25.3	29.4	38.0	39.5	41.0	40.9
Sum monoglycerides	1.8	1.7	2.5	2.5	3.4	3.3
Sum FFA	29.1	33.7	43.3	45.2	46.8	47.0

Table S2. Composition of fish oil samples (FO1/18/0d, FO1/18/10d), measured with gas chromatography (mg/g oil). n.d.is not detected (<0.02 mg/g oil).

	FO1/18/0 d	**FO1/18/10 d**
Saturated FFA		
C12:0	n.d.	0.11
C14:0	2.76	2.59
C15:0	0.25	0.29
C16:0	6.42	6.19
C17:0	0.12	0.12
C18:0	1.86	1.88
C20:0	0.25	0.19
C22:0	0.25	0.20
Unsaturated FFA		
C16:1	4.01	3.84
C18:3 (1)	0.96	0.80
C18:2	18.5	17.1
C18:3 (2)	5.75	5.10
9-18:1	42.3	41.0
11-18:1	3.53	3.52
cis-5,8,11,14,17-21:5	3.17	2.65
cis-13-21:1	2.93	2.53
5,8,11,14,17-21:5 methyl ester	4.43	3.41
cis-22:1 (1)	1.54	1.52
cis-22:1 (2)	0.69	0.75
Monoglycerids		
MG (1)	0.30	0.35
MG (2)	0.61	0.52
MG (3)	1.74	1.62
Sterols		
Cholesterol	1.58	1.49
Sum saturated FFA	11.9	11.6
Saturated FFA/Sum FFA	11.9%	12.3%
Sum unsaturated FFA	87.8	82.3
Sum monoglycerides	2.6	2.5
Sum FFA	99.7	93.9

Nina Bruun, Fiseha Tesfaye, Jarl Hemming, Meheretu Jaleta Dirbeba
and Leena Hupa

Effect of Storage Time on the Physicochemical Properties of Waste Fish Oils and Used Cooking Vegetable Oils

Energies 2021, 14, 101, 1–14.

III

energies

MDPI

Article

Effect of Storage Time on the Physicochemical Properties of Waste Fish Oils and Used Cooking Vegetable Oils

Nina Bruun *, Fiseha Tesfaye, Jarl Hemming, Meheretu Jaleta Dirbeba and Leena Hupa

Johan Gadolin Process Chemistry Centre, Åbo Akademi University, Piispankatu 8, FI-20500 Turku, Finland; fiseha.tesfaye@abo.fi (F.T.); jarl.hemming@abo.fi (J.H.); meheretu.dirbeba@abo.fi (M.J.D.); leena.hupa@abo.fi (L.H.)

* Correspondence: nina.bruun@abo.fi

Abstract: Waste fish oils (FOs) and used cooking vegetable oils (UCOs) are increasingly becoming alternative renewable fuels. However, different physicochemical aspects of these renewable fuels, including the effect of storage, are not well-known. In this work, the effect of the storage period on physicochemical properties of selected samples of FOs and UCOs was investigated. The bio-oils were stored at 4 °C for up to five years before each experimentation. The chemical properties were characterized using capillary gas chromatography with flame ionization detection (GC-FID) and high-performance size exclusion chromatography including an evaporative light scattering detector (HPSEC-ELSD). Water contents and acid numbers of the bio-oils were determined using the Karl Fischer (KF) titration and the ASTM D 664 methods. Furthermore, the average heating values and surface tension of the bio-oils were determined. According to the results obtained, for all bio-oil types, the concentrations of polymerized triglycerides, diglycerides, and fatty acids and monoglycerides had increased during the storage periods. The physical properties of the bio-oils also showed a small variation as a function of the storage period. The overall results observed indicate that the deterioration of the physicochemical properties of bio-oils can be controlled through storage in dark, dry, and cold conditions.

Keywords: free fatty acid; bio-oil; fuel aging; renewable energy sources

Citation: Bruun, N.; Tesfaye, F.; Hemming, J.; Dirbeba, M.J.; Hupa, L. Effect of Storage Time on the Physicochemical Properties of Waste Fish Oils and Used Cooking Vegetable Oils. *Energies* **2021**, *14*, 101. https://dx.doi.org/10.3390/en14010101

Received: 13 November 2020
Accepted: 24 December 2020
Published: 27 December 2020

1. Introduction

Used cooking vegetable oils (UCOs) and waste fish oils (FOs) are of increasing interest as economic feedstock for bio-oils or biodiesel production. Furthermore, compared to petroleum based oils, they are more eco-friendly [1–8]. However, they have limited oxidative stability as their source is, i.e., fresh vegetable oils [3]. Their contribution to a carbon-neutral energy system is illustrated in Figure 1.

Bio-oils usage in the transport sector is increasing. The usage of waste-derived oils, not in the food production chain, offers a feasible way to increase the share of carbon-neutral fuel alternatives. In the marine sector, sulfur-oxide (SO_x) emissions from engines cause fine dust generations that can lead to serious health issues [9]. The EU is actively promoting and passing legislations for a global maritime emissions cut. Recently, the United Nations specialized agency, the IMO—International Maritime Organization, agreed to reduce shipping greenhouse gas emissions by $\geq$50% until 2050 [10]. According to the revised Sulfur Directive, since the beginning of 2020, maximum sulfur content of marine fuels is reduced to 0.5%, i.e., down from the 2012 Sulfur Directive limit 3.5%, globally [9]. Bio-oils such as UCOs and FOs with a low sulfur content are excellent alternative marine fuels. Thus, the ongoing intensive research related to the bio-oils quality and usage can contribute to the transition towards increasing usage of the eco-friendly fuels.

Vegetable oils, consisting of triglycerides, are used worldwide in restaurants and households for frying food. During frying, the temperature of the oils can reach as high as 190 °C [11], which creates favorable conditions for several reactions to take place within

the oil and its surroundings. The oils' original properties are significantly affected during the frying step as the triglycerides degrade thermally and chemically [11]. In general, three major types of reactions may take place during frying: oxidation, hydrolysis, and thermal degradation of triglycerides [12]. These reactions may result in the formation of free fatty acids (FFAs), glycerol, monoglycerides, and diglycerides. An increase in saturated and monounsaturated fatty acids can also occur [1,11,13–16].

During the frying process, the cooking oils are exposed to moisture, air, and an elevated temperature ($140 < T(°C) < 180$), which cause hydrolytic and oxidation reactions of the oils. The hydrolytic reactions result in diglycerides, FFAs, monoglycerides, and glycerol. The oxidation reactions, which are the main reactions in the presence of air, result in oxidized polymers, dimers, and monomers [2,17–19].

In most cases, tocopherols, dimers of fatty acids, or sterols formed by peroxidation are bridged by oxygen. The oxidation and polymerization reactions that increase the viscosity of UCOs depend on the duration of frying [11,20]. In addition, many toxic substances are formed in the vegetable oils during frying. For this reason, in 2002, the European Commission has forbidden the addition of used cooking oils in animal feed [1]. The concentration of UCOs is increasing worldwide because of a surge in edible oil consumption [1]. UCOs are much cheaper than fresh vegetable oils. They can be directly used as marine engine fuel, for example, or by using a transesterification reaction, in biodiesel production [18] as depicted in Figure 1.

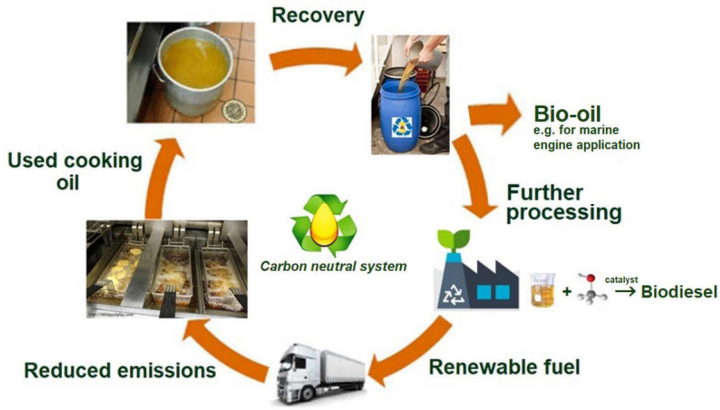

Figure 1. Schematic diagram showing the role of used cooking vegetable oils (UCOs) enabling a carbon neutral energy system.

The storage conditions of bio-oils contribute to the change in quality over time. Research on this topic is relatively fresh; the majority of the previous publications by different authors regarding the effect of storage on bio-oils quality have taken place between the years 2007 and 2019.

Various chemical reactions can occur during the storage of bio-oils and biodiesels constituting FFAs and water [1,21,22]. For UCOs, the FFA value, water content, viscosity, and density are variables that increase compared to fresh vegetable oil [1,23]. Light, heat, and dissolved metal ions are conducive to vegetable oils oxidation and increased acidity. Oxidation begins at the carbon double bond and the reaction mechanism is described as a chain reaction of free radicals [24,25].

Over an extended period, inappropriate storage conditions cause oxidation of oils, which lead to higher viscosity and necessity for filtration prior to use in an engine [26]. When storing bio-oils, the following conditions should be met: impurities removed, cool and constant temperature conditions, and protected from exposure to light (including

sunlight) [26]. To determine the oxidation rate of bio-oils at elevated temperatures, some researchers [3,24,27] conducted experiments in an oven ranging from 80 to 110 °C.

Ushakov et al. [28] demonstrated that crude fish-oils show a higher acidity and viscosity, as well as lower lubricity than conventional diesel fuels. The fish-oils' poor fuel properties could be due to impurities like FFAs (a primary oxidation product), pigments, minerals, moisture, and phospholipids in unrefined fish-oil [29]. Higher FFA and phospholipid levels reduce the fuel quality of fish-oils, requiring additional refining processes, such as degumming and neutralization. Phospholipids in fish-oils polymerize due to heat and build up deposits on the combustion chamber walls and the surfaces of cylinders in engines. The deposits can also clog injectors and valves [26,30]. The hydrolysis of triglycerides in the presence of water may lead to high FFA due to bad feedstock storage conditions. The high FFA cause low stability of oil during storage and corrosion during usage [30,31]. Generally, the water content of bio-oil hinders ignition, decelerates flame propagation, and decreases the heating value [30,32].

Surface tension profoundly influences the product quality of fuels, detergents, inkjet products, lubricants, and pharmaceuticals. In addition, in wetting, penetration, foaming and formation of droplets, surface tension of a liquid have a determinant role [33,34], thus governing a liquid's physicochemical behavior. Surface tension varies with pressure, temperature, and for mixtures, also on the mixture composition. If the fuel is used in internal engines, the injection system's droplet formation and the atomization properties related to the ignition quality are greatly influenced by surface tension [35,36]. Increasing surface tension results in increased spray atomization, which suggests a better mixing of fuel with air [37]. Recently, Morón-Villarreyes et al. [35] measured the surface tension of biodiesels, taking water as a reference liquid utilizing the drop weight technique by applying Tate's Law. Tyowua et al. [38] measured vegetable oils' surface tension by the du Noüy tensiometer method at room temperature. It is a well-known fact that the fuel atomization process that affects the combustion process depend on surface tension. However, there are only limited number of published information regarding the surface tension of UCOs and FOs to be used as unmodified fuels in diesel engines.

In our previous works, the chemical, physical, and thermal properties and corrosivity of fresh UCOs and FOs were analyzed [27,39]. In this work, the storage time effect on the bio-oils' physicochemical and thermal properties was investigated. Samples of the bio-oils were placed in a refrigerator at 4 °C for up to five years before each measurement. In general, the results obtained contribute to the understanding of the impact of storage time on the quality of bio-oils.

2. Materials and Methods

2.1. Materials

The properties and composition of two waste fish oils (FO1-15 and FO1-18) and six used cooking oils (UCO1-15, UCO2-15, UCO3-15, UCO1-18, UCO2-18, and UCO3-18) were measured. The samples were kindly provided by VG EcoFuel Oy (Uusikaupunki, Finland). The numbers after each sample name FO and UCO refer to the batch and the year of delivery, i.e., for example FO1-15 means 1st fish oil sample received in 2015 and UCO1-18 means 1st used cooking oil sample received in 2018. The FOs were produced from the gutting remains of rainbow trout after extracting the edible oil, while the filtered UCOs originated from frying vegetable oils used in restaurants. As a reference for all bio-oils, a commercial product (COref) was used. The composition of COref is mostly aliphatic hydrocarbons, in which the dominant compounds are linear saturated hydrocarbons with composition up to C30, the largest single compounds being in the range C14–C26. The bio-oils were stored over the whole time (from 2 to 5 years) in a refrigerator in white opaque plastic bottles with screw plastic lids at 4 °C before the analyses.

2.2. Methods

2.2.1. Chemical Properties

- Water content and acid number

KF (Karl Fischer) titration with an automatic coulometric titrator (Metrohm 851 Titrando instrument) connected to the oven (860 KF Thermoprep) at 110 °C was used to measure the oils' water content. The bio-oil's acid number (AN) was measured by the ASTM D 664 method using the Solvotrode glass electrode in a Metrohm 888 Titrando. More details of the experimental procedure and equipment used for the water content and AN measurements are given in [39].

- Oil composition

Capillary gas chromatography with flame ionization detection (GC–FID) (Perkin Elmer Autosystem XL) was used to quantify the amount of FFAs and monoglycerides in silylated oil samples. The experimental error for this method is estimated to be ±5%. An Agilent J&W HP-1, 25 m (L) × 0.200 mm (ID) column with film thickness 1.1×10^{-7} m was used. As a carrier hydrogen gas was used with a flow rate of 0.8 mL/min. Details on the oven temperatures and gas flow rates can be found in [39]. By GC-MS analysis with an HP 6890-5973 GC-MSD instrument, the individual components were identified, using as carrier helium gas.

By applying a wide-bore short column GC-FID (PerkinElmer Clarus 500) di- and triglycerides were analyzed. Parameters of the column (Agilent HP-1/SIMDIST) were 0.15 µm (film thickness) and ~6 m (L) × 0.530 mm (ID). Hydrogen was the carrier gas with a flow rate of 7 mL/min. Details of the temperatures in a wide-bore GC-oven and gas flow rates can be found in [39].

- Elemental analyses

High-performance size-exclusion chromatography connected to an evaporative light scattering detector (HPSEC-ELSD, Shimadzu Corporation, Kyoto, Japan, Shimadzu 10A series modular HPLC; and SEDERE SA, ELSD detector, Sedex 85 LT-ELSD), using tetrahydrofuran as eluent, was used to detect polymerized triglycerides, triglycerides, diglycerides, and fatty acids and monoglyceride.

The C and H contents of the FOs, UCOs, and COref were analyzed using a FLASH 2000 organic elemental analyzer from Thermo Scientific (Cambridge, UK). The elemental analysis was performed in the year 2020 for all the oil samples collected during the years 2015 and 2018. Elemental analysis with the organic elemental analyzer was carried out as follows: First, the analyzer was calibrated with organic analytical standards, i.e., methionine, cysteine, sulfanilamide, and BBOT (2,5-Bis(5-tert-butyl-2-benzoxazol-2-yl) thiophene), all from Thermo Scientific (Cambridge, UK). Then, about 2 mg samples of the oils were weighed into tin capsules, which were partly filled with an adsorbent—Chromosorb W/AW from ThermoQuest Italia S.p.A. (Milan, Italy). The adsorbent was used to minimize the loss of volatile organic compounds from the oils during analysis with the analyzer. Next, the tin capsules with the oil samples contained in them were combusted in the combustion chamber of the analyzer. The CO_2 and H_2O gas mixture from the combustion chamber was then separated in the chromatographic column of the analyzer, and the gases were detected by the thermal conductivity detector (TCD) of the analyzer. Finally, the electrical signals from the TCD were processed using Eager Xperience software, version 1.2. For each oil, the experiments were repeated three times, and the average values on a wt% oil basis were reported. Further details of the experimental procedures for the elemental analysis with the organic elemental analyzer are available in [40].

2.2.2. Density, Kinematic Viscosity, and Surface Tension Measurements

By applying a pycnometer, the density of all samples was measured at 21 °C. A Cannon Fenske (reverse flow) viscometer, capillary 511 20, using the ASTM D 2515 method,

in a thermostatic bath at 40 ± 0.5 °C, were applied to measure kinematic viscosity. Each sample was measured in three replications.

The surface tension of the bio-oils was measured using the du Noüy KSV Sigma 70 tensiometer. The electrobalance and the moving mechanism were collected on a PC. For reproducibility checks, the measurements of each sample were conducted three times. Before the measurements, the platinum du Noüy ring was heated to glowing in a blue Bunsen flame and between each measurement purified with ethanol and acetone and dried in contamination-free air. The sample container was purified with ethanol and acetone and dried. The container was filled with 40 mL of bio-oil sample before each surface tension measurement. The temperature during the measurements was 24 °C.

2.2.3. Thermal Properties

The higher heating values (HVs) of the bio-oils were determined by burning them in an adiabatic oxygen bomb calorimeter (model Parr 1341), according to SFS-EN 14918:2009. Bio-oil samples weighing between 400 and 800 mg were put in the bomb calorimeter and charged with oxygen at a pressure of ~30 atm. The experiments were run twice for each sample.

3. Results and Discussion

3.1. Oil Composition

3.1.1. Polymerized Triglycerides, Diglycerides, and Fatty Acids and Monoglycerides

During the two and five years of storage, the polymerized triglycerides, diglycerides, and fatty acids and monoglycerides of all FOs and UCOs had increased (Table 1). Apparent differences were measured for the polymerized triglycerides in FO compared to those in UCOs during the five-year storage period.

Table 1. Summary of the contents of polymerized triglycerides, diglycerides, and fatty acids and monoglycerides in the bio-oils after different storage times using high-performance size exclusion chromatography (HPSEC). n.d. stands for not detected (detection limit < 0.3%).

Sample	Polymerized Triglycerides (%)		Diglycerides (%)		Fatty Acids and Monoglycerides (%)	
	Year of Analysis		Year of Analysis		Year of Analysis	
	2015	**2020**	**2015**	**2020**	**2015**	**2020**
FO1-15	n.d.	4.3	0.3	1.7	0.7	n.d.
UCO1-15	5.6	6	12.6	14.6	4.2	6.1
UCO2-15	5.6	6	13.8	15.3	4.6	6.6
UCO3-15	4.8	6.6	6.2	8.2	1.7	3.1
	2018	**2020**	**2018**	**2020**	**2018**	**2020**
FO1-18	n.d.	1.7	7.6	11.8	10.8	14.0
UCO1-18	1.2	5.7	4.5	10.1	1.1	4.7
UCO2-18	1.3	5.1	5.10	10.3	1.6	4.9
UCO3-18	1.3	6	5.2	10.8	1.6	5.8

No marked differences in the patterns of changes in the polymerized triglycerides or fatty acids and monoglycerides of the UCOs were analyzed after the storage periods (Table 1). In contrast, the changes in the contents of polymerized triglycerides or fatty acids and monoglycerides were not consistent. When comparing the two series, the original batch's oil component share is likely to vary depending on the batch preparation day, thus most likely depending on the raw material variations for the oil.

The increased concentrations of polymerized triglycerides, diglycerides, and fatty acids and monoglycerides could be due to the effect of the storage period on hydrolysis and oxidation reactions in the bio-oils [1,11,13,16,22].

3.1.2. Total Free Fatty Acid

Total FFAs of the bio-oils were analyzed by the GC method with an estimated accuracy of ± 5%. For FO1-15, the change in total FFA between those measured in 2015 and 2020 are insignificant. For the used cooking vegetable oil samples, the overall change in the total FFAs were noticeably outside the experimental error margins and are presented in Figure 2. As can be seen in Figure 2, the total FFAs of the UCOs had decreased in the batches stored for a five-year period. However, the trends after two years for the batches from 2018 did not show consistent results.

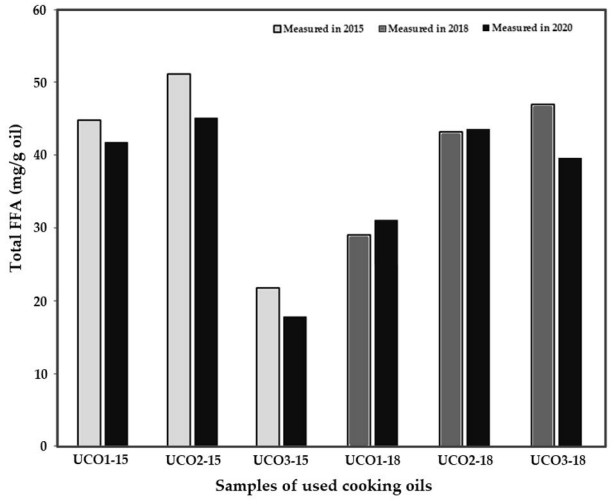

Figure 2. Change in total free fatty acids (FFAs) of different UCOs measured as received and after two and five years' storage.

According to Santos et al. [11], the oxidation and polymerization reactions within the UCOs also depend on the duration of frying prior to the recovery of the UCOs. Differences in the total FFAs for different bio-oil samples before and after the storage were assumed to depend partly on variations in the frying periods. A summary of the total FFAs together with the saturated, unsaturated and monoglycerides obtained by the GC analyses are provided in Table S1.

3.1.3. Acid Number

The ANs for the FOs and UCOs are presented in Figure 3. The AN of the bio-oils was analyzed with the ASTM D 664 method. The highest increase in AN was observed during a two-year storage period for FO1-18, i.e., 2.5 mg KOH/g. The waste fish oil already had a high level of AN (about 25 mg KOH/g oil) when delivered. It did not meet the requirements for the bio-fuels for marine engine applications, with the maximum limit of 15 mg KOH/g oil. AN for the higher quality FO1-15, with the low initial value (1.7 mg KOH/g oil), increased only by 0.8 mg KOH/g oil during the five-year storage period.

For the used cooking vegetable oil UCO1-15, the acid number increased from 8.9 mg KOH/g oil to 11.1 mg KOH/g oil during the five-year storage. For UCO1-18, UCO2-18, and UCO3-18, the AN has increased between 0.5 and 1.3 mg KOH/g oil in two years.

The AN of all bio-oils increased consistently during the two and five year periods of storage. The assumption is, that the increase in acidity depends on the hydrolysis and oxidation reactions [24,41].

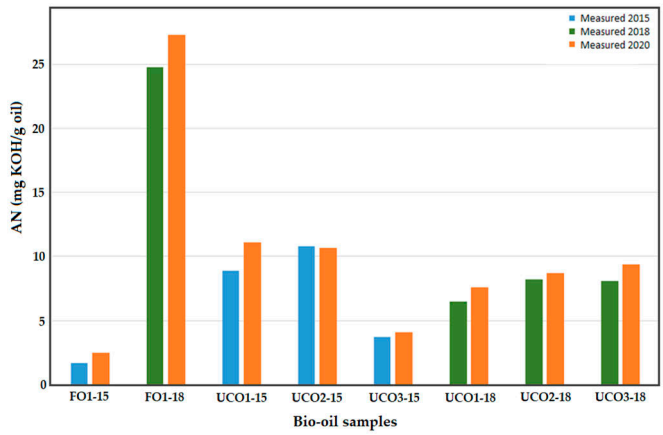

Figure 3. Acid number for bio-oils measured in the years 2015, 2018, and 2020.

The theoretical acid numbers (mg KOH/g oil) were calculated according to Equation (1) using the GC analysis determined total FFAs of the samples. The measured and calculated acid number values as functions of the total measured FFA content are shown in Figure 4. The differences between the measured and calculated values are assumed to depend partly on volatile fatty acids, such as formic acid, acetic acids, or some inorganic acids that are not detected in the GC analysis. Some oil samples, for example, FO1-18 may also include a preservative (formic acid) added against ageing [27]. The total FFA concentrations analyzed using GC (given in Table S1) were converted to theoretical ANs, mg KOH/g oil. All the GC analyses of the oil samples received in 2015 and 2018 were made in 2020.

$$\mathrm{AN}\left(\frac{\text{mg KOH}}{\text{g}}\text{oil}\right) = [\text{Total FFA}]\left(\frac{\text{mmol}}{\text{g}}\right)\cdot 56.1\ \text{mg KOH/mmol} \quad (1)$$

3.1.4. Water Content

The water content for the bio-oil samples was measured with the KF titration method. Generally, the water content of all bio-oils had increased during the storage (Table 2), as also reported by Meng et al. [42]. As shown in Table 2, the water content of FO1-15 had increased by 430 ppm after five years of storage time. The water content in the five-year old UCO samples, UCO1-15, UCO2-15, and UCO3-15, had increased by about 240–560 ppm. The increase in water content of UCO1-18, 111 ppm in two years, was in line with the five-year samples. According to specifications for marine engines, the water content of biofuels must be below 0.2% v/v [43]. Thus, all the samples except for FO1-18 had a water content below this limit, both before and after the storage.

Table 2. Water content of bio-oils measured in the years 2015, 2018, and 2020.

Water Content (ppm)					
	Year			Year	
Sample	**2015**	**2020**	**Sample**	**2018**	**2020**
FO1-15	473	900	FO1-18	2473	2720
UCO1-15	538	1094	UCO1-18	1662	1773
UCO2-15	706	1015	UCO2-18	1449	1734
UCO3-15	740	977	UCO3-18	1403	1686

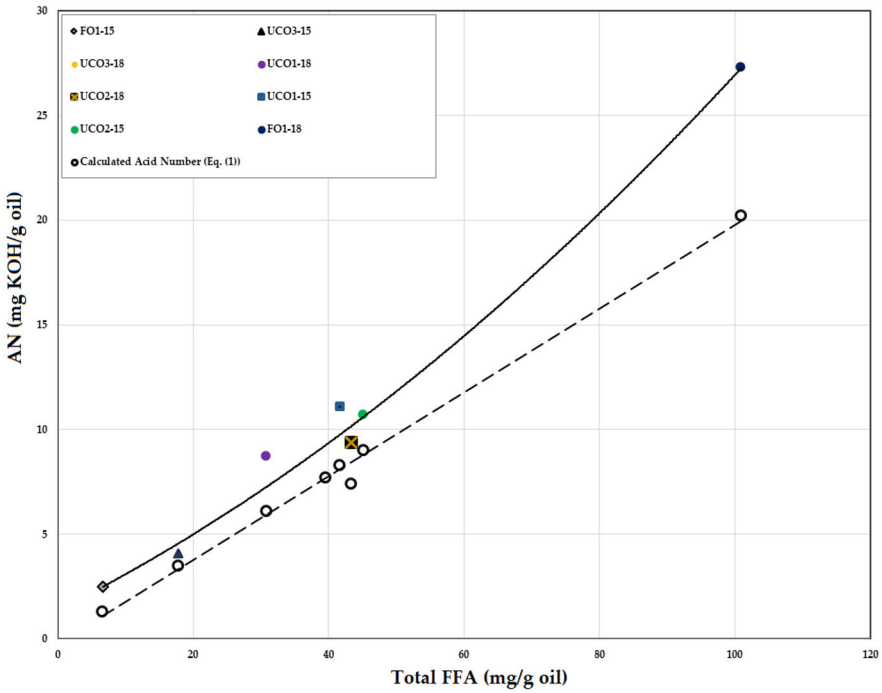

Figure 4. Measured and theoretically calculated acid number (AN) values as functions of the measured total FFA after two and five years' storage. The solid and dashed lines give the least-square fitting of the experimental and calculated values, respectively.

According to Karmakar et al. [44], water molecules are attracted to free fatty acids because of their hygroscopic properties. Mono- and diglycerides also effectively bind water into vegetable oil fuels [45]. This increase of water content with aging could be higher if stored at room temperature and in a relatively open system of storage.

3.1.5. Elemental Composition: H and C Contents of the Oils

Table 3 lists the carbon and hydrogen contents and their ratio on a wt% for the FOs, UCOs, and COref measured with the CHNS-O (carbon, hydrogen, nitrogen, sulfur, and oxygen) elemental analyzer. The C/H-ratio of most oils was in the range of 6.4 to 6.6, independently of the storage time.

The C/H-ratios are typical for triglycerides, such as triolein, trilinolein, tripalmitolein, and tristearin, found in waste fish oils [46,47] and used cooking oils [48].

For COref, consisting of hydrocarbons [27], the carbon and hydrogen concentrations were higher than those in the bio-oils. Our bio-oil studies show that over a maximum of five years there was not much oxidation in our samples, because all the measured H and C contents were on the same level for the bio-oils.

In this work, the values were roughly the same before and after the storage, thus verifying that the amount of volatile species due to oxidation reactions was small in cold storage conditions.

Table 3. H and C contents and mass ratios of the bio-oils and a commercial product analyzed with CHNS-O elemental analyzer. The overall average standard deviation is 0.4.

Sample	C (wt%)	H (wt%)	C to H Ratio (Mass Basis)
FO1-15	79.1	12.1	6.5
FO1-18	76.6	11.8	6.5
UCO1-15	76.8	12.0	6.4
UCO2-15	76.2	11.9	6.4
UCO3-15	76.3	11.9	6.4
UCO1-18	76.4	11.9	6.4
UCO2-18	76.8	11.0	7.0
UCO3-18	76.7	12.0	6.4
COref	86.2	13.1	6.6

3.2. Thermal Properties

HV of the Bio-Oils

All the measured HVs of the oils before and after storage are collected to Table 4. The average heating value of the bio-oils was 39.8 ± 0.3 MJ/kg oil, comparable to the typical value ~40 MJ/kg [49] for heavy fuel oils and biodiesel prepared from waste cooking oils 39.4 MJ/kg [50]. The heating value for the reference oil (COref) is significantly higher, 45.7 MJ/kg oil. According to Capuano et al. [2], used cooking vegetable oils have mean heating values in the range 32.2–41.8 MJ/kg and the average value determined for the bio-oils in this work falls in this range. The HVs of vegetable oils are lower than those of diesel due to high oxygen content [51]. According to Jiménez Espadafor et al. [52] and Hoekman et al. [50], the oxygen atoms in the triglyceride molecules, about 11%, are responsible for a 4% decrease in the heating value. The oxygen atoms in the fatty acids in the bio-oils could explain the circa 12% difference in the HVs compared to aliphatic hydrocarbons COref [27].

The chemical and physical changes during the storage time (maximum five years) had not significantly affected the heating values of the original bio-oils. The studies of Wahyudi et al. [51] on vegetable oils suggest that the oxidation reaction has a noticeable impact on the HVs of the oils. CHNS-O elemental analyses (Table 3) of the bio-oils in this work show that the composition of the bio-oils was not affected over the five years of storage. This is consistent with the negligible changes in the HVs measured after the long storage times.

According to Liu et al. [53], the HV of biodiesel produced from Jatropha curcas showed a marked decrease in an accelerated oxidation test upon the oil-blend oxidation. The atmosphere in our storage conditions was likely to prevent oxidation, thus explaining the almost insignificant changes in the HV over different storage periods.

Table 4. The heating value of the fish oils (FOs) and UCOs samples determined before and after storage periods of two and five years.

Sample	Heating Value (MJ/kg Oil)		Sample	Heating Value (MJ/kg Oil)	
	2015	2020		2018	2020
FO1-15	39.8	40.1	FO1-18	40.3	39.7
UCO1-15	40	39.5	UCO1-18	39.6	40.0
UCO2-15	40	39.6	UCO2-18	39.7	40.0
UCO3-15	39.9	39.8	UCO3-18	39.7	39.7

3.3. Physical Properties

Goodrum and Eitcman [37] indicated that dynamic viscosity, density, surface tension, vapor pressure, and specific heat are the most relevant physical properties of oils.

3.3.1. Density of the Bio-Oils

During the storage periods of the bio-oils, density increased or remained at the same level (Table 5). A relatively small increase was measured for the fish oil FO1-18, which is an increase of 3 kg/m^3 in two years. The only exception was UCO2-18, for which the density decreased slightly from 917 kg/m^3 to 914 kg/m^3 in five years. The water content for the same soil increased by 285 ppm (from 1449 ppm to 1734 ppm, Table 2), which probably can also have affected the density change.

Table 5. Physical properties of bio-oils before and after two and five years of storage.

Sample	Kinematic Viscosity (mm^2/s) 40 °C Year of Analysis		Density (kg/m^3) 21 °C Year of Analysis		Surface Tension (mN/m) Year of Analysis	
	2015	**2020**	**2015**	**2020**		**2020**
FO1-15	31.9	36.4	916	917	-	33.25
UCO1-15	40.6	43.6	914	915	-	32.91
UCO2-15	41.3	43.6	916	916	-	32.99
UCO3-15	44.3	44.1	915	916	-	33.03
	2018	**2020**	**2018**	**2020**		**2020**
FO1-18	26.6	35.7	916	919	-	32.97
UCO1-18	40.7	41.0	916	916	-	33.01
UCO2-18	40.7	40.0	917	914	-	33.14
UCO3-18	40.3	41.7	916	918	-	33.12

3.3.2. Kinematic Viscosity of the Oils

Kinematic viscosities measured for each bio-oil sample at 40 °C showed a tendency of increasing with the storage time (Table 5). The only exceptions are the kinematic viscosities of UCO3-15, UCO1-18, and UCO2-18, which remain within the experimental error range of $\pm$0.7 mm^2/s. For FO1-18, the increase in kinematic viscosities was the highest, 9.1 mm^2/s in two years. The kinematic viscosities of FO1-15, UCO1-15, UCO2-15, and UCO3-18 increased by an average of 2.8 mm^2/s during the storage periods. For the UCO samples, the concentration of polymerized triglycerides had increased during the storage periods (Table 1), thus contributing to the observed viscosity increases.

After examining several different vegetable oils, Sahasrabudhe et al. [54] concluded that the viscosity and density varied depending on the oil type. In contrast, the variations in the types of the oils did not affect the bio-oils' surface tension. The temperature (between 22 and 200 °C) had a significant effect on all three physical properties. At the saturation level, the number of carbon atoms [55] and the configuration of the double bond (cis or trans) [53,56] affect the kinematic viscosity.

3.3.3. Surface Tension

Unlike the density and kinematic viscosity, the surface tension of the bio-oils was measured only in 2020 (Table 5), i.e., bio-oils received in 2015 were measured in 2020, and those received in 2018 were also measured in 2020. The values varied between 32.9 and 33.3 mN/m at 24 °C, with each measurement accuracies of $\pm$0.03 mN/m. The older bio-oils' surface tension values (received in 2015) were consistently lower than those of the more recent bio-oils (received in 2018). Even if the differences between each measured value were not significant (~0.5%), they imply that the storage period has had a minor effect on the bio-oils' overall surface tension.

The narrow range of the surface tension values obtained for the bio-oil samples is consistent with the results observed by Goodrum at al. [37]. They reported that four different triglyceride samples had very close surface tension values. Sahasrabudhe et al. [54] reported similar surface tension values for different samples of vegetable oils. Surface tensions determined by Tyowua et al. [38], using the du Noüy tensiometer method at 25 °C, for sunflower, olive, and rapeseed oils were 32.2, 33.1, and 33.8 mN/m, respectively.

Given that there was a 1 °C temperature difference, the surface tension values reported by Tyowua et al. [38] agree with the FOs and UCOs surface tensions determined in our work.

The surface tension of COref was 30.6 ± 0.007 mN/m at 24 °C, which is out of the bio-oils range. As described in the Materials section, the composition of COref is mostly aliphatic hydrocarbons, including the largest single compounds in the range C14–C26. According to the data available in [57], the surface tension of hexacosane ($C_{26}H_{54}$) was reported to be 28.6 mN/m at 51.8 °C. Considering the general trend of decrease in surface tension with increasing temperature, the measured surface tension of COref is comparable to that of hexacosane ($C_{26}H_{54}$).

3.4. Observations

The physicochemical properties of the bio-oils stored for two and five years showed slow decreasing or increasing trend. Several studies [21,23,45,58,59] suggested that exposure of bio-oils to air, light, traces of metal, elevated temperatures, and moisture can accelerate the deterioration of the properties of bio-oils and/or biodiesels. The observed slow aging of the bio-oils in this work was assumed to depend on the storage conditions: closed plastic bottles, and cold and dark environment. Furthermore, the small physicochemical property changes observed in the cold storage conditions can be considered as an indication of larger changes at elevated temperatures.

4. Conclusions

The effect of a prolonged storage time on the physical, chemical, and thermal properties of fish-oils (FOs) and used cooking oils (UCOs) was investigated. Different analytical techniques were applied to examine the effect of storage on their fuel qualities. Based on the results obtained from the different techniques, the following conclusions were drawn.

After five years storage period, greater changes about 4.3% were measured in the composition of the polymerized triglycerides in FOs than in UCOs. The changes in fatty acids and monoglycerides were smaller in FOs than in UCOs. In general, the total FFAs of the UCOs slightly decreased by ~7.7% during storage. The decrease in the total FFAs for the UCOs was related to the increased concentration of polymerized triglycerides. The acid number and water content of the bio-oils increased slightly during storage. The acid numbers of the bio-oils were well below the fuel quality limit set, e.g., for fuels in marine engines.

The density of the bio-oil samples did not show any marked changes after the storage periods. The kinematic viscosity increased slightly ~7.9% with the storage time. The increases in the polymerized triglycerides during storage may have contributed to the viscosity increase. The surface tension values of the bio-oils implied a minor decreasing trend ~0.5% with prolonged storage time. The average heating value did not significantly change with the storage time. This observation was supported by the unchanged ratio between C and H in oils.

The results confirm that storing bio-oils in dark, cold, and air tight plastic containers can retain their fuel quality specifications through a slowed aging process. However, commercial bio-oils with acceptable fuel qualities for usage are usually stored in tanks where the temperature is not as low as in our experiments; in such cases, the aging process may proceed faster.

Supplementary Materials: The following is available online at https://www.mdpi.com/1996-1073/14/1/101/s1: Table S1. Composition of bio-oils measured with a gas chromatography (mg/g oil).

Author Contributions: Conceptualization, N.B., L.H., and F.T.; methodology, N.B., J.H., and M.J.D.; formal analysis, N.B., J.H., F.T., L.H., and M.J.D; investigation, N.B., F.T., L.H., J.H., and M.J.D.; writing—original draft, N.B. and F.T.; writing—review and editing, L.H., F.T., J.H., and M.J.D.; supervision, L.H. and F.T.; project administration, L.H.; funding acquisition, N.B., L.H., and F.T. All authors have read and agreed to the published version of the manuscript.

Funding: This research was funded by the Swedish Cultural Foundation in Finland, and the Academy of Finland project "Thermodynamic investigation of complex inorganic material systems for improved renewable energy and metals production processes" (decision no. 311537). The APC was funded by Åbo Akademi University. VG EcoFuel Oy and Neste Oyj are gratefully acknowledged for providing the oil samples.

Informed Consent Statement: Not applicable.

Data Availability Statement: Data is contained within the article and its supplementary material.

Conflicts of Interest: The authors declare no conflict of interest.

References

1. Kulkarni, M.G.; Dalai, A.K. Waste cooking oil—An economical source for biodiesel: A review. *Ind. Eng. Chem. Res.* **2006**, *45*, 2901–2913. [CrossRef]
2. Capuano, D.; Costa, M.; Di Fraia, S.; Massarotti, N.; Vanoli, L. Direct use of waste vegetable oil in internal combustion engines. *Renew. Sustain. Energy Rev.* **2017**, *69*, 759–770. [CrossRef]
3. Mannekote, J.K.; Kailas, S.V. The effect of oxidation on the tribological performance of few vegetable oils. *J. Mater. Res. Technol.* **2012**, *1*, 91–95. [CrossRef]
4. Chhetri, A.B.; Watts, K.C.; Islam, M.R. Waste cooking oil as an alternative feedstock for biodiesel production. *Energies* **2008**, *1*, 3–18. [CrossRef]
5. Saeed, R.H.S.; Kassem, Y.; Çamur, H. Effect of biodiesel mixture derived from waste frying-corn, frying-canola-corn and canola-corn cooking oils with various ages on physiochemical properties. *Energies* **2019**, *12*, 3729. [CrossRef]
6. Behçet, R. Performance and emission study of waste anchovy fish biodiesel in a diesel engine. *Fuel Process. Technol.* **2011**, *92*, 1187–1194. [CrossRef]
7. Hemmer, M.; Badent, R.; Ströck, G. Einsatzfähigkeit von Rapsöl als Isoliermedium in Mittelspannungstransformatoren. In *Nachwachsende Rohstoffe für die Chemie 8, Tübingen, Germany, 26–27 March 2003*; Landwirtschaftsverlag: Münster, Germany, 2003; pp. 591–599.
8. Tye, C.T. Recent advances in waste cooking oil management and applications for sustainable environment. In *Handbook of Research on Resource Management for Pollution and Waste Treatment*; Affam, A.C., Ezechi, E.H., Eds.; IGI Global: Hershey, PA, USA, 2020; pp. 47–63.
9. Moirangthem, K. *Alternative Fuel for Marine and Inland Waterways: An Exploratory Study*; European Commission JRC: Luxembourg, 2016; pp. 1–44.
10. European Commission (EC). Reducing Emissions from the Shipping Sector. Available online: https://ec.europa.eu/clima/policies/transport/shipping_en (accessed on 7 December 2020).
11. Santos, J.C.O.; Santos, I.M.G.; Souza, A.G. Effect of heating and cooling on rheological parameters of edible vegetable oils. *J. Food Eng.* **2005**, *67*, 401–405. [CrossRef]
12. Di Pietro, M.E.; Mannu, A.; Mele, A. NMR determination of free acids in vegetable oils. *Processes* **2020**, *8*, 410. [CrossRef]
13. Talbot, G. The stability and shelf life of fats and oils. In *The Stability and Shelf Life of Food*, 2nd ed.; Subramaniam, P., Ed.; Elsevier: Amsterdam, The Netherlands, 2016; pp. 461–503.
14. Marmesat, S.; Rodrigues, E.; Velasco, J.; Dobarganes, C. Quality of used frying fats and oils: Comparison of rapid tests based on chemical and physical oil properties. *Int. J. Food Sci. Technol.* **2007**, *42*, 601–608. [CrossRef]
15. Totani, N.; Yawata, M.; Mori, T.; Hammond, E.G. Oxygen content and oxidation in frying oil. *J. Oleo Sci.* **2013**, *62*, 989–995. [CrossRef]
16. Gnanasekaran, D. Green fluids from vegetable oil: Power plant. In *Vegetable Oil based Bio-lubricants and Transformer Fluids: Applications in Power Plants*; Gnanasekaran, D., Chavidi, V.P., Eds.; Springer Nature: Singapore, 2018; pp. 3–26.
17. Gutiérrez González-Quijano, R.; Dobarganes, M.C. Analytical procedures for the evaluation of used frying fats. In *Frying of Food: Principles, Changes, New Aproaches*; Varela, G., Bender, A.E., Morton, I.D., Eds.; VCH: Weinheim, Germany, 1988; pp. 141–154.
18. Enweremadu, C.C.; Mbarawa, M.M. Technical aspects of production and analysis of biodiesel from used cooking oil—A review. *Renew. Sustain. Energy Rev.* **2009**, *13*, 2205–2224. [CrossRef]
19. Gertz, C.; Klostermann, S.; Kochhar, S.P. Testing and comparing oxidative stability of vegetable oils and fats at frying temperature. *Eur. J. Lipid Sci. Technol.* **2000**, *102*, 543–551. [CrossRef]
20. Tenbohlen, S.; Koch, M. Aging performance and moisture solubility of vegetable oils for power transformers. *IEEE Trans. Power Deliv.* **2010**, *25*, 825–830. [CrossRef]
21. Sazzad, B.S.; Fazal, M.A.; Haseeb, A.S.M.A.; Masjuki, H.H. Retardation of oxidation and material degradation in biodiesel: A review. *Rsc Adv.* **2016**, *6*, 60244–60263. [CrossRef]
22. Demirbas, A.; Karslioglu, S. Biodiesel production facilities from vegetable oils and animal fats. *Energy Sourses Part A* **2007**, *29*, 133–141. [CrossRef]
23. Bouaid, A.; Martinez, M.; Aracil, J. Long storage stability of biodiesel from vegetable and used frying oils. *Fuel* **2007**, *86*, 2596–2602. [CrossRef]

24. Xu, Y.; Qian, S.; Liu, Q.; Wang, Z.D. Oxidation stability assessment of a vegetable transformer oil under thermal aging. *IEEE Trans. Dielectr. Electr. Insul.* **2014**, *21*, 683–692. [CrossRef]
25. Fox, N.J.; Stachowiak, G.W. Vegetable oil-based lubricants—A review of oxidation. *Tribol. Int.* **2007**, *40*, 1035–1046. [CrossRef]
26. Sidibé, S.S.; Blin, J.; Vaitilingom, G.; Azoumah, Y. Use of crude filtered vegetable oil as a fuel in diesel engines state of the art: Literature review. *Renew. Sustain. Energy Rev.* **2010**, *14*, 2748–2759. [CrossRef]
27. Bruun, N.; Khazraie Shoulaifar, T.; Hemming, J.; Willför, S.; Hupa, L. Characterization of waste bio-oil as an alternate source of renewable fuel for marine engines. *Biofuels* **2019**. [CrossRef]
28. Ushakov, S.; Valland, H.; Æsøy, V. Combustion and emissions characteristics of fish oil fuel in a heavy-duty diesel engine. *Energy Convers. Manag.* **2013**, *65*, 228–238. [CrossRef]
29. Yin, H.; Solval, K.M.; Huang, J.; Bechtel, P.J.; Sathivel, S. Effects of oil extraction methods on physical and chemical properties of red salmon oils (Oncorhynchus nerka). *J. Am. Oil Chem. Soc.* **2011**, *88*, 1641–1648. [CrossRef]
30. Blin, J.; Brunschwig, C.; Chapuis, A.; Changotade, O.; Sidibe, S.S.; Noumi, E.S.; Girard, P. Characteristics of vegetable oils for use as fuel in stationary diesel engines—Towards specifications for a standard in West Africa. *Renew. Sustain. Energy Rev.* **2013**, *22*, 580–597. [CrossRef]
31. Jayasinghe, P.; Hawboldt, K. A review of bio-oils from waste biomass: Focus on fish processing waste. *Renew. Sustain. Energy Rev.* **2012**, *16*, 798–821. [CrossRef]
32. Adeoti, I.A.; Hawboldt, K. Comparison of biofuel quality of waste derived oils as a function of oil extraction methods. *Fuel* **2015**, *158*, 183–190. [CrossRef]
33. Lee, B.B.; Ravindra, P.; Chan, E.S. New drop weight analysis for surface tension determination of liquids. *Colloids Surf. A Physicochem. Eng. Aspects* **2009**, *332*, 112–120. [CrossRef]
34. Gianino, C. Measurement of surface tension by the dripping from a needle. *Phys. Educ.* **2006**, *41*, 440–444. [CrossRef]
35. Morón-Villarreyes, J.A.; Soldi, C.; DeAmorim, A.M.; Pizzolatti, M.G.; DeMendonça, A.P., Jr.; D'Oca, M.G.M. Diesel/biodiesel proportion for by-compression ignition engines. *Fuel* **2007**, *86*, 1977–1982. [CrossRef]
36. Graboski, M.S.; McCormick, R.L. Combustion of fat and vegetable oil derived fuels in diesel engines. *Prog. Energy Combust. Sci.* **1998**, *24*, 125–164. [CrossRef]
37. Goodrum, J.W.; Eitcman, M.A. Physical properties of low molecular weight triglycerides for the development of bio-diesel fuel models. *Bioresour. Technol.* **1996**, *56*, 55–60. [CrossRef]
38. Tyowua, A.T.; Targeman, M.; Binks, B.P. Comparison of vegetable oil–silicone oil interfacial tension data from the du Noüy ring and the spinning drop methods. *Niger. Ann. Pure Appl. Sci. Maiden Ed.* **2018**, 209–213. [CrossRef]
39. Bruun, N.; Demesa, A.G.; Tesfaye, F.; Hemming, J.; Hupa, L. Factors affecting the corrosive behavior of used cooking oils and a non-edible fish oil that are in contact with ferrous metals. *Energies* **2019**, *12*, 4812. [CrossRef]
40. Dirbeba, M.J.; Aho, A.; DeMartini, N.; Brink, A.; Mattsson, I.; Hupa, L.; Hupa, M. Fast pyrolysis of dried sugar cane vinasse at 400 and 500 °C: Product distribution and yield. *Energy Fuels* **2019**, *33*, 1236–1247. [CrossRef]
41. Pölczmann, G.; Tóth, O.; Beck, Á.; Hancsók, J. Investigation of storage stability of diesel fuels containing biodiesel produced from waste cooking oil. *J. Clean. Prod.* **2016**, *111*, 85–92.
42. Meng, J.; Moore, A.; Tilotta, D.C.; Kelley, S.S.; Adhikair, S.; Park, S. Thermal and storage stability of bio-oil from pyrolysis of torrefied wood. *Energy Fuels* **2015**, *29*, 5117–5126. [CrossRef]
43. Ollus, R.; Juoperi, K. Alternative fuels experiences for medium-speed diesel engines. In Proceedings of the 25th CIMAC Congress on Combustion Engine Technology, Vienna, Austria, 21–27 May 2007; International Council on Combustion Engines: Frankfurt, Germany, 2007.
44. Karmakar, A.; Karmakar, S.; Mukherjee, S. Properties of various plants and animals feedstocks for biodiesel production. *Bioresour. Technol.* **2010**, *101*, 7201–7210. [CrossRef]
45. Gregg, F. *SVO: Powering Your Vehicle with Straight Vegetable Oil*; New Society Publishers: Gabriola Island, BC, Canada, 2008; pp. 29–79.
46. Yahyaee, R.; Ghobadian, B.; Najafi, G. Waste fish oil biodiesel as a source of renewable fuel in Iran. *Renew. Sustain. Energy Rev.* **2013**, *7*, 312–319. [CrossRef]
47. Wisniewski, A.; Wiggers, V.R.; Simionatto, E.L.; Meier, H.F.; Barros, A.A.C.; Madureira, L.A.S. Biofuels from waste fish oil pyrolysis: Chemical composition. *Fuel* **2010**, *89*, 563–568. [CrossRef]
48. Abidin, S.Z.; Patel, D.; Saha, B. Quantitative analysis of fatty acids composition in the used cooking oil (UCO) by gas chromatography-mass spectrometry (GC-MS). *Can. J. Chem. Eng.* **2013**, *91*, 1896–1903. [CrossRef]
49. Czernik, S.; Bridgwater, A.V. Overview of applications of biomass fast pyrolysis oil. *Energy Fuels* **2004**, *18*, 590–598. [CrossRef]
50. Hoekman, S.K.; Broch, A.; Robbins, C.; Ceniceros, E.; Natarajan, M. Review of biodiesel composition, properties, and specifications. *Renew. Sustain. Energy Rev.* **2012**, *16*, 143–169. [CrossRef]
51. Wahyudi, W.; Nadjib, M.; Bari, M.F.; Permana, F.W. Increasing of quality biodiesel of Jatropha seed oil with biodiesel mixture of waste cooking oil. *J. Biotech Res.* **2019**, *10*, 183–189.
52. Jiménez Espadafor, F.; Torres García, M.; Becerra Villanueva, J.; Moreno Gutiérrez, J. The viability of pure vegetable oil as an alternative fuel for large ships. *Transp. Res. Part D.* **2009**, *14*, 461–469. [CrossRef]
53. Liu, Z.W.; Li, F.S.; Wang, W.; Wang, B. Impact of different levels of biodiesel oxidation on its emission characteristics. *J. Energy Inst.* **2019**, *92*, 861–870. [CrossRef]

54. Sahasrabudhe, S.N.; Rodriguez-Martinez, V.; O'Meara, M.; Farkas, B.F. Density, viscosity and surface tension of five vegetable oils at elevated temperatures: Measurement and modeling. *Int. J. Food Prop.* **2017**, *20*, 51965–51981. [CrossRef]
55. Prankl, H.; Wörgetter, M.; Rathbauer, J. Technical performance of vegetable oil methyl esters with a high iodine number. In Proceedings of the 4th Biomass Conference of the Americas, Oakland, CA, USA, 29 August–2 September 1999.
56. Knothe, G.; Steidley, K.R. Kinematic viscosity of biodiesel fuel components and related compounds. Influence of compound structure and comparison to petrodiesel fuel components. *Fuel* **2005**, *84*, 1059–1065. [CrossRef]
57. Yaws, C.L.; Richmond, P.C. Chapter 21 - Surface tension-Organic compounds. In *Thermophysical Properties of Chemicals and Hydrocarbons*; Yaws, C.L., Ed.; William Andrew Publishing: Norwich, NY, USA, 2009; pp. 686–781. [CrossRef]
58. Bajpai, D.; Tyagi, V.K. Biodiesel: Source, production, composition, properties and its benefits. *J. Oleo Sci.* **2006**, *55*, 487–502. [CrossRef]
59. Das, L.M.; Bora, D.K.; Pradhan, S.; Naik, M.K.; Naik, S.N. Long-term storage stability of biodiesel produced from Karanja oil. *Fuel* **2009**, *88*, 2315–2318. [CrossRef]

Nina Bruun, Juho Lehmusto, Jarl Hemming, Fiseha Tesfaye and Leena Hupa

Metal Rod Surfaces after Exposure to Used Cooking Oils

Sustainability 2022, 14, 355, 1–15.

IV

sustainability

MDPI

Article

Metal Rod Surfaces after Exposure to Used Cooking Oils

Nina Bruun *, Juho Lehmusto, Jarl Hemming, Fiseha Tesfaye and Leena Hupa

Johan Gadolin Process Chemistry Centre, Åbo Akademi University, Henrikinkatu 2, FI-20500 Turku, Finland; juho.lehmusto@abo.fi (J.L.); jarl.hemming@abo.fi (J.H.); fiseha.tesfaye@abo.fi (F.T.); leena.hupa@abo.fi (L.H.)
* Correspondence: nina.bruun@abo.fi

Abstract: Used cooking oils (UCOs) have a high potential as renewable fuels for the maritime shipping industry. However, their corrosiveness during storage and usage are some of the concerns yet to be investigated for addressing compatibility issues. Thus, the corrosion of steels and copper exposed to the UCOs was studied through the immersion of metal rods for different periods. The changes on the rod surfaces were analyzed with a scanning electron microscope (SEM). After the immersion, the copper concentration dissolved in the bio-oils was measured using inductively coupled plasma-optical emission spectrometry (ICP-OES). The free fatty acids and glycerides were analyzed using gas chromatography with flame ionization detection (GC-FID). The acid number (AN), water concentration, as well as density and kinematic viscosity of the bio-oils were determined with standard methods. The UCOs with the highest water content were corrosive, while the oils with lower water concentrations but higher ANs induced lower corrosion. After mixing two different UCOs, the metal corrosion decreased with an increasing concentration of the oil with lower corrosive properties. The lower corrosion properties were most likely due to the monounsaturated fatty acids, e.g., oleic acid in oils. These acids formed a barrier layer on the rod surfaces, thereby inhibiting the permeation of oxygen and water to the surface. Even adding 0.025 wt% of tert-butylamine decreased the corrosivity of UCO against polished steel rod. The results suggested that mixing several oil batches and adding a suitable inhibitor reduces the potential corrosive properties of UCOs.

Keywords: corrosion; inhibitor; used cooking oil; renewable energy sources

Citation: Bruun, N.; Lehmusto, J.; Hemming, J.; Tesfaye, F.; Hupa, L. Metal Rod Surfaces after Exposure to Used Cooking Oils. *Sustainability* **2022**, *14*, 355. https://doi.org/10.3390/su14010355

Academic Editors: Luca Marchitto and Cinzia Tornatore

Received: 14 November 2021
Accepted: 25 December 2021
Published: 29 December 2021

1. Introduction

Used cooking vegetable oils (UCOs) are waste streams and of great interest as renewable fuels. Thus, they neither compete with the food chain nor utilize farmland for their production. These circumstances make UCOs an attractive feedstock for future transportation fuels for maritime shipping, aviation, and material production [1,2]. The current demand of EU and UK for UCOs and UCO-based biodiesel (UCOBD) is 2.8 Mt/y. The maximum worldwide UCO and UCOBD production is predicted to be between 3.1 and 3.3 Mt/y by 2030 [2]. On a global scale, the need for UCOs and UCOBDs is 27–37 Mt/y in 2030 if the projected EU share of UCOBDs in renewable transport fuels is achieved [2].

UCOs are mixtures of triglycerides, diglycerides, monoglycerides, and fatty acids contaminated by derivatives from the food frying process, such as free fatty acids (FFAs), heterocycles, Maillard reaction products, and metal traces originating from pads and food leaching [3–5]. UCOs are also raw materials for other industries, e.g., production of bioplasticizers, syngas, and sorbents for volatile organic compounds (VOCs) [6–8].

In the utilization of UCOs, corrosivity during storage and usage are some of the concerns yet to be investigated for addressing materials compatibility issues with the UCOs. According to the experimental investigation of Fazal et al. [9], on the surface of metals exposed to biodiesel as well as water and oxygen at room temperature and for different periods, corrosion products consisting of metal-oxides, -carbonates, and -hydroxides can

be formed. Figure 1 illustrates the overall phenomena at the interface of a metal and biodiesel as described in literature [9]. Despite the compositional differences between UCO and biodiesel, the same phenomena depicted in Figure 1 could occur also at metal/UCO interfaces under similar conditions.

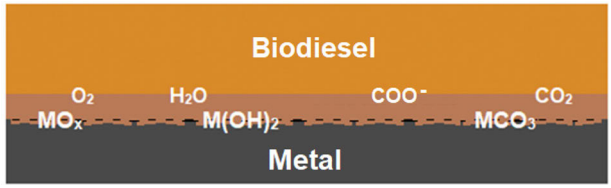

Figure 1. Schematic illustration of the phenomena at the interface of a metal (M) and biodiesel exposed to the atmosphere at room temperature and different periods. COO^- represents short-chain radicals formed by breaking down of long-chain molecules.

Corrosion in fuel tanks, fuel injection systems, and deterioration of the hot parts in the exhaust gas stream originates partly from fuel properties [10]. In petroleum production, oxidation leading to corrosion is controlled by antioxidants, while corrosion inhibitors hinder oxidation through adsorption on reactive sites of potentially catalytic metal surfaces forming a monomolecular layer of the functional group that prevents metal contacting directly with the fuel [11]. For example, an eco-friendly formulation of *Opuntia dillenii* seed oil was reported to act as a corrosion inhibitor to protect iron in an acidic environment, such as acid rain [12]. This oil is a significant source of fatty acids, sterols, and vitamin E, which forms a barrier layer on the iron surface and minimize the contact between the metal surface and the corrosive solution [12].

According to Bruun et al. [13], oleic acid or oleic acid and glycerol additions prevented corrosion of steel rods exposed to UCOs. Fazal et al. [14] reported a significant increase in corrosion rate upon immersion of metals in fossil and biodiesel samples at 27 °C, 50 °C, and 80 °C for 50 days. They concluded that the oxidation instability of the oil contributed to the corrosion mechanism. Immersion tests of metal coupons in various diesel-biodiesel mixtures at 43 °C for two months were carried out by Hu et al. [15]. Their results showed that diesel containing biodiesel components led to a tenfold higher corrosion rate than plain fossil diesel. Copper and carbon steel were the most susceptible to corrosion, while stainless steel showed good resistance [15]. Copper has been found to act as a strong catalyst for oxidizing palm biodiesel [16]. Alves et al. [17] reported that small metal ions released during a stainless steel surface corrosion promoted biodiesel oxidation. Accordingly, the fuel quality and its oxidative stability changed.

Natural additives, such as rosmarinic acid, curcumin, and gingerol, have been found to increase the oxidative stability of soybean biodiesel and the corrosion resistance of carbon steel in the oil [18]. Curcumin was found the best additive concerning oxidative stability, while rosmarinic acid showed better performance as a corrosion inhibitor. The effects were related to the presence of phenolic compounds or oxygen in the molecular structures of these compounds [18].

Polar amine groups in amine-based inhibitors have been reported to be capable of ionizing at interfaces and adsorbing heterocyclic moiety via nitrogen atoms, which enhanced corrosion inhibiting properties of metal surfaces [19,20]. Well-known corrosion inhibitors include organic compounds that contain nitrogen, oxygen, or sulfur atoms, heterocyclic compounds, and pi electrons [21]. The polar functional groups present in inhibitors are considered the center of reaction for adsorption [22]. Water content, temperature, microbial growth, and raw material used for biodiesel production influence the corrosion rate. The amount of unsaturated free fatty acid in the raw material for biodiesel production has a high impact on the oxidation rate. The metals commonly used in compression

ignition engines, such as copper and copper alloys, steel, and aluminum, are prone to corrosion [23,24]. Inhibitors ethylenediamine, tert-butylamine (TBA), and n-butylamine formed a stable metal oxide protective layer and thus retarded the corrosion in biodiesel [23,25].

In our previous works, the chemical, physical, and thermal properties and the effect of storage time on the corrosivity of bio-oils were investigated [13,26,27]. The corrosiveness of different bio-oils during storage and usage are some of the concerns yet to be investigated for addressing compatibility issues. Thus, the corrosion of steels and copper exposed to the UCOs was studied through the immersion of metal rods for different periods. This work aimed to find out whether different UCO batches have variations in their corrosive properties. Additionally, preliminary studies of the corrosivity of oil mixtures and adding a corrosion inhibitor to the most corrosive batch were carried out.

2. Materials and Methods

Eight freshly processed cooking oils (UCO1–UCO8) collected from fast food companies were received from VG EcoFuel Oy (Uusikaupunki, Finland) and studied in detail. In the abbreviations of the oils, numbers presented different oil batches. All used cooking oils are vegetable-based and filtered. Prior to the experiments, the oils were stored in a refrigerator.

TBA (98%), used as a corrosion inhibitor, was purchased from Sigma-Aldrich (Saint Louis, MO, USA). The other chemicals used for chemical analyses are described in [13,26,27]. All chemicals and solvents used in the experiment were of analytical reagent grade.

Capillary gas chromatography with flame ionization detection (GC-FID) (Perkin Elmer Autosystem XL (Waltham, MA, USA)) was used to quantify the amount of FFAs and monoglycerides in silylated oil samples. The experimental error for this method is estimated to be ±5%. An Agilent J&W HP-1 (Santa Clara, CA, USA), 25 m (L) × 0.200 mm (ID) column with film thickness 0.11 μm was used. Hydrogen was used as a carrier gas with a flow rate of 0.8 mL/min. Details on the oven temperatures and gas flow rates can be found in [13]. The individual components were identified by capillary gas chromatography-mass spectrometry (GC-MS) analysis with a Hewlett-Packard (HP) 6890-5973 GC-quadrupole-MSD instrument (Palo Alto, CA, USA), using helium as carrier gas.

By applying a wide-bore short column GC-FID (PerkinElmer Clarus 500 (Waltham, MA, USA)), di- and triglycerides were analyzed. Dimensions of the column (Agilent HP-1/SIMDIST (Santa Clara, CA, USA)) were 0.15 μm (film thickness) and 6 m (L) × 0.530 mm (ID). Hydrogen was the carrier gas with a flow rate of 7 mL/min. Details of the temperatures in a wide-bore GC oven and gas flow rates can be found in our previous study [13].

Karl Fischer (KF) titration with an automatic coulometric titrator (Metrohm 851 Titrando instrument (Herisau, Appenzell Ausserrhoden, Switzerland)) connected to an oven (860 KF Thermoprep (Herisau, Appenzell Ausserrhoden, Switzerland)) was used to determine the water content of the oils. In the measurements, 100 mg of the sample sealed in a glass tube was studied. The KF measurements were performed under a dry N2 gas atmosphere flowing with a rate of 90 mL/min. The water release of the UCOs was measured at 110 °C three times for each sample.

ASTM D 664 method using Metrohm 888 Titrando (Herisau, Appenzell Ausserrhoden, Switzerland) titrator with the Solvotrode glass electrode (Affoltern, Zürich, Switzerland) was applied to measure the acid number (AN) of the UCOs. Samples of the bio-oils were dissolved in 125 mL of a solution of toluene, propan-2-ol, and deionized water (500:495:5 *v*/*v*/*v*) and then titrated with 0.1 M KOH in propan-2-ol. The amount of KOH in propan-2-ol was determined by titration of potassium hydrogen phthalate. The blank test was carried out three times. The theoretical AN was calculated according to a previous study, where the GC analysis results of the total FFA concentrations were converted to theoretical ANs, mg KOH/g oil [27].

The density of all the samples was measured at 21 °C using a 100 mL pycnometer (Wertheim, Baden-Württemberg, Germany). The kinematic viscosity was measured using a Cannon–Fenske (reverse flow) viscometer (Hofheim am Taunus, Hesse, Germany), capillary 51120, using the ASTM D 2515 method in a thermostatic bath at 40 ± 0.5 °C. Three analyses for each sample were performed.

2.1. Experimental Setup and Procedure

2.1.1. Immersion Test

An immersion test was applied at room temperature to investigate the corrosive behavior of UCOs in contact with steels and copper rods. The experiments were performed in test tubes of 15 mL mounted on a rotary mixer rotated at a constant speed of 56 rpm. The rod was placed in a 7-mL oil sample, and the test was conducted over a period of 1, 3, 5, and 10 days (1 d, 3 d, 5 d, and 10 d). During the experiments, the samples were wrapped with duct tape to avoid exposure to light. After the immersion test, the rod was removed from the oil and cleaned ultrasonically using a mixture of toluene and 2-propanol (1:1 *v*/*v*). The oils from each experiment were subjected to liquid-liquid extraction using 1 mL of sulfuric acid (95%) and 8 mL of deionized water in a test tube, then vigorously shaken for 1 min. After the extraction, the mixture was filtered using WhatmanTM quantitative filter paper grade No 42 (ashless, Whatman International Ltd., Maidstone, UK), and the aqueous solution was taken for subsequent spectrophotometric analysis. Each experiment was repeated in triplicates.

The polished rods were used to maximize the interaction between the oil and the surface, thus giving us a good starting point to study corrosion. Unpolished samples were used to mimic real-life situation. Mild-annealed steel was used to study the effect of alloying on corrosion resistance.

The capability of the corrosion inhibitor TBA to suppress the corrosivity of bio-oils was investigated using a polished steel rod exposed to three different concentrations of TBA in UCO2 for three days.

Copper was chosen for the immersion test, as it is used in internal combustion engine systems, and gaskets utilize copper-based alloys and copper, respectively [24]. According to [28], copper may oxidize biodiesel and generate sediments.

2.1.2. Metal Rods

The steel rod (98.64 wt% Fe, 1.00 wt% Mn, 0.21 wt% Si, 0.11 wt% C, 0.03 wt% P, and 0.02 wt% S) used in the immersion tests was a H44 all-round welding rod with a diameter of 1.6 mm, obtained from AGA (Finland). The mild annealed steel rod (98.79 wt% Fe, 1.0 wt% Mn, 0.15 wt% Si, and 0.06 wt% C) and the copper rod (99.9 wt% Cu) had 1.5 and 1.0 mm diameters, respectively. All rods were cut in 85-mm long pieces, and the ends were polished to a similar roughness (visually) as the surfaces of the rod.

Surface polishing of the steel rod was carried out to standardize the starting point for the experiments. The surface was polished first with grinding paper Buehler CarbiMetTM, Grit 280 [P320], and then with Buehler-Met® II, Silicon Carbide grinding paper, Grit 360 [P600].

2.1.3. Dissolved Metal Ions in Oils

The amount of iron dissolved in oils during the experiment was determined using a spectrophotometer (Perkin-Elmer Lambda 25 (Waltham, MA, USA)) by analyzing the amount of total dissolved iron in the aqueous phase after the liquid-liquid extraction step. The spectra were measured between 400 and 600 nm with a scan rate of 480 nm·min^{-1} using a quartz cuvette with a one cm path length.

After the immersion tests with copper rods, dissolved copper in the bio-oils was measured using inductively coupled plasma-optical emission spectrometry (ICP-OES, Perkin Elmer Optima 5300 DV (Waltham, MA, USA)). HNO_3 (65%) and H_2O_2 were added

to digest the sample in a microwave oven (Anton Paar, Multiwave 3000 (Graz, Styria, Austria)). Three analyses were performed of each immersion solution.

2.1.4. Metal Surface Morphology after Oil Exposure

The corrosion on the surfaces of the steel, mild annealed steel, and copper rods was analyzed with a scanning electron microscopy (SEM) LEO Gemini 1530 (Oberkochen, Baden-Württemberg, Germany) with a Thermo Scientific Ultra Dry Silicon Drift Detector—SDD (Madison, WI, USA).

3. Results and Discussion

3.1. Physicochemical Properties

3.1.1. Diglycerides, Free Fatty Acids, and Monoglycerides

First, the differences in the contents of diglycerides, FFAs, and monoglycerides of the eight UCOs were analyzed. There were no big differences in the amounts of diglycerides (mean value 6.9%), FFAs (mean value 3.3%), and monoglycerides (mean value 0.3%). The rest of the analyzed compounds were triglycerides. The mean value and variations of the saturated and unsaturated free fatty acids and monoglycerides are given in Table 1. Detailed composition of the total FFAs of the UCOs can be found in Table 2. The total FFA values were significantly elevated, especially for UCO8 and UCO5 and probably also for UCO4 (assuming the normal FFA level between 27–28.4 mg/g (Table 2)) since the differences were bigger than 5%. The total FFA values and the AN values (Table 3) indicate similar trends consistently. The unsaturated fatty acid, oleic acid (9-18:1), was 21.7 mg/g in UCO8 and 18.7 mg/g in UCO5. In UCO4, oleic acid was analyzed to be 16.9 mg/g.

Table 1. Total FFA, total saturated FFA, total unsaturated FFA, and total monoglycerides in UCO1-UCO8 samples with capillary column GC-FID.

GC Analysis	Mean Value (mg/g)
Total saturated FFA	3.5 ± 0.7
Total unsaturated FFA	26.6 ± 3.6
Total monoglycerides	1.6 ± 0.6
Total FFA	30.1 ± 3.6

Table 2. Composition of used cooking oil samples UCO1–UCO8 measured with gas chromatography (mg/g oil). n.d. is not detected.

Analyzed Compositions	UCO1	UCO2	UCO3	UCO4	UCO5	UCO6	UCO7	UCO8
Saturated FFA								
C14:0	0.06	0.06	0.04	0.04	0.05	0.05	0.04	0.06
C16:0	1.88	1.82	1.71	1.79	1.80	1.73	1.65	2.14
C17:0	0.07	0.04	0.06	0.07	0.05	0.04	0.07	0.04
C18:0	2.10	2.21	0.72	0.77	0.82	0.72	0.72	0.92
C20:0	0.24	0.25	0.22	0.24	0.26	0.20	0.23	0.28
C22:0	0.19	0.19	0.15	0.16	0.20	0.16	0.15	0.18
Unsaturated FFA								
C16:1	0.07	0.09	0.09	0.08	0.09	0.08	0.08	0.09
C18:3	1.34	1.27	1.57	1.66	1.81	1.48	1.50	2.06
C18:2	5.33	5.41	6.09	6.48	7.20	5.91	6.24	8.36
9-18:1	14.9	14.8	16.0	16.9	18.7	15.24	15.93	21.71
11-18:1	1.84	1.82	1.10	1.20	1.24	0.94	0.97	1.32
cis-13-21:1	0.22	0.24	0.29	0.31	0.35	0.29	0.27	0.40
C20:5	n.d.	n.d.	0.10	0.08	0.10	0.02	0.04	0.03

cis-22:1	0.20	0.22	0.17	0.19	0.18	0.10	0.14	0.20
Monoglycerids								
MG(1)	0.10	0.11	0.11	0.17	0.16	0.08	0.17	0.27
MG(2)	0.29	0.28	0.36	0.41	0.54	0.19	0.40	0.65
MG(3)	0.89	0.88	1.02	1.11	1.49	0.50	1.11	1.67
Sterols								
cholesterol	0.13	0.10	0.20	0.10	0.11	0.15	0.08	0.11
farnesol	0.18	0.20	0.19	0.19	0.17	n.d.	n.d.	n.d.
campesterol	0.41	0.42	0.44	0.42	0.41	0.43	0.41	0.38
sitosterol	0.70	0.72	0.71	0.64	0.66	0.71	0.72	0.67
sitostanol	0.06	0.06	0.06	0.03	0.05	0.05	0.05	0.06
Total saturated FFA	4.55	4.58	2.90	3.07	3.18	2.91	2.85	3.61
Saturated FFA/Total FFA	16.0%	16.1%	10.3%	10.2%	9.7%	10.8%	10.2%	9.6%
Total unsaturated FFA	23.9	23.8	25.4	26.9	29.7	24.0	25.2	34.2
Total monoglycerides	1.28	1.28	1.49	1.69	2.19	0.77	1.68	2.58
Total FFA	28.4	28.4	28.3	30.0	32.9	27.0	28.0	37.8

Table 3. Water content, theoretical and measured acid numbers, and concentration of Fe in oils after immersing polished iron rods for three days. The values are averages of three parallel measurements.

Sample	Water Content	Theoretical AN	Measured AN	Immersion Test (3 d)
	(ppm)	(mg KOH/g Oil)	(mg KOH/g Oil)	Fe (ppm)
UCO1	1850	5.7	6.9	12
UCO2	1776	5.7	6.5	389
UCO3	2180	5.6	6.9	102
UCO4	2067	6.0	7.0	14
UCO5	2493	6.5	8.0	74
UCO6	3748	5.4	6.7	449
UCO7	3089	5.6	6.9	571
UCO8	2664	7.5	8.8	59
		Mean value		
UCO1–UCO8	2483	6	7.2	209

3.1.2. Water Content

The water content of the oils is given in Table 3. In general, the water content of only two oils was less than the specification limit, 0.2% *v*/*v* [10] for marine engines. FFAs attract water molecules because of their hygroscopic properties. Additionally, mono- and di-glycerides also bind water into vegetable oil fuels [29,30]. Thus, corrosion of the equipment and tanks during the storage can occur if using such oils [26,31]. Therefore, high water content should be taken into account, and strategies for dewatering in tanks should be planned. It was noticed that the visual appearance of the bio-oils (UCO3-UCO8) with a water content >2000 ppm was turbid, while the oils with water content below 2000 ppm looked clear.

3.1.3. Theoretical Acid Number

The theoretical ANs (mg KOH/g oil) were calculated according to Equation (1), and the values are shown in Table 3. When analyzing the total FFA concentrations, no volatile

fatty acids, like formic or propionic acids, were detected. These compounds are sometimes added as preservatives to bio-oils [27].

$$\mathrm{AN}\left(\frac{\text{mg KOH}}{\text{g}}\text{oil}\right) = [\text{Total FFA}]\left(\frac{\text{mmol}}{\text{g}}\right) \cdot 56.1 \text{ mg KOH/mmol} \quad (1)$$

3.1.4. Measured Acid Number

The average measured ANs are shown in Table 3. For all oils, the measured values were higher than the calculated theoretical values. The difference can partly depend on volatile fatty acids not seen in the FFA measurement.

Although UCO8 showed high AN values and relatively high water content, the concentration of dissolved iron was low. Considering that AN value <5 mg KOH/g oil implies a minimal corrosion risk, all the oils should have induced some corrosion [10]. On the other hand, the AN values were well below the 15 mg KOH/g oil, a limit set by the engine manufacturers. Notably, the highest concentrations of iron in oils (UCO6 and UCO7) correlate with water contents. In contrast, UCO2 had a low water content and intermediate acid number but showed a relatively high concentration of iron after the immersion test. This implies that the corrosive properties cannot directly be correlated with the water content and acid number.

3.1.5. Density and Kinematic Viscosities of the Bio-Oils

The densities of the UCO1–UCO8 samples analyzed at 21 °C varied only slightly with the average value of 916 ± 1.3 kg/m^3, which is lower than the density of water, 998 kg/m^3. According to the marine diesel engines manufacturer, the density of the liquid biofuel for four-stroke engines should be lower than 991 kg/m^3 [10].

The kinematic viscosities of UCO1-UCO8 analyzed at 40 ± 0.5 °C showed only slight variations with an average value of 39.4 ± 0.3 mm^2/s. The higher kinematic viscosity values of the UCOs compared to a refined commercial product (9.1 mm^2/s) could be due to impurities like starch, polymerized triglycerides, and meat traces [26].

3.2. Corrosion of the Metal Surfaces

3.2.1. Iron-Based Rods

Iron concentration dissolved from the unpolished reference steel rod surfaces into UCO2 increased during the test from 58 ppm (1 d), 84 ppm (3 d), 308 ppm (5 d) to 370 ppm (10 d) (see Figure 2). The values are averages of three parallel samples. For polished steel rod, the iron concentration dissolved into UCO2 first increased up to 5 d (406 ppm) but then decreased to 351 ppm at 10 days. A similar increasing trend during the five first days followed by a lower concentration at 10 days was measured for mild annealed polished steel rods in UCO2. In general, lower ion concentrations were measured for the mild annealed steel rods than for the polished steel rods.

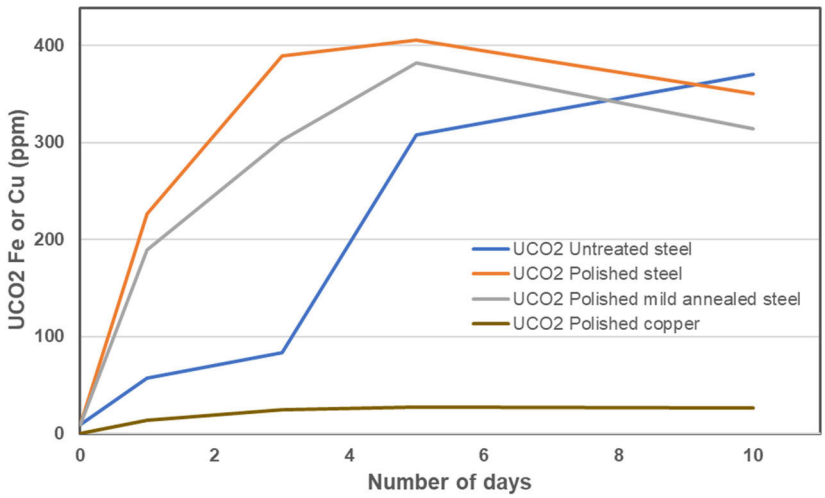

Figure 2. Changes in iron and copper concentrations dissolved from untreated and polished steel rods, polished mild annealed steel rods, and polished copper rods into UCO2 as a function of exposure time. The cumulative error for the measured values is 3%.

For the polished samples, the dissolved iron concentration increased up to five days, after which the amount of dissolved iron started slowly decreasing. The decrease suggested formation of iron-containing precipitates. This was, however, not verified. Unlike the polished samples, iron continued dissolving from the untreated steel rod, probably because the dissolved iron concentration did not reach saturation during the experiment. No precipitates could be verified on the rod surfaces nor in oils.

The SEM secondary electron images in Figure 3 show the surface morphology of an untreated steel rod, a polished steel rod, and a polished annealed steel rod. The unpolished steel, polished steel, and polished mild anneal steel rod surfaces are shown in Figure 3A–C. The surface morphology of the steel rods is rather even before corrosion. However, polishing gives steep scratches on the surfaces. After immersion for 10 days, the surface morphologies are smoother (Figure 3D–F). As seen in the SEM images, the oil exposure clearly affected the surface morphology of rods, thus suggesting corrosion. This is in agreement with the measured ion concentration in the oil after the exposure.

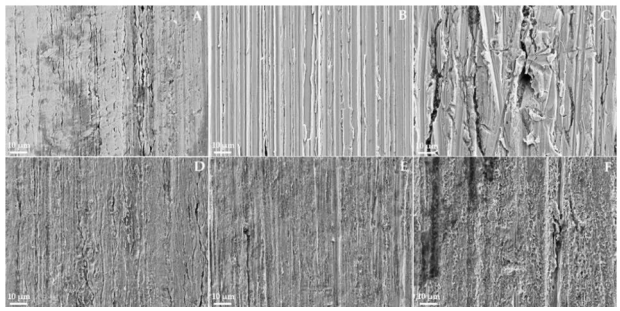

Figure 3. SEM images before oil exposure of (**A**) untreated steel, (**B**) polished steel, and (**C**) polished mild annealed steel. SEM images after 10 days of exposure to UCO2 (**D**) untreated steel, (**E**) polished steel, and (**F**) polished mild annealed steel.

- Iron Concentrations Dissolved from the Rods

Table 4 shows the relative concentrations of iron dissolved from polished steel rods into the different oil batches at different time points. If the measured concentration was less than 50 ppm, the dissolution was considered low (L). Again, concentrations higher than 200 ppm indicated high dissolution (H), while the concentration in between was considered as medium dissolution (M). The average iron concentration in the oils before the exposures was around 8 ppm. UCO1 and UCO4 dissolved a very low iron concentration (8–14 ppm); the reason for this could be that their water concentration is the lowest, and FFAs concentration is among the highest. UCO3, UCO5, and UCO8 dissolved a medium iron concentration (50–199 ppm). The water concentrations were between 2200–2700 ppm, and the ANs were highest compared to the other oils.

Table 4. Relative iron dissolution from polished steel rods into different UCO batches. L, low (8–49 ppm); M, medium (50–199 ppm); H, high (200–600 ppm); n.a., not analyzed.

No. of Days	UCO1	UCO2	UCO3	UCO4	UCO5	UCO6	UCO7	UCO8
1d	L	H	M	n.a.	M	n.a.	n.a.	n.a.
3d	L	H	M	L	M	H	H	M
5d	L	H	L	n.a.	M	n.a.	n.a.	n.a.
10d	L	H	L	n.a.	M	n.a.	n.a.	n.a.

UCO2, UCO6, and UCO7 dissolved a high iron concentration (200–600 ppm). For UCO6 and UCO7, the water content was the highest, between 3100–3750 ppm, and for UCO2, the water content was 1800 ppm, which was also close to the maximum approved level of 2000 ppm of water in oil [10]. The ANs were 6.5–6.9 mg KOH/g oil, which was lower compared to UCO5 and UCO8 samples' ANs (8–8.8 mg KOH/g oil).

The immersion test for three days with a polished steel rod showed higher corrosivity of UCO2, UCO6, and UCO7 (200–600 ppm) but the medium level of corrosivity (50–199 ppm) with UCO3, UCO5, and UCO8 (see Figure 4). In contrast, UCO1 and UCO4 showed the lowest corrosivity (8–49 ppm).

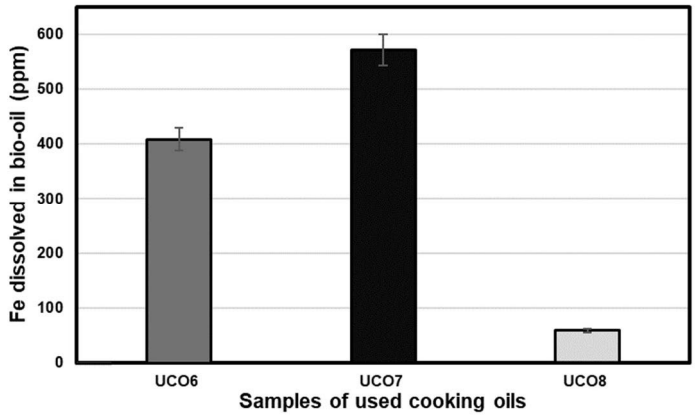

Figure 4. Iron concentration in UCO6, UCO7, and UCO8 after three days in contact with polished steel rods.

Results of the immersion test for all UCO samples for the three days are presented in Table 3 together with the corresponding values for AN and water contents. As the immersion test results presented in Table 3 show that the corrosion properties of these oils

(UCO8, UCO5, and UCO4) were lowest compared to the other oils, it could be possible that unsaturated FFAs, e.g., oleic acid, acts as a surfactant on the steel surface and decreases the corrosive properties of UCO oils, as was noticed in a previous study [13]. Fatty acids, such as oleic acid, linoleic acid, and linolenic acid derivatives, are environmentally-friendly corrosion inhibitors protecting mild steel, etc. [32]. Oleic acid was used as a surfactant and bonded covalently to the surfaces of magnetite nanoparticles [33]. A seed oil, *Opuntia dillenii*, which consists of fatty acids, was shown to form a barrier layer on the surface of iron by preventing contact of the metal surface and the corrosive solution [12].

- Exposure to Different UCO Mixtures

The more corrosive UCO2 was mixed with the low corrosive UCO4 in fractions of 9:1, 8:2, 7:3, and 1:1. The immersion test during 3 d with a polished steel rod was implemented. Three replications for each sample were performed. Figure 5 shows the iron concentrations dissolved in the oils. When UCO2 was used in the immersion test, an average iron concentration of 277 ppm was dissolved. As the fractions with decreasing concentration of UCO2 were tested, the concentration of dissolved iron in oil also decreased. The results show that by adding the low corrosive UCO4 oil to a very corrosive UCO2 oil, the harmful corrosive properties of the bio-oil mixture decreased. For utilization of different UCO batches, it would be very important to know the quality of each batch. The most corrosive batches should be blended with the less corrosive batches in a certain proportion such that the influence of the more corrosive oils is minimized.

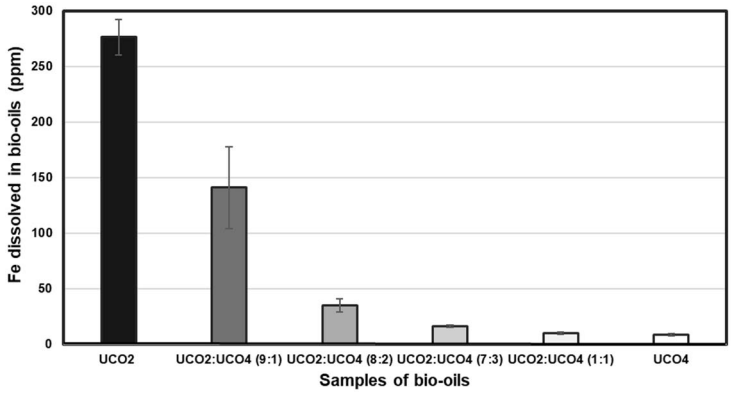

Figure 5. Iron concentration dissolved from polished steel rods into various mixtures of UCO2 and UCO4.

The SEM secondary electron images in Figure 6 show the surface morphology of the polished steel rods after three days of exposure to the following oil samples: (a) UCO2, (b) UCO2:UCO4 (9:1), (c) UCO2:UCO4 (8:2), and (d) UCO4. Figure 6a shows corrosion on the steel surface, 6b shows corrosion, and Figure 6c shows corrosion on the steel surface. Figure 6d shows a very smooth surface with very low corrosion.

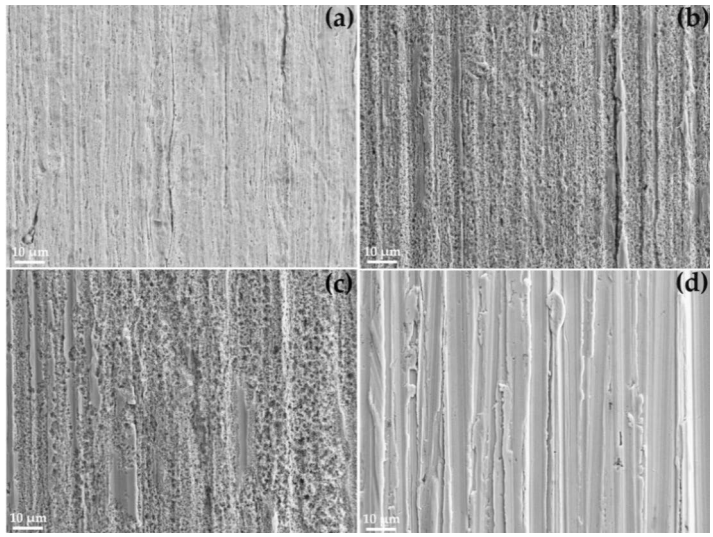

Figure 6. SEM secondary electron images of polished steel rod surfaces after 3 days of exposure to: (**a**) UCO2, (**b**) UCO2:UCO4 (9:1), (**c**) UCO2:UCO4 (8:2), and (**d**) UCO4.

As seen in the SEM images, the oil exposure clearly affected the surface morphology of rods, thus suggesting corrosion. The measured ion concentration in the oil after the exposure also supports this finding.

3.2.2. Copper Rod Corrosion

A polished copper rod was used in the immersion test. The concentration of copper in UCO2 was analyzed with ICP-OES. UCO2 dissolved copper during 1 d only 14 ppm, and during 3 d, 5 d, and 10 d, the level of dissolved copper was 25.9 ± 0.7 ppm (Table 5). The copper rods withstood corrosion much better than the steel rods when UCO2 was used. Figure 7A,B shows the minor change on the surfaces of the copper rod before and after expose to UCO2. For up to three days, copper kept dissolving, but after that, the copper content remained constant.

Table 5. Measured copper concentration (ppm) after exposure to UCO2 for different times.

No. of Days	0	1	3	5	10
Cu (ppm)	<6	14.4 ± 0.4	25.3 ± 0.3	26.7 ± 0.5	25.8 ± 0.5

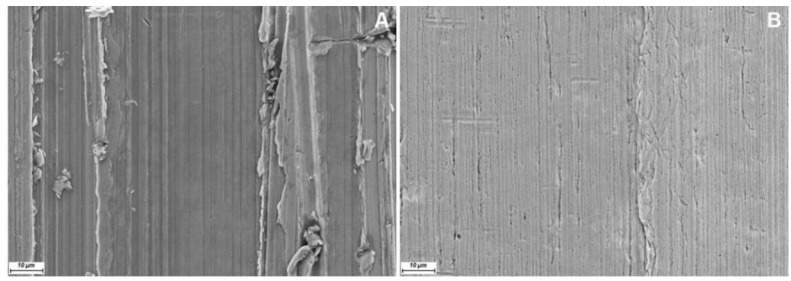

Figure 7. SEM secondary electron images of polished copper rod surfaces: (**A**) not exposed to the bio-oil and (**B**) exposed to UCO2 for 5 days.

The same batch of UCO2 was used in this copper test as in the test where UCO2 and UCO4 were mixed. A polished steel rod was used with UCO2 in the immersion test (3 d), and it was noticed that 277 ppm iron was dissolved into the oil (Figure 5).

When comparing the two rods in contact with the oil during the immersion test, the area 268.48 mm^2 of the polished copper rod was smaller compared to the polished steel rod's area of 431.57 mm^2. The concentration of copper dissolved from the rod was 0.09 ppm/mm^2, and the iron dissolved from the rod was 0.64 ppm/mm^2, which means that there was about 6.8 times higher concentration of iron compared to copper dissolved in UCO2 oil. These results indicate that the corrosive compounds in UCO2 caused more corrosion in contact with the polished steel rod surface compared to the copper rod surface.

Immersion tests with copper in UCOs could not be found in the open literature. Thus, we consider the corrosive properties of biodiesels for comparison. Biodiesel is chemically modified from UCOs and animal fats (that contain triglycerides and impurities like water, FFAs, etc.). During the chemical modification, including, e.g., transesterification, the production of biodiesel occurs, which is a mono-alkyl ester-based oxygenated fuel [34].

Immersion tests of copper, mild carbon steel, and stainless steel in biodiesel at 43 °C for two months were performed by Hu et al. [15]. According to their results, copper and mild carbon steel were observed to be more susceptible to corrosion than stainless steel. They also reported that chemical reactions controlled the corrosion mechanism of the metals [15]. Dissolved copper and iron were also found to act as strong catalysts to oxidize biodiesel [16]. Fazal et al. [9] also studied corrosion of copper in biodiesel and found out that after a certain immersion period (600–1200 h), the formation of oxygenated compounds on the surface of copper exposed to biodiesel reduced corrosion rate.

The immersion tests with biodiesel discussed above were done at elevated temperatures and for a longer immersion period [9,15,16,23,28]. During the biodiesel immersion tests, copper was most vulnerable to corrosion; however, in our shorter period of immersion testing at room temperature with UCO2, polished copper was observed to be less corroded compared to the polished steel rod. The reason could be that the concentration of dissolved copper at room temperature reached a saturation level during the three-day immersion test, or there could be chemical reactions that control the corrosion of the copper surface exposed to the UCO2.

3.2.3. Corrosion Inhibitor

The immersion tests were made for three days with a polished steel rod and the bio-oil UCO2. During the test, there was 310 ppm iron dissolved in UCO2. Table 6 shows that when 0.025 wt% or 0.25 wt% tert-butylamine (TBA) was added to UCO2, the concentration of dissolved iron decreased to 9 ppm in both samples. When 2.42 wt% TBA was added to UCO2, the iron dissolved from the polished steel rod was 14 ppm. To prevent corrosion of a polished steel rod, 0.025 wt% TBA was enough to add to UCO2. The low iron concentration (9 ppm) measured in the bio-oil was on the same level as when no steel rod had been in contact with oil.

Table 6. The immersion test (3 d) with a polished steel rod and UCO2. TBA was added to the oil in different concentrations.

TBA (wt%)	**0**	**0.025**	**0.25**	**2.42**
Fe (ppm)	310	9	9	14

Deyab et al. [21] reported that corrosion inhibitors contain organic compounds with nitrogen, oxygen, or sulfur atoms, heterocyclic compounds, and pi electrons. The polar functional groups present in inhibitors are considered to be the center of reaction for adsorption [22]. Inhibitors ethylenediamine, tert-butylamine (TBA), or n-butylamine form a stable metal oxide protective layer and thus inhibit the corrosion in biodiesel [23]. Physical

adsorption of amine-based inhibitors could have created a stable protective layer over the steel surface and thus prevented corrosion in our bio-oils [23,25].

As can be seen in Figure 8A,B, the steel rod surface after three-day immersion in UCO2 and TBA (0.025 wt%) is smoother than the immersion in UCO2 alone. The smoother surface observed when TBA was added originated from the smaller amounts of dissolved iron or less corrosion of the surface.

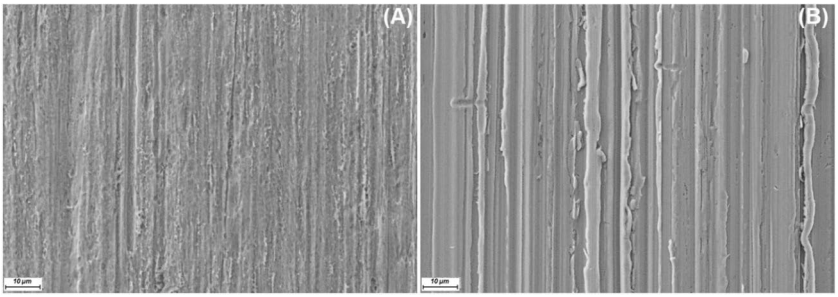

Figure 8. SEM secondary electron images of polished steel rod surfaces: (**A**) after exposure to UCO2 for 3 days and (**B**) after exposure to UCO2 and TBA (0.025 wt%).

Despite the promising results of TBA, notably inhibiting corrosion, it should be mentioned from the chemical safety point of view that it is classified as an acutely toxic substance. Therefore, more environmentally friendly chemicals as a replacement for TBA should be one of the focuses of future research in this area.

4. Conclusions

To study bio-oil-induced corrosion, unpolished and polished steel rods, polished mild annealed steel rods, and polished copper rods were immersed in vegetable-based used cooking oils at room temperature for up to 10 days. The iron content in the oils varied markedly depending on the oil sample. In general, the oils with the highest water concentrations (3100–3800 ppm) showed the highest corrosion properties although their acid number (AN) values of 6.7–6.9 mg KOH/g oil were not the highest. In contrast, the bio-oils with a lower level of water (2100–2700 ppm) but higher ANs (7–8.8 mg KOH/g oil) showed low corrosion properties. The oils with the highest ANs contained the highest concentrations of unsaturated free fatty acids, such as oleic acid. The unsaturated free fatty acids were assumed to have formed a protective layer on the rods, thereby preventing the permeation of oxygen and water to the metal surface. The copper rods withstood corrosion much better than the steel rods when UCO2 was used. For up to three days, copper kept dissolving, but after that, the copper content remained constant 25.9 ± 0.7 ppm. When a very corrosive oil was mixed with a non-corrosive oil, the amount of dissolved iron decreased notably. This suggests that mixing different bio-oils could be used as an advantage in corrosion prevention of fuel tanks and engines.

In the preliminary tests on the effect of corrosion inhibitors, it has been observed that adding even a very low concentration, 0.025 wt%, of TBA to the most corrosive used cooking oil clearly decreased the iron dissolution into the oil. Although more research needs to be carried out, the inhibiting effect could originate from the formation of a protective layer on the steel surface. However, due to the toxicity of TBA, more ecological alternatives should be studied.

Author Contributions: Conceptualization, N.B., L.H. and J.L.; methodology, N.B., L.H. and J.H.; formal analyses, N.B., J.H., L.H., J.L. and F.T.; investigation, N.B., L.H., J.L., J.H. and F.T.; writing—original draft, N.B.; writing—review and editing, F.T., L.H., J.L. and J.H.; supervision, L.H., J.L. and

F.T.; project administration, N.B. and L.H.; funding acquisition, N.B. and L.H. All authors have read and agreed to the published version of the manuscript.

Funding: This research was funded by the Swedish Cultural Foundation in Finland and the Otto A. Malm Foundation. Authors are also grateful to the CircVol 6Aika project for financial support as part of the activities of the Johan Gadolin Process Chemistry Centre at Åbo Akademi University. The APC was funded by Åbo Akademi University.

Institutional Review Board Statement: Not applicable.

Informed Consent Statement: Not applicable.

Data Availability Statement: Data are contained within the article.

Acknowledgments: VG EcoFuel Oy is gratefully acknowledge for providing the oil samples.

Conflicts of Interest: The authors declare no conflict of interest.

References

1. Moretti, C.; Junginger, M.; Shen, L. Environmental life cycle assessment of polypropylene made from used cooking oil. *Resour. Conserv. Recycl.* **2020**, *157*, 104750.
2. van Grinsven, A.; van den Toorn, E.; van der Veen, R.; Kampman, B.; Oil, C. *Used Cooking Oil (UCO) as Biofuel Feedstock in the EU*; CE Delft: Delft, The Netherlands, 2020; p. 200247.
3. Panadare, D.C.; Rathod, V.K. Applications of waste cooking oil other than biodiesel: A review. *Iran. J. Chem. Eng.* **2015**, *12*, 55–76.
4. Chung, T.Y.; Eiserich, J.P.; Shibamoto, T. Volatile compounds identified in headspace samples of peanut oil heated under temperatures ranging from 50 to 200 °C. *J. Agric. Food Chem.* **1993**, *41*, 1467–1470.
5. Wu, C.M.; Chen, S.Y. Volatile compounds in oils after deep frying or stir frying and subsequent storage. *J. Am. Oil Chem. Soc.* **1992**, *69*, 858–865.
6. Singhabhandhu, A.; Tezuka, T. The waste-to-energy framework for integrated multi-waste utilization: Waste cooking oil, waste lubricating oil, and waste plastics. *Energy* **2010**, *35*, 2544–2551.
7. Mannu, A.; Ferro, M.; DiPietro, M.E.; Mele, A. Innovative applications of waste cooking oil as raw material. *Sci. Prog.* **2019**, *102*, 153–160.
8. Lhuissier, M.; Couvert, A.; Amrane, A.; Kane, A.; Audic, J.L. Characterization and selection of waste oils for the absorption and biodegradation of VOC of different hydrophobicities. *Chem. Eng. Res. Des.* **2018**, *138*, 482–489.
9. Fazal, M.A.; Haseeb, A.S.M.A.; Masjuki, H.H. Corrosion mechanism of copper in palm biodiesel. *Corros. Sci.* **2013**, *67*, 50–59.
10. Ollus, R.; Juoperi, K. Alternative fuels experiences for medium-speed diesel engines. In Proceedings of the 25th CIMAC Congress on Combustion Engine Technology, Vienna, Austria, 21–27 May 2007; International Council on Combustion Engines: Frankfurt, Germany, 2007; pp. 538–552.
11. Kovács, A.; Tóth, J.; Isaák, G.; Keresztényi, I. Aspects of storage and corrosion characteristics of biodiesel. *Fuel Process. Technol.* **2015**, *134*, 59–64.
12. Rehioui, M.; Abbout, S.; Benzidia, B.; Hammouch, H.; Erramli, H.; Daoud, N.A.; Badrane, N.; Hajjaji, N. Corrosion inhibiting effect of a green formulation based on Opuntia Dillenii seed oil for iron in acid rain solution. *Heliyon* **2021**, *7*, e06674.
13. Bruun, N.; Demesa, A.G.; Tesfaye, F.; Hemming, J.; Hupa, L. Factors affecting the corrosive behavior of used cooking oils and a non-edible fish oil that are in contact with ferrous metals. *Energies* **2019**, *12*, 4812.
14. Fazal, M.A.; Haseeb, A.S.M.A.; Masjuki, H.H. Effect of temperature on the corrosion behavior of mild steel upon exposure to palm biodiesel. *Energy* **2011**, *36*, 3328–3334.
15. Hu, E.; Xu, Y.; Hu, X.; Pan, L.; Jiang, S. Corrosion behaviors of metals in biodiesel from rapeseed oil and methanol. *Renew. Energy* **2012**, *37*, 371–378.
16. Fazal, M.A.; Haseeb, A.S.M.A.; Masjuki, H.H. Comparative corrosive characteristics of petroleum diesel and palm biodiesel for automotive materials. *Fuel Process. Technol.* **2010**, *91*, 1308–1315.
17. Alves, S.M.; Dutra-Pereira, F.K.; Bicudo, T.C. Influence of stainless steel corrosion on biodiesel oxidative stability during storage. *Fuel* **2019**, *249*, 73–79.
18. Souza, C.A.C.; De Meira, M.; Assis, L.O.; De Barbosa, R.S.; Luna, S. Effect of natural substances as antioxidants and as corrosion inhibitors of carbon steel on soybean biodiesel. *Mater. Res.* **2021**, *24*, e20200234.
19. Komatsu, D.; Souza, E.C.; De Canale, L.C.F.; Totten, G.E. Effect of antioxidants and corrosion inhibitor additives on the quenching performance of soybean oil. *Stroj. Vestn. J. Mech. Eng.* **2010**, *56*, 121–130.
20. Li, P.; Lin, J.; Tan, K.; Lee, J. Electrochemical impedance and X-ray photoelectron spectroscopic studies of the inhibition of mild steel corrosion in acids by cyclohexylamine. *Electrochim. Acta* **1997**, *42*, 605–615.
21. Deyab, M.A. The inhibition activity of butylated hydroxytoluene towards corrosion of carbon steel in biodiesel blend B20. J. Taiwan Inst. *Chem. Eng.* **2016**, *60*, 369–375.

22. Deyab, M.A. Application of nonionic surfactant as a corrosion inhibitor for zinc in alkaline battery solution. *J. Power Source* **2015**, *292*, 66–71.
23. Singh, B.; Korstad, J.; Sharma, Y.C. A critical review on corrosion of compression ignition (CI) engine parts by biodiesel and biodiesel blends and its inhibition. *Renew. Sustain. Energy Rev.* **2012**, *16*, 3401–3408.
24. Yeşilyurt, M.K.; Öner, I.V.; Yilmaz, E.Ç. Biodiesel induced corrosion and degradation: Review. *Pamukkale Univ. Muh. Bilim. Derg.* **2019**, *25*, 60–70.
25. Fazal, M.A.; Sazzad, B.S.; Haseeb, A.S.M.A.; Masjuki, H.H. Inhibition study of additives towards the corrosion of ferrous metal in palm biodiesel. *Energy Convers. Manag.* **2016**, *122*, 290–297.
26. Bruun, N.; Khazraie Shoulaifar, T.; Hemming, J.; Willför, S.; Hupa, L. Characterization of waste bio-oil as an alternate source of renewable fuel for marine engines. *Biofuels* **2022**, *13*, 21–30.
27. Bruun, N.; Tesfaye, F.; Hemming, J.; Dirbeba, M.J.; Hupa, L. Effect of storage time on the physicochemical properties of waste fish oils and used cooking vegetable oils. *Energies* **2021**, *14*, 101.
28. Zuleta, E.C.; Baena, L.; Rios, L.A.; Calderón, J.A. The oxidative stability and its impact on the deterioration of metallic and polymeric materials: A review. *J. Braz. Chem. Soc.* **2012**, *23*, 2159–2175.
29. Karmakar, A.; Karmakar, S.; Mukherjee, S. Properties of various plants and animals feedstocks for biodiesel production. *Bioresour. Technol.* **2010**, *101*, 7201–7210.
30. Gregg, F. *SVO: Powering Your Vehicle with Straight Vegetable Oil*; New Society Publishers: Gabriola Island, BC, Canada, 2008; pp. 29–79.
31. Adeoti, I.A.; Hawboldt, K. Comparison of biofuel quality of waste derived oils as a function of oil extraction methods. *Fuel* **2015**, *158*, 183–190.
32. Swathi, P.N.; Rasheeda, K.; Samshuddin, S.; Alva, V.D.P. Fatty acids and its derivatives as corrosion inhibitors for mild steel—An overview. *J. Asian Sci. Res.* **2017**, *7*, 301–308.
33. Guardia, P.; Batlle-Brugal, B.; Roca, A.G.; Iglesias, O.; Morales, M.P.; Serna, C.J.; Labarta, A.; Batlle, X. Surfactant effects in magnetite nanoparticles of controlled size. *J. Magn. Magn. Mater.* **2007**, *316*, e756–e759.
34. Enweremadu, C.C.; Mbarawa, M.M. Technical aspects of production and analysis of biodiesel from used cooking oil—A review. *Renew. Sustain. Energy Rev.* **2009**, *13*, 2205–2224.

Nina Bruun, Juho Lehmusto, Fiseha Tesfaye, Jarl Hemming and Leena Hupa

Amino Acids Reduce Mild Steel Corrosion in Used Cooking Oils

Sustainability 2022, 14, 3858, 1–14.

V

sustainability

MDPI

Article

Amino Acids Reduce Mild Steel Corrosion in Used Cooking Oils

Nina Bruun *, Juho Lehmusto, Fiseha Tesfaye, Jarl Hemming and Leena Hupa

Johan Gadolin Process Chemistry Centre, Åbo Akademi University, Henrikinkatu 2, FI-20500 Turku, Finland; juho.lehmusto@abo.fi (J.L.); fiseha.tesfaye@abo.fi (F.T.); jarl.hemming@abo.fi (J.H.); leena.hupa@abo.fi (L.H.)
* Correspondence: nina.bruun@abo.fi

Abstract: In this study, we tested several amino acids as eco-friendly inhibitors against corrosion of mild steel by used cooking oils (UCOs). The corrosion inhibition was studied by immersing mild steel rods in the UCOs and reference fresh rapeseed and olive oils mixed with amino acids. The immersion tests were conducted at room temperature for three days. The roles of water and bio-oil preservatives (formic and propionic acids) in the corrosion were explored. The mild steel surface morphology changes after exposure to the oils were analyzed with a scanning electron microscope coupled with an energy dispersive spectroscope (SEM-EDS). The concentration of iron dissolved in the oils was determined with a spectrophotometer. A thick layer was analyzed on the surfaces of the mild steel rods immersed in the oils containing formic or propionic acid and water. This layer provided a minor barrier against corrosion. According to the Fourier transform infrared spectrometer (FTIR) analytical results, the layer consisted of an acid and iron salt mixture. All the tested amino acids decreased the concentration of dissolved iron in the UCOs; particularly, cationic amino acids, L-lycine and L-arginine showed adequate corrosion inhibition properties at low concentrations.

Keywords: biofuel utilization; corrosion inhibition; amino acids; mild steel; renewable energy sources

Citation: Bruun, N.; Lehmusto, J.; Tesfaye, F.; Hemming, J.; Hupa, L. Amino Acids Reduce Mild Steel Corrosion in Used Cooking Oils. *Sustainability* **2022**, *14*, 3858. https://doi.org/10.3390/su14073858

Academic Editors: Yang Guo and Yanhui Li

Received: 16 February 2022
Accepted: 23 March 2022
Published: 24 March 2022

1. Introduction

Used cooking oils (UCOs) are non-edible residues from restaurants, households, and the food processing industry. The global vegetable oil utilization leading to the generation of UCOs has significantly increased in recent decades due to the global population growth, the change in food habits, and the rise in the utilization of lipids [1]. The generation of UCOs is estimated to be around 20–32% of the total vegetable oil consumption [2,3].

Increasing interest in the circular economy and sustainable use of resources has made UCOs and UCO-based biodiesel attractive as renewable fuels for diesel engines, particularly for marine engine applications [4]. However, the UCOs must be used within a relatively short period of time after their collection and processing to avoid, e.g., the formation of corrosive degradation components [5,6]. In general, the acid number, viscosity, density, and water content are essential criteria for approving the UCOs as fuels [7]. However, the acid number and water do not directly correlate with the bio-oil properties and corrosivity [8]. The roles of different bio-oil components and corrosion inhibitors in the corrosive properties are not thoroughly understood.

The corrosivity of bio-oils can be lowered with corrosion inhibitors, which are added in small concentrations to alter the environment into a less corrosive one by interacting with the corrosive species [9,10]. Alternatively, the inhibitors interact with the metal to form a protective surface film [10–13]. Corrosion inhibitors with proven effective performance include those containing multiple bonds, N, O, S, and P organic compounds, in addition to some functional groups [13,14]. Organic compounds with -OH, -COOH, -NH_2, etc., are also excellent corrosion inhibitors, especially in acidic solutions [14]. The environmental legislation on toxicity, biodegradability, and bioaccumulation gives strict regulations and rules for

the usage and disposal of corrosion inhibitors in different countries [15]. Developing green or eco-friendly corrosion inhibitors with minimal side effects has been considered very important [16,17]. These inhibitors are generally categorized as inorganic or organic [17]. Organic green corrosion inhibitors include surfactants, amino acids, etc. [11]. Proteins in all animal and plant species are composed of twenty different amino acids [18]. Amino acids are biomolecules that have vital significance to all organisms. They form the building blocks of proteins and many essential substances such as neurotransmitters, hormones, and nucleic acids [19]. Amino acids are relatively cheap, non-toxic, biodegradable, soluble in aqueous media, and produced at high purity [14,20]. Amino acids possess at least one carboxyl group and one amino group. They can coordinate with metals through nitrogen or oxygen atoms in the carboxyl group [21]. The strength of the inhibitor-metal bond is an essential part of the corrosion inhibition degree of amino acids [21]. Amino acids can control corrosion of various metals such as pure iron, carbon steel, copper, zinc, nickel, tin, and aluminum alloys [20–22]. Furthermore, amino acids behave as corrosion inhibitors in acid medium, neutral medium, and de-aerated carbonate solution [21].

Short-chain carboxylic acids, including formic, acetic, propionic, and butyric acids, have been used as food preservatives for a long time [23,24]. Organic acids are commonly used as preservatives for animal feed (such as chicken, pig, and cattle) and human consumption [23,24]. The reactive carboxyl group present in organic acids makes them essential building blocks for many compounds such as drugs, pharmaceuticals, plastics, and fibers [25]. Rust and oxidation scales formed on the steel substrates can be removed by different inorganic or organic acids such as phosphoric, hydrochloric, sulfuric, formic, or acetic acid. The choice of the acid depends on the oxide scale's solubility in the solution and the content of various components in the steel. Acid solutions, e.g., hydrochloric and sulfuric acids, are used for pickling, de-scaling, cleaning, oil well cleaning, and pipeline cleaning [26]. The corrosion inhibitors added to these acid solutions must be stable and effective in the hot concentrated acid even in severe environments [27]. Rafiquee et al. [25] have studied the corrosion of mild steel in the presence and absence of inhibitors in 20% formic and 20% acetic acid solutions at 30 °C for 24 h. The polished mild steel exposed to the 20% formic acid solution without corrosion inhibitors showed abrasion and corrosion. In contrast, the metal surface exposed to the 20% formic acid solution containing 100 ppm of the inhibitor 2-amino-5-propyl-1,3,4-thiadiazoles (APT) was smoother, and the inhibitor had adsorbed on the surface [25]. Zhu et al. [28] have examined the effects of temperature and acetic acid concentration on the corrosion behavior of N80 carbon steel. An increased temperature was observed to enhance the dissolution of steel substrate and promote the main corrosion product $FeCO_3$ precipitation. The increased acetic acid enhanced the localized corrosion attack on N80 carbon steel [28].

Carbon steel coupons exposed to biodiesel and different antioxidants (e.g., tert-butylhydroquinone, propyl gallate, and curcumin) for 90 days were examined by Serqueira et al. [29]. After the exposure, the surfaces were analyzed with the SEM-EDX technique. The results indicated that antioxidants had adhered to the metallic surface, forming a protective film that may provide corrosion protection [29].

Qiang et al. [30,31] have studied the inhibition effect of 5-(Benzylthio)-1H-tetrazole (BTTA) and 5-Benzyl-1H-tetrazole (BTA) for Q235 steel (Fe 99.7 wt %) in 0.5 M sulfuric acid and copper in 0.5 M H_2SO_4 by applying weight loss measurement, electrochemical techniques, scanning electron microscopy (SEM), atomic force microscopy (AFM), etc. Their results suggested that corrosion of the metal surfaces could be significantly better inhibited when 2 mM BTTA was added to the acid solution, compared to 2 mM BTA.

The eco-friendly substance Losartan potassium (LP) for corrosion inhibition of mild steel in HCl medium was recently studied by applying the gravimetric, electrochemical, and scanning vibrating electrode techniques [32]. For 5 mM LP, the authors reported the inhibition performance to increase from about 89% at room temperature to 92% at 318 K.

Our previous works [8,33–35] discussed the chemical, physical, and thermal properties and the effect of storage time on the quality and corrosion properties of UCOs and fish oils.

In addition, the corrosion of different metal rods in oils was tested [8]. The immersion tests of the UCOs showed variations in corrosion properties depending on the oil batch [8,33]. An oleic acid layer on the steel rod after the immersion in one UCO batch was supposed to provide partial corrosion protection [8]. Thus, it was assumed that suitable additives in UCOs could form a protective layer or provide corrosion inhibition through some other mechanism.

This work studied the role of ten different amino acids, water, and formic and propionic acids in different UCO batches in the corrosion of mild steel rods. Fresh edible oils were used as references. The results provide a novel understanding of the efficiency of different amino acids in the corrosion resistance of mild steel rods in contact with oils.

2. Materials and Methods

2.1. Materials

The physicochemical properties of the studied bio-oils have been reported earlier in detail [8]. All the UCO samples were provided by VG EcoFuel Oy (Uusikaupunki, Finland). When naming the oil samples, numbers were used to note different oil batches. All the used cooking oils (filtered) were vegetable-based and obtained from fast food companies. In this work, oil samples from different batches were studied in immersion tests. A fresh edible vegetable oil (Keiju from Bunge Finland Oy, Raisio, Finland) and an organic extra virgin olive oil (Pirkka Luomu, from Granada, Spain) were used as reference samples. The UCOs and vegetable oil were stored in a refrigerator, whereas the olive oil was stored at room temperature.

The mild steel rods (98.64 wt % Fe, 1.00 wt % Mn, 0.21 wt % Si, 0.11 wt % C, 0.03 wt % P, and 0.02 wt % S) used in the immersion tests were cut from an H44 all-round welding rod with a diameter of 1.6 mm, obtained from Linde (Solna, Sweden). All chemicals and solvents used for the analyses were of analytical reagent grade. Formic acid (98–100%) was purchased from Riedel-de Haën (Seelze, Germany), and propionic acid (99.5%) and L-Methionine (98%) were acquired from Fluka AG, Sigma-Aldrich Chemie GmbH (Buchs, Switzerland). L-Alanine (99%) was provided by Sigma-Aldrich Chemie GmbH (Steinheim, Germany). L-Arginine (>98%), L-Cysteine (>98%), and L-Serine (>99%) were provided by Sigma Ultra, Sigma Chemical Co. (St. Louis, MO, USA). Glycine (>99.7%), L-Glutamic acid (>99%), L-Leucine (>99%), and L-Tyrosine (>99%) were provided by Merck (Darmstadt, Germany). L-Lysine (>97%) was acquired from SAFC (St. Louis, MO, USA). The concentrations of amino acids in the oil samples slightly varied due to difficulties in weighing the tiny amounts of powder or liquid needed for a particular concentration. Finally, formic and propionic acids and water were added to the oils to better understand the roles of various components in oil in mild steel corrosion.

2.2. Corrosion Test and Analyses

Corrosion tests were carried out at room temperature to investigate the inhibitive role of amino acids in UCO-induced corrosion of mild steel. The experiments were performed in test tubes of 15 mL, mounted on a rotary mixer rotated at a constant speed of 56 rpm. The steel sample was placed in a 7 mL oil sample for three days. After the immersion test, the sample was removed from the oil and cleaned ultrasonically using a mixture (1:1 v/v) of toluene (≥99.9%, Honeywell, Riedel-de-Haën, Seelze, Germany) and 2-propanol (≥99.8%, Sigma-Aldrich Chemie GmbH, Steinheim, Germany). Then, the oils were subjected to liquid–liquid extraction using 1 mL of sulfuric acid (95–97%, Sigma-Aldrich Chemie GmbH, Steinheim, Germany) and 8 mL of deionized water in a test tube, which was vigorously shaken for 1 min. After the extraction, the mixture was filtered using a quantitative ashless filter paper (Grade No. 42, Whatman International Ltd., Maidstone, England), and the filtrate was analyzed spectrophotometrically. Each experiment contained three parallel samples. More details on the experimental procedures were reported in [8,33].

The amount of iron dissolved in oils was determined from the filtrate after a liquid–liquid extraction step using a spectrophotometer (Perkin-Elmer Lambda 25, Waltham, MA,

USA). The spectra were measured between 400 and 600 nm with a scan rate of 480 nm min^{-1} using a quartz cuvette with a 1 cm path length.

The surface morphologies and the corrosion products were studied with a scanning electron microscope (SEM, LEO Gemini 1530 with a Thermo Scientific Ultra Dry Silicon Drift Detector (SDD), Oberkochen, Baden-Württemberg, Germany) coupled to an elemental X-ray detector (EDS, Energy Dispersive X-ray Spectroscopy, Thermo Scientific, Madison, WI, USA). Cross-sectional samples for SEM imaging were prepared by broad ion beam milling (BIB) (Ilion + Advantage Precision, Model 693, Gatan Inc., Pleasanton, CA, USA).

Organometallic species at the sample surfaces were identified with Fourier transform infrared spectroscopy (FTIR) using a Perkin-Elmer Spectrum Two™ spectrometer (Perkin-Elmer, Llantrisant, UK) with a spectrum area of 4000–450 cm^{-1} and a resolution of 4 cm^{-1}. The FTIR spectra were interpreted using the spectral analysis function (software KnowItAll Informatics System 2020, John Wiley Sons, Inc., Hoboken, NJ, USA).

2.3. Properties of UCO Batches without Additives

The chemical and physical properties (chemical composition, acid number, water content, density, viscosity, and kinematic measurements) of the UCOs have been reported in [8]. In short, no significant differences between the properties of the UCO batches were found. The mean value for total free fatty acids (FFAs) was about 30.1 ± 3.6 mg/g and the measured acid number (AN) was 7.2 ± 0.8 mg KOH/g oil (Table 1). The mean water content was 2483 ± 672 ppm [8].

Table 1. The physicochemical properties and immersion test results of UCOs [8] and the reference vegetable and olive oils. The UCO batches marked with bold were used for the corrosion tests in this work.

Sample	Measured AN	Water Content	Total FFA	Oleic Acid	Immersion Test (3 d)
	(mg KOH/g Oil)	(ppm)	(mg/g)	mg/g	Fe (ppm)
UCO1	6.9	1850	28.4	14.9	12
UCO2	**6.5**	**1776**	**28.4**	**14.8**	**390**
UCO3	6.9	2180	28.3	16.0	102
UCO4	7.0	2067	30.0	16.9	14
UCO5	8.0	2493	32.9	18.7	74
UCO6	**6.7**	**3748**	**27.0**	**15.2**	**449**
UCO7	**6.9**	**3089**	**28.0**	**15.9**	**571**
UCO8	**8.8**	**2664**	**37.8**	**21.7**	**59**
			Mean Value		
UCO1-UCO8	7.2 ± 0.8	2483.0 ± 672	30.1 ± 3.6	16.8 ± 2.4	209 ± 223
Vegetable oil	0.1	604	0.5	0.2	8
Virgin Olive oil	0.5	581	1.0	0.4	8

The immersion tests showed the highest iron concentrations, >390 ppm, after three days in UCO2, UCO6, and UCO7 [8]. After three days, the dissolved iron concentration in UCO8 was 60 ppm, much lower than in UCO6 (450 ppm) and UCO7 (570 ppm). Although UCO8 had a lower water content (2660 ppm) than the two other oils (3750 and 3090 ppm for UCO6 and UCO7, respectively), the differences in the dissolved iron cannot be explained by the water concentrations. UCO8 had the highest total FFAs, 37.8 mg/g oil, and AN (8.8 mg KOH/g oil) (Table 1). Furthermore, the unsaturated free fatty acid oleic acid content was 21.7 mg/g in UCO8, higher than in UCO6 (15.2 mg/g) and UCO7 (15.9 mg/g). According to our previous study [33], a layer formed of oleic acid on the mild steel rod surface. This layer might provide some corrosion protection and thus partly explain the differences in the observed iron contents.

Table 1 also shows the physicochemical properties and the immersion test results of the reference samples, fresh edible vegetable oil and virgin olive oil. The water contents of

these oils were about 600 ppm, and the measured ANs were 0.1 and 0.5 mg KOH/g oil for the vegetable and olive oil, respectively. After the immersion tests, these fresh oils showed low iron content, 8 ppm, the same level as before.

3. Results and Discussion

3.1. Corrosion Inhibition

3.1.1. UCO2 with Amino Acids

Figure 1 shows the dissolved iron concentration after immersion of the mild steel rods in UCO2 with various concentrations of the amino acids tested as corrosion inhibitors. Although significant differences were measured between the different amino acids' corrosion-inhibiting effects, all amino acids decreased the amount of iron dissolved to UCO2 during the three-day immersion. These results are in accordance with the published results of utilizing amino acids and their derivatives to prevent corrosion of metals and alloys in aqueous media [11,21]. Interestingly, a particular amino acid concentration did not have a marked impact on the iron concentration analyzed in the oil. The best corrosion inhibition was achieved with the cationic acids L-lycine and L-arginine. Low concentrations of these two amino acids almost totally inhibited the corrosion.

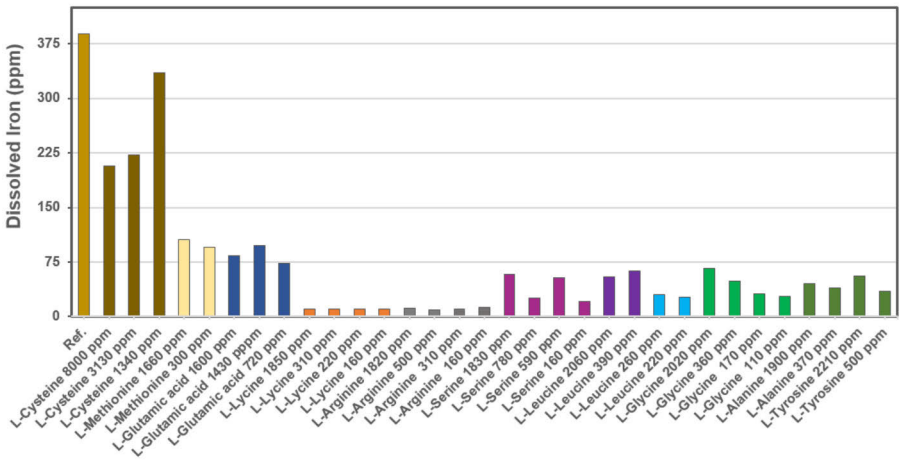

Figure 1. Iron dissolved (ppm) from the mild steel rods during 3 d immersion in UCO2 without and with different additions of amino acids.

Figure 2 shows SEM secondary electron images of polished steel rod surfaces after immersion in UCO2 and the different amino acids. Figure 2a shows the polishing scratches on the rod surface before the exposure. After the immersions, the surface morphologies were smoother (Figure 2b–e). The immersion affected the surface morphology of the rods for all other UCO2 additives but L-lycine (Figure 2f) and L-arginine (Figure 2g). Thus, the images suggest only minor corrosion, further supported by low iron concentrations in UCO2, around 10 ppm Fe with L-lycine and 12 ppm Fe with L-arginine.

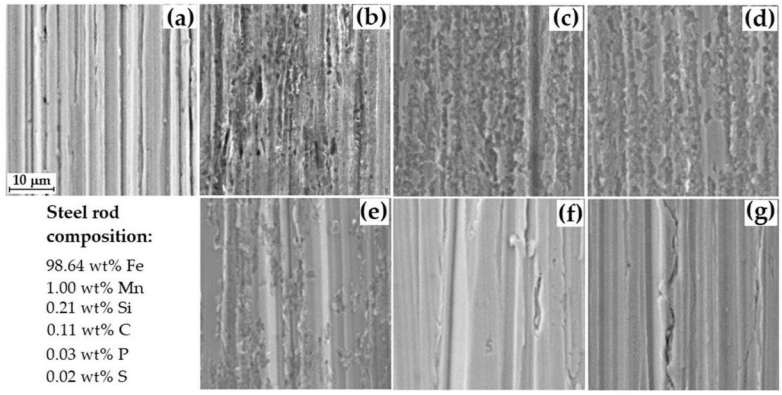

Figure 2. SEM images of polished mild steel surface exposed to UCO2 and amino acid additives: (**a**) before exposure, (**b**) after exposure without any additive, (**c**) with 300 ppm L-methionine, (**d**) 720 ppm L-glutamic acid, (**e**) 220 ppm L-leucine, (**f**) 160 ppm L-lycine, and (**g**) 160 ppm L-arginine. All images have the same magnification.

3.1.2. Impact of Water in UCO2 on Corrosion Inhibition with L-Lycine and L-Arginine

UCO batches with more than 3000 ppm water (UCO6 and UCO7 in Table 1) dissolved more iron than UCO2 with 1800 ppm water. Whether L-lycine and L-arginine were effective also in the presence of higher water content was tested by adding water to UCO2 and UCO2 mixtures with the two amino acids. Table 2 gives the water and amino acid contents in UCO2 and the measured average Fe concentration of three parallel samples with each UCO2 composition. The iron concentration difference in UCO2 shown in Tables 1 and 2 was assumed to depend on the difference in the experimental time points. The oil in Table 1 was fresh but, most likely, had aged during the five months of storage before the experiments shown in Table 2 were carried out. Nevertheless, the corrosivity of UCO2 increased with the water content. As indicated by the small amounts of dissolved iron in Table 2, both L-lycine and L-arginine effectively inhibited corrosion for the mixtures with higher water contents.

Table 2. Impact of water, L-lycine, and L-arginine content (ppm) in UCO2 on iron released from the mild steel rod during the three-day immersion test.

Chemicals in UCO2 (ppm)			Dissolved Fe (ppm)
H_2O	L-Lycine	L-Arginine	
1800	-	-	490
5500	-	-	530
4200	430	-	10
3400	-	380	10

The surface morphologies in Figure 3 verify the negligible iron dissolution into UCO2 with higher water contents in the presence of the amino acids. However, the SEM images in Figures 2 and 3 do not explain the corrosion inhibition mechanism induced by the amino acids. According to Rafiquee et al. [25], the inhibitive effect occurs when the inhibitors adsorb on the mild steel surface, thereby decreasing corrosion.

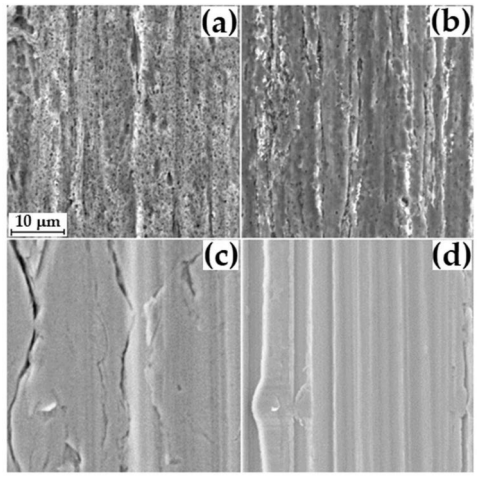

Figure 3. SEM secondary electron images of mild steel rod surfaces after immersion in UCO2 with (**a**) no additives, 1800 ppm water, (**b**) 5500 ppm water, (**c**) L-lycine 430 ppm + 4200 ppm water, and (**d**) L-arginine 380 ppm + 3400 ppm water. The scale is the same for all images.

3.1.3. Amino Acids, L-Lycine and L-Arginine in Different UCO Batches

The corrosion-inhibiting effects of L-lycine and L-arginine were also tested with UCO6 and UCO7, which had shown significant corrosion of the mild steel rods in earlier experiments (Table 1) [8]. In addition, the batch UCO8 showing less intense corrosion was included in the experiment series.

Adding 300 ppm L-lycine to UCO6, UCO7, and UCO8 decreased the iron dissolution to 15–20 ppm. Similarly, 300 ppm L-arginine in UCO6, UCO7, and UCO8 decreased the dissolved iron concentration to 22–44 ppm.

Figure 4 shows SEM images of the mild steel rod surfaces after immersion in UCO6, UCO7, and UCO8 without and with 300 ppm L-lycine. The rods immersed in oil batches containing L-lycine had similar surface morphology as before the exposure, suggesting that the amino acid effectively suppressed the corrosion.

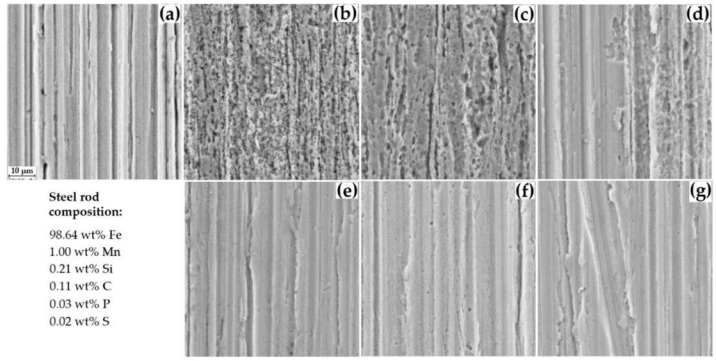

Figure 4. SEM secondary electron images of mild steel rod surfaces: (**a**) before exposure and after three days in (**b**) UCO6, (**c**) UCO7, (**d**) UCO8, (**e**) UCO6+ L-lycine 300 ppm, (**f**) UCO7+ L-lycine 300 ppm, and (**g**) UCO8+ L-lycine 300 ppm. The magnification is the same for all images.

3.1.4. Formic and Propionic Acids in UCOs with Amino Acid Inhibitors

The three-day immersion test was used to measure the impact of two carboxylic acids, formic and propionic acids, on the corrosive properties of used cooking oils with and without amino acids.

The iron concentration in UCO6 without any additives was 450 ppm. After immersion in UCO6 containing formic acid and added water, the iron content was lower, around 230 ppm. Adding 300 ppm L-lycine to the UCO6 mixture with formic acid and water slightly decreased the iron content to 180 ppm (Figure 5). Similar trends were also seen in UCO7, i.e., the iron content in the oil decreased from 570 to 190 and further to 140 ppm upon adding formic acid and water, followed by L-lycine addition (Figure 5).

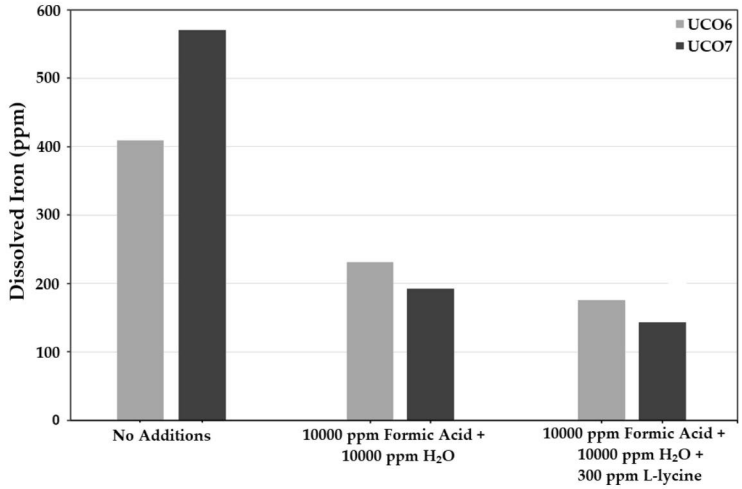

Figure 5. Mean iron concentrations in UCO6 and UCO7 with different additives after three days of immersion. All values are the means of three parallel experiments.

The SEM images of the steel surface after immersion in UCO6, UCO7, and UCO8 with additions of formic acid (10,000 ppm), water (10,000 ppm), and L-lycine (300 ppm) show a surface layer of large (>10 μm) particles (Figure 6). The surface layer structure is similar to that reported by Rafiquee et al. [25] for mild steel after being in contact with a 20% formic acid solution.

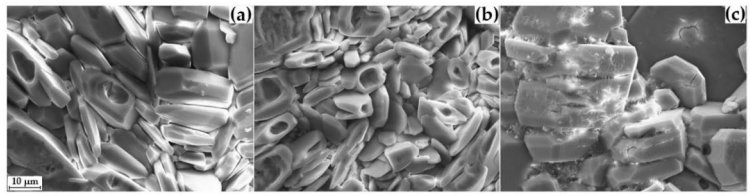

Figure 6. SEM images of rod surfaces after immersion in oils with formic acid (10,000 ppm), water (10,000 ppm), and L-lycine (300 ppm): (**a**) UCO6, (**b**) UCO7, and (**c**) UCO8. The magnification is the same for all images.

SEM-EDS analysis suggested that the layer consisted mainly of carbon and oxygen, with some iron and manganese. The rod cross-section was revealed by BIB cutting for

the SEM analysis. According to the image analysis, the layer mean thickness was 46 µm (Figure 7).

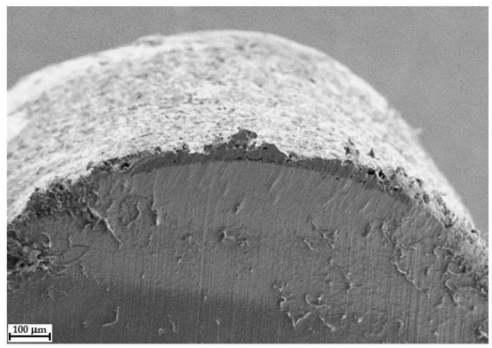

Figure 7. SEM image of rod surface layer after 3 days in UCO6 + formic acid, water, and L-lycine.

The layer was removed from the rod surface and then analyzed using FTIR. The spectrum in Figure 8 and the absorption bands and their interpretations in Table 3 suggest that the layer consisted of formic acid and iron salt.

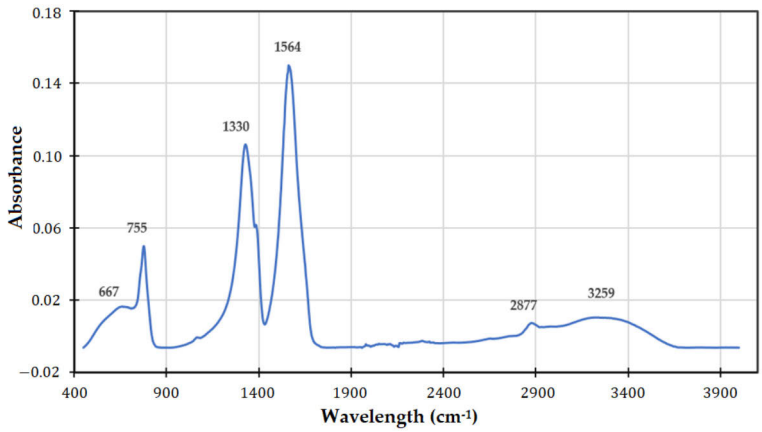

Figure 8. FTIR spectrum of the removed scale from mild steel surface after immersion in UCO6 with formic acid, water, and L-lycine.

Table 3. Peaks in the FTIR spectrum (Figure 8) and their interpretation.

Peak (cm^{-1})	Strength	Structure	Interpretation
3259	Weak	-OH (hydroxyl)	Iron oxide or water
2877	Weak	-CH stretching	Organic compound
1564	Strong	Asymmetric C=O stretching of carboxylic acid salt	Iron and carboxylic acid salt, formic acid
1330	Weak	Symmetric C=O stretching of carboxylic acid salt	Iron and carboxylic acid salt, formic acid
755	Weak	Rocking of primary amine salt	
667	Weak	Unknown	

3.2. Corrosion in Fresh Edible Oils

The impact of formic and propionic acid on corrosion was studied by immersing the mild steel rods in fresh olive and vegetable (rapeseed) oils with acid and water additions.

3.2.1. Olive Oil with Formic Acid, Propionic Acid, and Water

The iron content in fresh olive oil and vegetable oil was 7 ppm. After immersing mild steel rods in oils, the iron level was still on the same level (8 ppm). Adding (1) water (10,000 ppm), (2) formic acid (10,000 ppm), or (3) propionic acid (10,000 ppm) gave only a negligible increase in the iron content (8–11 ppm) (Table 4). However, adding 10,000 ppm formic acid and water resulted in 200 ppm iron in olive oil. Similarly, 10,000 ppm propionic acid and 10,000 ppm water increased the iron content in olive oil to 1200 ppm (Table 4).

Table 4. Iron content in olive and rapeseed oils after immersing mild steel rods in oils with different concentrations of formic acid, propionic acid, and water.

Additive (ppm)			Iron Content (ppm)	
Formic Acid	**Propionic Acid**	**Water**	**Olive Oil**	**Rapeseed Oil**
-	-	-	8	8
-	-	10,000	10	9
10,000	-	-	11	11
10,000	-	10,000	200	170
-	10,000	-	8	9
-	10,000	10,000	1200	1550

After the immersion, SEM images of the rod surface morphologies were in line with the dissolved iron concentrations in oil mixtures. Adding only water, formic acid, or propionic acid in olive or rapeseed oils did not induce corrosion noticeably. However, marked corrosion occurred as soon as both an acid and water were present simultaneously. The corrosion was observed with increased concentrations of iron in the oils (Table 4) and changed morphologies of the steel surfaces (Figure 9).

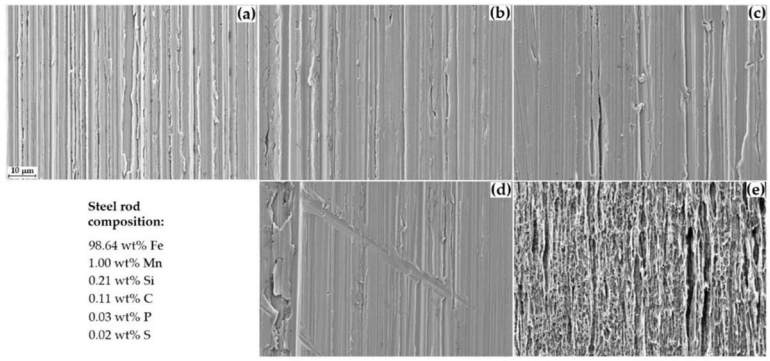

Figure 9. SEM images of steel surfaces: (**a**) before immersion, and after three days in (**b**) rapeseed oil, (**c**) rapeseed oil + 10,000 ppm water, (**d**) rapeseed oil + 10,000 propionic acid, and (**e**) rapeseed oil + 10,000 propionic acid + 10,000 ppm water. The magnification is the same in all images.

The observed corrosion by an acid–water mixture originates from the dissociation of acid in aqueous solutions. According to Kahyarian et al. [36], acetic acid, often used as a model for short-chain carboxylic acids, does not directly participate in the corrosion reaction. Instead, after acetic acid has dissociated in water, the hydrogen ions participate in the cathode reaction and thus induce steel corrosion; in contrast, undissociated acid does

not possess similar corrosivity. Similar behavior has been reported for formic acid, which is readily dissociated in aqueous solutions, increasing the conductivity and the corrosion rate of the solution [37–39]. Furthermore, acid concentration, solution temperature, and pH affect the corrosion rate [38–40]. Since formic acid is a relatively strong acid, any bio-oil containing formic acid can be considered corrosive towards steels with a Cr concentration below 11 wt % [41]. The steel studied contained no Cr, thus explaining the high measured amount of dissolved iron. It should be mentioned that the possible phase separation of oil and acid–water was not examined. Therefore, it cannot be said with certainty whether only one phase or two separate phases existed in the oil mixture.

3.2.2. L-Lycine and L-Arginine in Rapeseed Oils Containing Carboxylic Acids and Water

L-lycine and L-arginine were tested as corrosion inhibitors in fresh oil mixtures containing carboxylic acid and water.

The immersion tests in rapeseed oil with propionic acid–water additions led to heavy corrosion of iron (Figure 10), and 300 ppm L-lycine or L-arginine in the oil mixture slightly decreased the corrosion. At the higher addition (3000 ppm), the amino acids did not decrease the corrosion to an acceptable level.

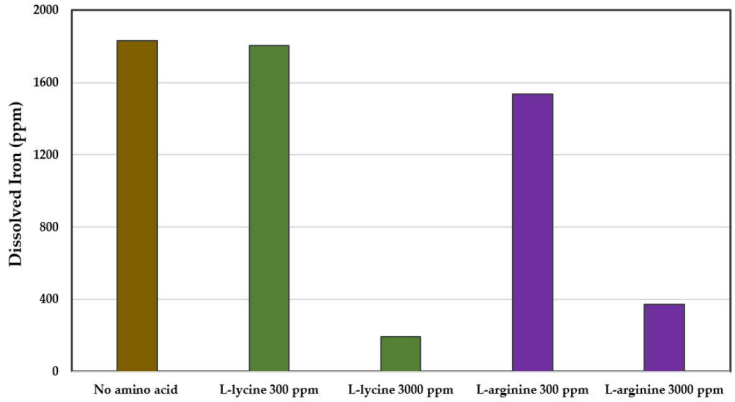

Figure 10. The concentration of iron dissolved from the mild steel immersed in rapeseed oil containing 10,000 ppm propionic acid and water with different amounts of either L-lycine or L-arginine.

After immersion of a polished mild steel rod (3 d) in rapeseed oil containing 10,000 ppm formic acid and water, 210 ppm iron was analyzed in the oil. When L-lycine 300 ppm was added to the oil mixture, the iron content was 180 ppm.

An increase in the L-lycine concentration to 3000 ppm in rapeseed oil containing 10,000 ppm formic acid and water somewhat decreased the corrosion. However, the iron concentration, 100 ppm, was still high. Similar results, i.e., a decrease in the concentration of metal ion, were measured in the oil–water–formic acid mixture with 300 ppm L-arginine (Figure 11).

Although amino acids decrease corrosion, the concentration needed for corrosion inhibition is likely high. The aging of bio-oils might lead to increased water content and the formation of carboxylic acids, which could induce significant corrosion. However, amino acids L-lycine and L-arginine effectively suppress room temperature corrosion if the oil does not simultaneously include water and carboxylic acid.

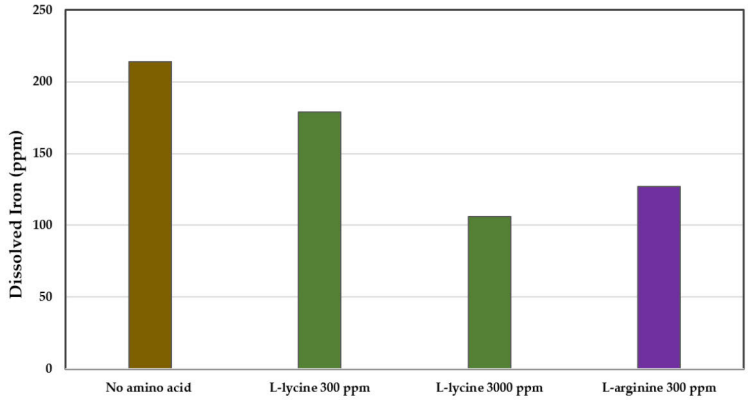

Figure 11. The concentration of iron dissolved from the mild steel in rapeseed oil containing formic acid and water with either L-lycine or L-arginine.

4. Conclusions

The corrosivity of used cooking oils was addressed in this study with three-day immersion tests of polished mild steel rods. Furthermore, the roles of contaminants, bio-oil preservatives, and corrosion inhibitors in bio-oil-induced corrosion were examined with oil samples containing added water, short-chain carboxylic acids, and amino acids. Among the ten studied amino acids, L-lycine and L-arginine showed noticeable corrosion inhibition effects, even when low concentration were added to an used cooking oil. More importantly, the level of corrosion inhibition was maintained even after the addition of water to the oil.

A minor increase in corrosion resistance was observed when a short-chained carboxylic acid (formic or propionic acid) was added to the oil. The improved corrosion resistance could have originated from a thin layer, which was formed on the surface of the sample. However, the simultaneous presence of water and one of the carboxylic acids led to corrosion of the sample rods. Furthermore, neither L-lycine nor L-arginine could provide notable corrosion protection when both water and a carboxylic acid were present in the oil. This suggests that used cooking oils contaminated with water and containing short-chained carboxylic acids increase the corrosion of mild steels. This should be taken into account when selecting the materials for oil storage vessels.

Author Contributions: Conceptualization, N.B., L.H. and J.L.; methodology, N.B., L.H. and J.H.; formal analyses, N.B., J.H., L.H., J.L. and F.T.; investigation, N.B., L.H., J.L., J.H. and F.T.; writing—original draft, N.B.; writing—review and editing, L.H., F.T., J.L. and J.H.; supervision, L.H., J.L. and F.T.; project administration, N.B. and L.H.; funding acquisition, N.B. and L.H. All authors have read and agreed to the published version of the manuscript.

Funding: This research was funded by the Swedish Cultural Foundation in Finland. The authors are also grateful to the CircVol 6Aika project for financial support as part of the activities of the Johan Gadolin Process Chemistry Centre at Åbo Akademi University. The APC was funded by Åbo Akademi University.

Institutional Review Board Statement: Not applicable.

Informed Consent Statement: Not applicable.

Data Availability Statement: Data are contained within the article.

Acknowledgments: VG EcoFuel Oy is gratefully acknowledged for providing the oil samples.

Conflicts of Interest: The authors declare no conflict of interest.

References

1. Cárdenas, J.; Orjuela, A.; Sánchez, D.L.; Narváez, P.C.; Katryniok, B.; Clark, J. Pre-treatment of used cooking oils for the production of green chemicals: A review. *J. Clean. Prod.* **2021**, *289*, 125129. [CrossRef]
2. Ribau, M.; Nogueira, R.; Nunes, L.M. Quantitative assessment of the valorisation of used cooking oils in 23 countries. *Waste Manag.* **2018**, *78*, 611–620.
3. Orjuela, A. Industrial Oleochemicals from Used Cooking Oils (UCOs): Sustainability Benefits and Challenges. In *Advances in Carbon Management Technologies: Biomass Utilization, Manufacturing, and Electricity Management*; Sikdar, S.K., Princiotta, F., Eds.; CRC: Boca Raton, FL, USA, 2021; Volume 2, pp. 74–96.
4. Stathatou, P.M.; Bergeron, S.; Fee, C.; Jeffrey, P.; Triantfyllou, M.; Gershenfeld, N. Towards Decarbonization of Shipping: Direct Emissions & Life Cycle Impacts from a Biofuel Trial Aboard an Ocean-Going Dry Bulk Vessel. Available online: https://pubs.rsc.org/en/content/articlehtml/2022/se/d1se01495a (accessed on 15 January 2022).
5. Fu, J.; Turn, S.Q.; Takushi, B.M.; Kawamata, C.L. Storage and oxidation stabilities of biodiesel from waste cooking oil. *Fuel* **2016**, *167*, 89–97. [CrossRef]
6. Pölczmann, G.; Tóth, O.; Beck, Á.; Hancsók, J. Investigation of storage stability of diesel fuels containing biodiesel produced from waste cooking oil. *J. Clean. Prod.* **2016**, *111*, 85–92. [CrossRef]
7. Tsoutsos, T.; Tournaki, S.; Gkouskos, Z.; Paraíba, O.; Giglio, F.; García, P.Q.; Braga, J.; Adrianos, H.; Filice, M. Quality characteristics of biodiesel produced from used cooking oil in Southern Europe. *ChemEngineering* **2019**, *3*, 19. [CrossRef]
8. Bruun, N.; Lehmusto, J.; Hemming, J.; Tesfaye, F.; Hupa, L. Metal rod surfaces after exposure to used cooking oils. *Sustainability* **2022**, *14*, 355. [CrossRef]
9. Sanyal, B. Organic compounds as corrosion inhibitors in different environments—A review. *Prog. Org. Coat.* **1981**, *9*, 165–236. [CrossRef]
10. Raja, A.S.; Rajendran, S.; Sathiyabama, J.; Angel, P. Corrosion control by aminoacetic acid (glycine)—An overview. *Int. J. Innov. Res. Sci. Eng. Technol.* **2014**, *3*, 11455–11467.
11. El Ibrahimi, B.; Jmiai, A.; Bazzi, L.; El Issami, S. Amino acids and their derivatives as corrosion inhibitors for metals and alloys. *Arab. J. Chem.* **2020**, *13*, 740–771. [CrossRef]
12. Kovács, A.; Tóth, J.; Isaák, G.; Keresztényi, I. Aspects of storage and corrosion characteristics of biodiesel. *Fuel Process. Technol.* **2015**, *134*, 59–64. [CrossRef]
13. Fazal, M.A.; Sazzad, B.S.; Haseeb, A.S.M.A.; Masjuki, H.H. Inhibition study of additives towards the corrosion of ferrous metal in palm biodiesel. *Energy Convers. Manag.* **2016**, *122*, 290–297. [CrossRef]
14. Hamadi, L.; Mansouri, S.; Oulmi, K.; Kareche, A. The use of amino acids as corrosion inhibitors for metals: A review. *Egypt. J. Pet.* **2018**, *27*, 1157–1165. [CrossRef]
15. Sastri, V.S. *Green Corrosion Inhibitors: Theory and Practice*; Wiley: Hoboken, NJ, USA, 2011; pp. 257–258.
16. Moretti, G.; Guidi, F.; Grion, G. Tryptamine as a green iron corrosion inhibitor in 0.5 M deaerated sulphuric acid. *Corros. Sci.* **2004**, *46*, 387–403. [CrossRef]
17. Raja, P.B.; Sethurama, M.G. Natural products as corrosion inhibitor for metals in corrosion media—A review. *Mater. Lett.* **2008**, *62*, 113–116. [CrossRef]
18. Kilberg, M.S.; Häussinger, D. Amino Acid Transport in Liver. In *Mammalian Amino Acid Transport: Mechanisms and Control*; Kilberg, M.S., Häussinger, D., Eds.; Springer: Boston, MA, USA, 1992; pp. 133–148.
19. Wu, G. *Amino Acids: Biochemistry and Nutrition*, 2nd ed.; CRC Press: Boca Raton, FL, USA, 2022; pp. 1–32.
20. Mendonça, G.L.F.; Costa, S.N.; Freire, V.N.; Casciano, P.N.S.; Correia, A.N.; de Lima-Neto, P. Understanding the corrosion inhibition of carbon steel and copper in sulphuric acid medium by amino acids using electrochemical techniques allied to molecular modelling methods. *Corros. Sci.* **2017**, *115*, 41–55. [CrossRef]
21. Gowri, S.; Sathiyabama, J.; Rajendran, S. Corrosion inhibition by amino acids—An over review. *Eur. Chem. Bull.* **2012**, *11*, 470–476.
22. Gece, G.; Bilgiç, S. A theoretical study on the inhibition efficiencies of some amino acids as corrosion inhibitors of nickel. *Corros. Sci.* **2010**, *52*, 3335–3443. [CrossRef]
23. Adams, D.; Boopathy, R. Use of formic acid to control vibriosis in shrimp aquaculture. *Biologia* **2013**, *68*, 1017–1021. [CrossRef]
24. Haque, M.N.; Chowdhury, R.; Islam, K.M.S.; Akbar, M.A. Propionic acid is an alternative to antibiotics in poultry diet. *Bangladesh J. Anim. Sci.* **2009**, *38*, 115–122. [CrossRef]
25. Rafiquee, M.Z.A.; Khan, S.; Saxena, N.; Quraishi, M.A. Influence of some thiadiazole derivatives on corrosion inhibition of mild steel in formic acid and acetic acid media. *Port. Electrochim. Acta* **2007**, *25*, 419–434. [CrossRef]
26. Yang, H.-M. Role of organic and eco-friendly inhibitors on the corrosion mitigation of steel in acidic environments—A state-of-art review. *Molecules* **2021**, *26*, 3473. [CrossRef] [PubMed]
27. Bouklah, M.; Ouassini, A.; Hammouti, B.; El Idrissi, A. Corrosion inhibition of steel in 0.5 M H_2SO_4 by [(2-pyridin-4-ylethyl) thio] acetic acid. *Appl. Surf. Sci.* **2005**, *250*, 50–56. [CrossRef]
28. Zhu, S.D.; Fu, A.Q.; Miao, J.; Yin, Z.F.; Zhou, G.S.; Wei, J.F. Corrosion of N80 carbon steel in oil field formation water containing CO_2 in the absence and presence of acetic acid. *Corros. Sci.* **2011**, *53*, 3156–3165. [CrossRef]
29. Serqueira, D.S.; Pereira, J.F.S.; Squissato, A.L.; Rodrigues, M.A.; Lima, R.C.; Faria, A.M.; Richter, E.M.; Munoz, R.A.A. Oxidative stability and corrosivity of biodiesel produced from residual cooking oil exposed to copper and carbon steel under simulated storage conditions: Dual effect of antioxidants. *Renew. Energy* **2021**, *164*, 1485–1495. [CrossRef]

30. Qiang, Y.; Li, H.; Lan, X. Self-assembling anchored film basing on two tetrazole derivatives for application to protect copper in sulfuric acid environment. *J. Mater. Sci. Technol.* **2020**, *52*, 63–71. [CrossRef]
31. Qiang, Y.; Zhi, H.; Guo, L.; Fu, A.; Xiang, T.; Jin, Y. Experimental and molecular modeling studies of multi-active tetrazole derivative bearing sulfur linker for protecting steel from corrosion. *J. Mol. Liq.* **2022**, *351*, 118638. [CrossRef]
32. Qiang, Y.; Guo, L.; Li, H.; Lan, X. Fabrication of environmentally friendly Losartan potassium film for corrosion inhibition of mild steel in HCl medium. *Chem. Eng. J.* **2021**, *406*, 126863. [CrossRef]
33. Bruun, N.; Demesa, A.G.; Tesfaye, F.; Hemming, J.; Hupa, L. Factors affecting the corrosive behavior of used cooking oils and a non-edible fish oil that are in contact with ferrous metals. *Energies* **2019**, *12*, 4812. [CrossRef]
34. Bruun, N.; Khazraie Shoulaifar, T.; Hemming, J.; Willför, S.; Hupa, L. Characterization of waste bio-oil as an alternate source of renewable fuel for marine engines. *Biofuels* **2022**, *13*, 21–30. [CrossRef]
35. Bruun, N.; Tesfaye, F.; Hemming, J.; Dirbeba, M.J.; Hupa, L. Effect of storage time on the physicochemical properties of waste fish oils and used cooking vegetable oils. *Energies* **2021**, *14*, 101. [CrossRef]
36. Kahyarian, A.; Brown, B.; Nešić, S. The unified mechanism of corrosion in aqueous weak acids solutions: A review of the recent developments in mechanistic understandings of mild steel corrosion in the presence of carboxylic acids, carbon dioxide, and hydrogen sulfide. *Corrosion* **2020**, *76*, 268–278. [CrossRef]
37. Invernizzi, A.J.; Sivieri, E.; Trasatti, S.P. Corrosion behaviour of duplex stainless steels in organic acid aqueous solutions. *Mater. Sci. Eng. A* **2008**, *485*, 234–242. [CrossRef]
38. Sekine, I.; Hatakeyama, S.; Nakazawa, Y. Effect of water content on the corrosion behaviour of type 430 stainless steel in formic and acetic acids. *Electrochim. Acta* **1987**, *32*, 915–920. [CrossRef]
39. Singh, M.M.; Gupta, A. Corrosion behaviour of mild steel in formic acid solutions. *Mater. Chem. Phys.* **1996**, *46*, 15–22. [CrossRef]
40. Gjertsen, S.B.; Palencsar, A.; Seiersten, M.; Hemmingsen, T.H. The effect of volatile organic acids and CO_2 on the corrosion rate of carbon steel from a top-of-line-corrosion (TLC) perspective. *IOP Conf. Ser. Mater. Sci. Eng.* **2021**, *1201*, 012079. [CrossRef]
41. Jun, J.; Frith, M.G.; Connatser, R.M.; Keiser, J.R.; Brady, M.P.; Lewis, S. Corrosion susceptibility of Cr-Mo steels and ferritic stainless steels in biomass-derived pyrolysis oil constituents. *Energy Fuels* **2020**, *34*, 6220–6228. [CrossRef]

RECENT REPORTS FROM THE COMBUSTION AND MATERIALS RESEARCH GROUP OF THE JOHAN GADOLIN PROCESS CHEMISTRY CENTRE:

19-01	Jingxin Sui	Initial stages of Alkali Salt Induced High Temperature Corrosion Mechanisms: Experimental studies using a combination of chronoamperometry, scanning electron microscopy, X-ray photoelectron spectroscopy and time-of-flight secondary ion mass spectrometry
19-02	Hanna Kinnunen	The Role and Corrosivity of Lead in Recycled Wood Combustion
19-03	Jonne Niemi	Effects of Temperature Gradient on Ash Deposit Aging and Heat Exchanger Corrosion
20-01	Meheretu Jaleta Dirbeba	Thermochemical Conversion Characteristics of Vinasse
20-02	Thomas Kronberg	Properties of raw glazes – The impact of composition, firing and functional coatings

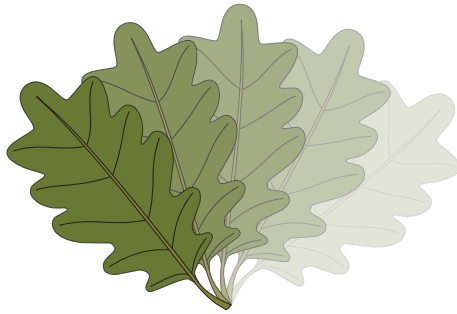

ISBN 978-952-12-4202-1 (printed)
ISBN 978-952-12-4203-8 (digital)
Åbo/Turku, Finland 2022

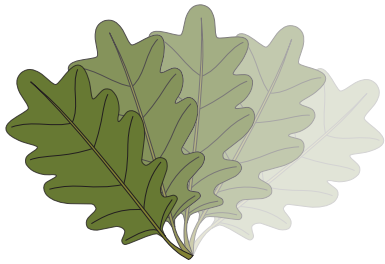

Johan Gadolin
Process Chemistry Centre

9 789521 242021 >

ISBN 978-952-12-4202-1